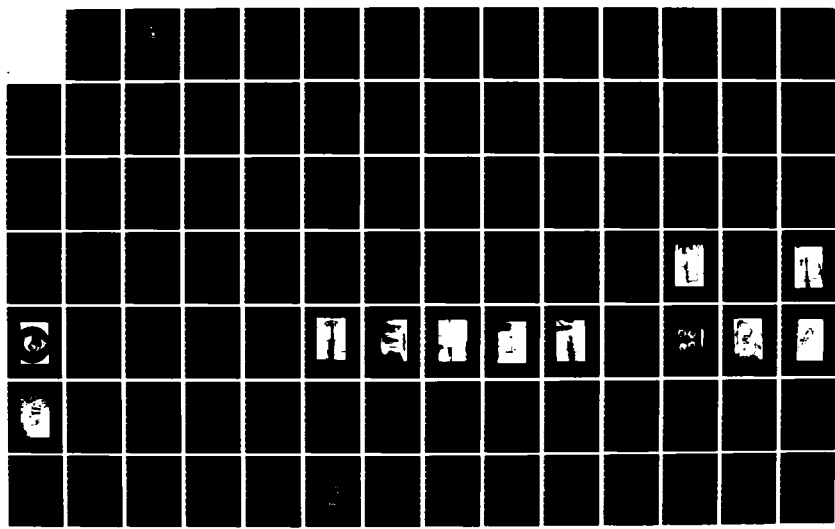
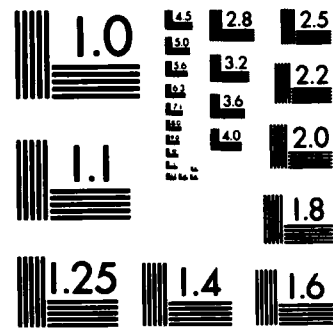


AD-A136 745 DESIGN AND TESTING OF SCALED EJECTOR-DIFFUSERS FOR JET 1/2
ENGINE TEST FACILITY APPLICATIONS(U) NAVAL POSTGRADUATE
SCHOOL MONTEREY CA J W MOLLOY SEP 83

UNCLASSIFIED

F/G 14/2 NL





MICROCOPY RESOLUTION TEST CHART
NATIONAL BUREAU OF STANDARDS-1963-A

AD A 136745

(2)

NAVAL POSTGRADUATE SCHOOL

Monterey, California



THESIS

DESIGN AND TESTING OF
SCALED EJECTOR-DIFFUSERS FOR
JET ENGINE TEST FACILITY APPLICATIONS

by

James William Molloy

September 1983

Thesis Advisor:

P.F. Pucci

Approved for public release; distribution unlimited

SELECTED
JAN 12 1984
S DTIC D
E

DTIC FILE COPY

84 01 12 022

UNCLASSIFIED

SECURITY CLASSIFICATION OF THIS PAGE (When Data Entered)

REPORT DOCUMENTATION PAGE		READ INSTRUCTIONS BEFORE COMPLETING FORM
1. REPORT NUMBER	2. GOVT ACCESSION NO.	3. RECIPIENT'S CATALOG NUMBER
		AD-H136 745
4. TITLE (and Subtitle) Design and Testing of Scaled Ejector-Diffusers for Jet Engine Test Facility Applications		5. TYPE OF REPORT & PERIOD COVERED Engineer's Thesis September 1983
7. AUTHOR(s) James William Molloy		6. PERFORMING ORG. REPORT NUMBER
9. PERFORMING ORGANIZATION NAME AND ADDRESS Naval Postgraduate School Monterey, CA 93943		10. PROGRAM ELEMENT, PROJECT, TASK AREA & WORK UNIT NUMBERS
11. CONTROLLING OFFICE NAME AND ADDRESS Naval Postgraduate School Monterey, CA 93943		12. REPORT DATE September 1983
14. MONITORING AGENCY NAME & ADDRESS (if different from Controlling Office)		13. NUMBER OF PAGES 141
		15. SECURITY CLASS. (of this report)
		15a. DECLASSIFICATION/DOWNGRADING SCHEDULE
16. DISTRIBUTION STATEMENT (of this Report) Approved for public release; distribution unlimited		
17. DISTRIBUTION STATEMENT (of the abstract entered in Block 20, if different from Report)		
18. SUPPLEMENTARY NOTES		
19. KEY WORDS (Continue on reverse side if necessary and identify by block number) Supersonic Ejector-Diffuser Pressure Recovery		
20. ABSTRACT (Continue on reverse side if necessary and identify by block number) →Design, fabrication and cold flow testing of a modeled jet engine test facility were conducted in an effort to provide an inexpensive vehicle to study geometric variations in diffuser geometry which could improve system efficiency. The design, is based on Mach number similitude, and consists of two configurations currently in use at the Naval Air Propulsion Center, Trenton, New Jersey. A constant area diffuser and a variable area diffuser with translating centerbody were modeled. Baseline mapping of the		

UNCLASSIFIED

SECURITY CLASSIFICATION OF THIS PAGE (When Data Entered)

20. Abstract (contd)

operating characteristics for each diffuser with representative scaled engines was conducted to provide a reference against which alternative geometries would be evaluated. The constant area plus two variants were tested. A five-sixths and two-thirds reduction were studied to investigate the potential for increasing efficiency for a specific engine diffuser combination at NAPC. Secondary flow provisions were incorporated into the design to allow variation of this parameter. The modeling results were consistent with theory and the test apparatus produced repeatable results. A two dimensional double ramp (wedge) capable of being translated in a rectangular duct was suggested as an alternative diffuser geometry.

Accession For	
NTIS GRAFI	<input checked="" type="checkbox"/>
DTIC TAB	<input type="checkbox"/>
Unrestricted	<input type="checkbox"/>
Classification	
Rev.	
Distribution/	
Availabilit Codes	
1. Standard and/or	
Dist	Special
A-1	



S-N 0102-LF-014-6601

UNCLASSIFIED

SECURITY CLASSIFICATION OF THIS PAGE (When Data Entered)

Approved for public release; distribution unlimited

Scaled Ejector-Diffusers For
Jet Engine Test Facility Applications

by

James William Molloy
Commander, United States Navy
B.S., United States Naval Academy, 1969

Submitted in partial fulfillment of the
requirements for the degree of

MASTER OF SCIENCE IN MECHANICAL ENGINEERING
and
MECHANICAL ENGINEER

from the

NAVAL POSTGRADUATE SCHOOL
September 1983

Author:

James W. Molloy

Approved by:

Paul J. Lucci

Thesis Advisor

P.J. Marto

Chairman, Department of Mechanical Engineering

James C. Oliver

Dean of Science and Engineering

ABSTRACT

Design, fabrication and cold flow testing of a modeled jet engine test facility was conducted in an effort to provide an inexpensive vehicle to study geometric variations in diffuser geometry which could improve system efficiency. The design is based on Mach number similitude and consists of two configurations currently in use at the Naval Air Propulsion Center, Trenton, New Jersey. A constant area diffuser and a variable area diffuser with translating centerbody were modeled. Baseline mapping of the operating characteristics for each diffuser with representative scaled engines was conducted to provide a reference against which alternative geometries would be evaluated. The constant area plus two variants were tested. A five-sixths and two-thirds reduction were studied to investigate the potential for increasing efficiency for a specific engine diffuser combination at NAPC. Secondary flow provisions were incorporated into the design to allow variation of this parameter. The modeling results were consistent with theory and the test apparatus produced repeatable results. A two dimensional double ramp (wedge) capable of being translated in a rectangular duct was suggested as an alternative diffuser geometry.

TABLE OF CONTENTS

I.	INTRODUCTION	10
A.	PROBLEM FORMULATION	10
B.	LITERATURE SURVEY	12
C.	RESEARCH OBJECTIVES	14
II.	THEORY AND ANALYSIS	17
A.	FLOW CHARACTERIZATION	19
B.	OPERATING CHARACTERISTIC	20
C.	ENERGY CONSIDERATIONS	21
III.	EXPERIMENTAL APPARATUS	22
A.	TEST CELL/ENGINE ASSEMBLY	22
B.	EXHAUST PLENUM	23
C.	DIFFUSER ASSEMBLIES	23
1.	Straight Tube Diffuser	24
2.	Variable Area Diffuser	24
D.	ENGINES	25
E.	AIR SUPPLY	25
F.	INSTRUMENTATION	26
G.	DATA ACQUISITION	27
IV.	EXPERIMENTAL PROCEDURES	29
V.	DISCUSSION OF RESULTS	31
A.	MODEL DESIGN/CONSTRUCTION	32
B.	ENGINE DESIGN	33
C.	DATA BASE	33
D.	PARAMETRIC VARIATIONS	34
	1. A_e/A^*	34

2. Secondary Flow	36
3. Ad/A*	38
E. F404 IMPROVEMENT	39
F. SYSTEMS EFFICIENCY	40
VI. CONCLUSIONS AND RECOMMENDATIONS	44
A. CONCLUSIONS	44
B. RECOMMENDATIONS	44
APPENDIX A: DEVELOPMENT	91
APPENDIX B: NAPC TEST FACILITY IMPROVEMENT PROGRAM . . .	95
APPENDIX C: DIFFUSER PROPOSALS	100
APPENDIX D: EXPERIMENTAL PROCEDURE	104
APPENDIX E: SECOND THROAT DIFFUSERS	106
APPENDIX F: SCALED DRAWINGS	108
APPENDIX G: DATA TABLES	116
APPENDIX H: COMPUTER PROGRAMS	133
LIST OF REFERENCES	139
INITIAL DISTRIBUTION LIST	141

LIST OF FIGURES

Figure 1.	Typical Turbojet Test Cell	46
Figure 2.	Variable Geometry Diffuser With Centerbody . .	47
Figure 3.	Generalized Flow Characterization of Expanding Jet with Secondary Flow	48
Figure 4.	Simplified Test Cell	49
Figure 5.	Shock Strength Model	50
Figure 6.	Model Test Facility With Straight Tube Diffuser	51
Figure 6a.	Model Test Facility Schematic	52
Figure 7.	Scale Model Test Cell with Variable Area Diffuser	53
Figure 7a.	F404 Engine Assembly	54
Figure 8.	Test Cell Cross Section	55
Figure 9.	Straight Tube Diffuser (Full Scale)	56
Figure 9a.	Straight Tube Diffuser (Two-Thirds)	57
Figure 9b.	Straight Tube Diffuser (Five-Sixths)	58
Figure 10.	Pressure Tap Arrangement	59
Figure 11.	Constant Area Diffuser with Inserts	60
Figure 12.	Variable Area Diffuser Exploded View	61
Figure 13.	Remotely Operated Drive Mechanism	62
Figure 14.	Pressure Taps (Variable Area Diffuser)	63
Figure 15.	Variable Area Profile	64
Figure 16.	Test Engine Models	65
Figure 17.	Allis Chalmers Twelve Stage Compressor . . .	66
Figure 18.	Scanivalve Pressure Scanner	67

Figure 19.	Model Test Facility Remote Operating Station .	68
Figure 20.	Operating Curve (F404 Non A/B)	69
Figure 20a.	Operating Curve (F404 A/B)	70
Figure 21.	Operating Curve (TF30 Non A/B)	71
Figure 21a.	Operating Curve (TF30 A/B)	72
Figure 22.	F404 Fully Started	73
Figure 23.	F404 Baseline	74
Figure 24.	TF30 Baseline	75
Figure 25.	Optional Presentation of Operating Curves . .	76
Figure 26.	AE/A* Effects	77
Figure 27.	Secondary Flow Effects (Five-Sixths)	78
Figure 28.	Secondary Flow Effects (Two-Thirds)	79
Figure 29.	AD/A* Effects	80
Figure 30.	Static Pressure Profiles	81
Figure 31.	F404 Improvement Summary	82
Figure 32.	Taper Effects (F404 Non A/B)	83
Figure 33.	Taper Effects (F404 A/B)	84
Figure 34.	Test Facility Illustration	85
Figure 35.	Generalized Exhaust Fan Efficiency	86
Figure 36.	Engine Test Facilities	87
Figure 37.	Variable Exhaust Ejector-Diffuser	88
Figure 38.	Conceptual Wedge Design	89
Figure 39.	Instrumentation Schematic	90

NOMENCLATURE

A^*	Nozzle Throat Area (L^2)
A_e	Nozzle Exit Area (L^2)
A_d	Second Throat Area (L^2)
H_t	Specific Fan Work ($L^2 T^{-2}$)
L/D	Length to Diameter Ratio
M	Mach Number
\dot{m}	Mass flow (MT^{-1})
P/ρ	Flow Energy (LT^{-2})
P_{T8}	Total Nozzle Pressure ($ML^{-1} T^{-2}$)
P_{14}	Exhaust Pressure ($ML^{-1} T^{-2}$)
P_{S9}	Cell Pressure ($ML^{-1} T^{-2}$)
P_o	Stagnation Pressure ($ML^{-1} T^{-2}$)
$v^2/2g_c$	Kinetic Energy (LT^{-2})
Z	Potential Energy (LT^{-2})
β	Orifice to Pipe Diameter Ratio
η_{aej}	Air Ejector Efficiency
η_f	Fan Efficiency

I. INTRODUCTION

The ability to efficiently exercise control over the energies entrained within a supersonic airstream has been the quest of aerodynamicists for several decades. The designers of wind tunnels, jet inlets, gas dynamic lasers and jet engine test facilities have each addressed the gas dynamics of this topic. Each design has had to incorporate a method to decelerate the flow, generally, through a mechanical device such as a diffuser. The complexities of treating the recompression of a real fluid in the presence of a boundary layer have defied analytic modeling of a supersonic diffuser to any great extent. The design approaches taken have been empirically based, which has led to a wide variety of diffusers tailored to meet the unique operating environment at a particular facility. This study is sponsored by one such facility challenged with one of the consistent fascinations of modern engineering: how to extend the limits of one's design in the presence of new technology or shifting economic variables.

A. PROBLEM FORMULATION

Ground testing of jet engines has long been an integral part of the design and maintenance practice in both the military and commercial aviation industries. Organizations, chartered with the testing of these engines, strive to generate a test envelope which closely approximates the operating envelope

which the engine will encounter in service. Advances in engine technology have imposed added demands upon the test engineer to extend the test envelope accordingly. This challenge has proven a classic cost effectiveness exercise, wherein, as higher altitude testing at increased power is pursued from one end of the spectrum, the attendant cost of exhausting the effluent in an innocuous manner to the environment spirals. The economic challenge continues to compound over the life cycle of the facility as energy costs associated with demands on the exhausters escalate.

Test cell philosophy has focused foremost on achieving a sufficiently flexible design which will accommodate a wide range of engines. Large exhaust mechanisms, capable of handling a wide range of exhaust states, were adequate when the motive energy cost was only a small fractional cost of the total price of testing. Strategies to enhance pressure recovery prior to the exhauster were developed but optimization of the design in this regard was not a bonafide concern. The present testing scenario reveals that the associated costs in exhausting the effluent rivals any of the other cost variables and percentage improvements in efficient pressure recovery through retrofit of the original design merit consideration.

A typical test cell design is as depicted in Figure 1. The engine to be tested is mounted on a test bed and located in the test cell such that the exhaust will be vented into an augmenting tube which acts as an ejector-diffuser assembly.

The kinetic energy of the exhaust stream is converted by the diffuser into a pressure for presentation to the exhauster. Each cell is nominally equipped for secondary flow in which secondary air is entrained with exhaust jet gas to provide engine cooling and dilute the combustion products. Allowance is made for relative positioning of the test bed and diffuser to reconcile potential problems with pressure gradients under conditions of secondary flow which may influence the operating envelope.

B. LITERATURE SURVEY

Several searches were conducted to survey the available literature for supersonic ejector-diffuser studies and theoretical discussions germane to this investigation. An online computer search of several national data bases was conducted using the keyword, keyphrase approach. Results of the search revealed over 10,000 documents generally associated with the broad topic area, of which, a highly focused search indicated over 300 documents with relevant material. A hardcopy of the latter with a brief synopsis of each report, was procured for further review. The survey was restricted to English or English translations but evidence of many foreign papers on the subject was apparent. In no respect is the review considered all-inclusive.

A synopsis of the most recognized works gives a flavor for the approach adopted. In 1949, pioneer work, which appears as a baseline in most studies related to supersonic

diffusers is attributed to Neumann and Lustwerk (Ref. 1). This study included a one-dimensional theoretical analysis, and an experimental modeling with flow visualization by Schlierin photography of a constant area diffuser. A "transverse shock" was observed and categorized as the operative mechanism controlling diffusion. An optimum diffuser with an L/D of 10 was identified. In 1958, Lukasiewicz (Ref. 2), studied data from several existing wind tunnel diffusers, concluding that fixed geometry diffusers can approach the pressure recoveries established from normal shock theory. Pressure recovery, far in excess of that obtainable with a constant area diffuser, was established for systems which employed variable area diffusers. In 1954, Hastings (Ref. 3) established the beneficial effect in diffuser performance of auxiliary ejection to partially evacuate test cells. Numerous additional studies with specific design goals have been conducted to optimize test facility operation. The most extensive noted were those conducted by Panesci and German (Ref. 4), for Arnold Engineering Development Center in the 60's in which variable geometry diffusers with a centerbody were employed. Here again, pressure recovery far in excess of that achievable with constant area diffusers was observed.

Generalized studies to characterize pertinent parameters governing the flow phenomenon in rectangular diffusers were conducted by Merkli (Ref. 5) in 1976 and Waltrip and Billig (Ref. 6) in 1973. Merkli focused upon Mach number, diffuser length, boundary layer and Reynolds number as controlling

parameters. Reynolds effects were discounted as minimal with Mach number and diffuser length the significant parameters. Waltrip and Billig corroborated previous works establishing 8 - 12 tube diameters as the required recovery zone. They also focused on an oblique shock system as the governing mechanism.

Ginoux {Ref. 7} compiled an excellent summary of a short course in Supersonic Ejectors conducted at the von Karman Institute. The short course was an attempt to focus on the most advanced initiatives and progress in theoretical modeling and design of high efficiency ejectors.

C. RESEARCH OBJECTIVES

The Naval Air Propulsion Center at Trenton, New Jersey, as a major jet engine test facility, has experienced the technological advances in engine design which have approached the design limits of their ejector-diffuser assemblies exacting a heavy burden on power consuming exhauster machinery to maintain simulated altitudes. As an adjunct to a much larger study, a cold flow modeling of their existing plant was sponsored by the center. The principal goal, assuming satisfactory modeling of the test facility, was to test alternative diffuser geometries in anticipation of enhancing overall efficiency. The modeling process was such that, Mach number similitude could be maintained, any efficiency increases over the baseline would be due largely to geometric effects.

As discussed in the general treatment on diffuser theory, the two principle types of diffusers, a fixed area and a variable area, were modeled. In both diffusers recompression of the supersonic flow is accomplished by a complex-shock mechanism under the influence of a boundary layer, with post shock subsonic diffusion following recognizable theory. The experimental technique devised was to establish the diffuser characteristic on a non-dimensional basis as a baseline against which 'new' geometries may be judged. Operating envelopes for each diffuser design would be duplicated as far as practicable with the same engines. Whereas the phenomenon by which recompression occurs would not be directly studied, a pressure histogram along the diffuser was recorded in order to postulate the character of the operative mechanism. It was anticipated that attempting to control the shock mechanism would likely provide the largest gains in efficiency as opposed to manipulating the subsonic diffusion process.

The scope of the investigation would be guided by studying only those configuration changes which could readily be retrofitted into the existing space limitations of the parent facility. Conceptual designs would be unbounded by any environmental or stress-related constraints, allowing a sponsor's cost benefit analysis to sort out those aspects of new design proposals.

Despite successful construction of a highly flexible model, a major portion of the stated objectives could not be accomplished within the timeframe allotted to this phase of

the study. As baseline testing proceeded into the variable geometry diffuser, Figure 2, an unanticipated heating and vibration phenomenon was observed. The extent and nature of the phenomenon was not readily ascertainable but was in evidence only with the use of the centerbody configuration. The problem was of such proportion as to potentially taint the conclusiveness of future work involving devices imbedded in the jet stream. A separate detailed study of the phenomenon was ordered and a new set of objectives was established in concert with the sponsor.

In an effort to optimize test cell geometry for one of the more heavily tested engines (F404), a series of liners which would reduce the cross section for diffusion were designed for insertion into the full scale straight tube diffuser. Engines were tested in anticipation of achieving better diffuser efficiency by seeking to optimize the ratio of nozzle area to diffuser cross section for the highest pressure recovery.

The details of the model design and testing in the context of this narrower objective are contained in the thesis proper. The conceptual work related to the original objective with a proposal for an alternative method of diffusion are discussed in Appendices A and C.

II. THEORY AND ANALYSIS

Pressure recovery in a supersonic jet engine test facility is accomplished by a mechanical device called a diffuser. Two types of diffusers are recognized, the fixed or constant area diffuser and the variable geometry diffuser. The fixed geometry normally is associated with fairly constant input parameters such as mass flow rate, stagnation temperature and pressure. The variable area geometry is utilized where fluctuations in fluid characteristics or engine geometry (such as variation in exhaust area accompanying jet engine testing from the non-afterburning to afterburning mode) are an integral part of the testing. Each type of diffuser may serve an ancillary role to eject secondary air used in cooling the engine assembly and test cell.

In each diffuser the operative mechanism which accomplishes the first order pressure recovery from supersonic to subsonic conditions is a shock system. Subsequent pressure recovery must follow the guidelines for subsonic diffusion. Projecting an improvement in efficiency accompanying any alternative geometry would require a projection of the probably shock patterns and the interaction of that shock system with a postulated boundary layer. This interaction, in simple geometries, has not been conclusively researched; hence, this type of approach in the presence of complex geometries is not warranted. Analytic models to guide the design of a new geometry for jet engine

testing abound in the literature but generally assume the most convenient of assumptions. The model is generally one dimensional steady state using a simplified control volume and serves to bound the expectations only. Academic interests aside, a purely empirical approach is warranted. The approach adopted herein calls for establishment of baseline models of proper similitude with the existing facility from which characteristic curves can be drawn and against which alternative designs may be mapped and contrasted.

Acceptance of any observed change in system efficiency merits consideration only if dynamic similitude of the flow field has been verified between the baseline model and the parent facility. With supersonic compressible flow, Shapiro {Ref. 8}, is replete with support documentation illustrating the role of Mach number as the significant parameter in characterization of the flow. Merkli {Ref. 5}, in a series of experiments with rectangular constant area supersonic diffusers, concluded that Reynolds number has little effect on the pressure recovery. Mach number, as the ratio of kinetic energy to internal energy, was thus chosen as the best parameter upon which to base model development. Geometric compatibility was governed by the constraints of the engines to be tested and the limits imposed by the available air supply at the model test facility. The influence of temperature between cold ambient testing and prototype testing with hot exhaust gases would be addressed in the discussion of results as how it might impact the operative pressure recovery.

mechanism. Appendix A provides a more detailed study of modeling/scaling considerations peculiar to this study.

A. FLOW CHARACTERIZATION

Flow at the exit plane of the nozzle achieves supersonic proportions whose Mach number may be approximated by analyzing a Prandtl-Meyer corner flow from the nozzle exit to diffuser entrance. The increase in area from the exit plane to the diffuser allows the jet to expand supersonically as it fills the available volume. A Prandtl-Meyer expansion may also be utilized to estimate the pre-shock Mach number. Shocking, due to perturbation of the jet stream with the boundary layer as reported in several other workd {Ref 8} will assume an oblique character. The oblique shock system will, upon attainment of subsonic conditions, blend into a turbulent, well-mixed stream which would diffuse in accordance with subsonic theory. The oblique shock system would be expected to migrate along the diffusers length for a given geometry of diffuser, in some proportion to the driving pressure. The oblique shock system, as discussed by Shapiro, {Ref. 8}, will either be strong or weak as governed by the stability of the flow, the nature of the boundary layer interaction and a multiplicity of lesser related factors. Pressure variations caused by area change conceivably promote an alternating compression and expansion character to the flow wherein the jet may tend to pulse. Restricting the flow to a constant area would tend to damp out this type of behavior. Figure 3 illustrates the anticipated character of the flow.

B. OPERATING CHARACTERISTICS

The operation of the variable area ejector-diffuser provides insight into the complexities involved when designing or redesigning a new pressure recovery mechanism. Utilizing the simplified arrangement of Figure 4 to guide the discussion, the operation of this device may be described. As the total pressure is increased, flow in the nozzle accelerates until sonic conditions ($M=1$) are attained at the throat. Increasing total pressure or holding total pressure at this level and reducing the back pressure will cause a normal shock to stand in the supersonic region of the nozzle. A further lowering will cause the shock to pass into the test cell and into the diffuser. With a second throat, once the shock has been swallowed, the diffuser is considered started after which exhaust pressure may be raised shifting the shock to zones where stagnation pressure loss is less. A minimum loss will occur if the shock is located at the second throat. This may be accomplished by adjusting the axial position of the centerbody. The minimum flow area of the diffuser, A_d , must be greater than A^* or the cell would become choked and altitude simulation could not proceed. The band of pressures, where cell pressure is independent of exhaust pressure, establishes the operating range of the diffuser. Conservatively, the shock is maintained upstream of the throat to preclude reverting to a higher cell pressure due to fluctuations in the flow field.

C. ENERGY CONSIDERATIONS

The presence of a shock wave arising from the supersonic starting process represents an increase in entropy at the expense of stagnation pressure. The entropy rise (pressure loss) is greatest across a normal shock as opposed to that across several oblique shocks. A simple illustration using Figure 5 makes the point. For a flow of Mach 2.0 at the diffuser entrance, a one-dimensional normal shock gives a stagnation pressure ratio across the shock of .721 with a post shock Mach number of .475. Using a device to diffuse the flow in oblique steps, then allowing for a normal shock, should increase the stagnation pressure ratio compared to the normal shock alone.

Choosing turning angles of 6 degrees for each of two successive redirections of the flow followed by a gradual turn prompting a normal shock yields an overall stagnation pressure ratio of .951. The pair of oblique shocks increases the stagnation pressure rise by a factor of 1.32. In the limit, an infinite number of small oblique shocks will tend towards an ideal recompression.

III. EXPERIMENTAL APPARATUS

Each of the scale model altitude test facilities constructed consisted of a common test cell, and an exhaust plenum with a variable diffuser assembly as illustrated in Figures 6 and 6a. Primary and secondary air were provided by a common source, an Allis-Chalmers twelve stage axial compressor. Exhaust plenum pressure was controlled by an air ejector driven by the common air supply from the axial compressor.

A. TEST CELL/ENGINE ASSEMBLY

The test cell, Figures 7, 7a, and 8, housed engines and provided a plenum for secondary air flow. The cell was fabricated from aluminum and of cylindrical design measuring 15 inches in length and 12 inches in diameter (I.D.). The upstream flange assembly (1) provides a mating surface for the primary air piping, structural support for a cantilevered engine housing (2) and an air seal assembly. Dry silicon rubber seals guarding against air intrusion are prescribed owing to the vacuum created for altitude simulation. A 3 inch diameter penetration (3) at the base is provided for secondary flow connections. The downstream flange (4) accommodates diffuser assembly attachment and incorporates a similar air sealing arrangement. Ports for direct sampling of cell pressure and remote connectors for engine pressures were provided.

The engine assembly, also of aluminum, consists of 3 inch (I.D.) entrance piping (5) which in addition to its flow straightening function served as the support for the engine mounting assembly (6). The mounting assembly served to transition the flow from the entrance piping to the 2 inch (I.D.) conformal entrance duct. The mounting assembly introduced one element of versatility via a variable spacer ring (7). The spacer ring allows for 2 inches of horizontal realignment of engines should variation in standoff distance to the diffuser be required. The engine mounting surface (8) was machined to provide a retaining collar and indented for set screw assembly of engines.

B. EXHAUST PLENUM

Interfacing between the exhaust air ejector assembly and the diffuser assemblies was an exhaust plenum 3 foot by 3 foot in cross section by 4 feet long. The plenum houses a remotely operated traversing mechanism used to drive the multiple angle centerbody assembly which is peculiar to the variable diffuser geometry. A maintenance access/inspection port is provided to assist in alignment. A six inch access connects to the air ejector piping to provide closure with the atmosphere and a means of back pressure control.

C. DIFFUSER ASSEMBLIES

Two scaled diffuser assemblies, Figures 2 and 9, were developed to establish the baseline against which alternative designs can be compared.

1. Straight Tube Diffuser

The model consists of a 15.25 inch long 2.71, inch (I.D.) cylindrical ejector-diffuser. Pressure taps were installed to record the pressure recovery process and are illustrated in Figure 10. Taps were placed at one (1) inch intervals along the length of the diffuser. Sealing was achieved by rubber seals in the end flanges. The length to diameter ratio was 5.62.

Two variations of this geometry, Figures 9a and 9b, were developed to investigate extending the operating envelope of the test cell to enhance efficiency and economy of operation. As depicted in Figures 9a, 9b, and 11 inserts were added to achieve a 5/6 and 2/3 reduction in diameter. Two end inserts (9) were included to allow investigation of sudden expansion versus gradual diffusion in the end section.

2. Variable Area Diffuser

Variable area diffusion was developed by traversing a multiple angle conical centerbody (Figures 2 and 12) within a 24 inch long cylindrical to conical diffuser. The overall length to inlet diameter ratio was 6.92.

The centerbody was 16.5 inches long having a leading cone of half angle 19.8 degrees and three trailing truncated cones of 10.8, 8.9, and 2.6 degrees, respectively, with a cylindrical afterbody. Centering was provided by a reinforced spider (10) which provided bearing support for 3/4 inch steel drive shaft. The shaft was coupled to an electrically operated

drive mechanism, Figure 13, which was remotely activated, allowing travel of 6 inches with positive mechanical and electrical limits. Positioning circuitry generated a plus/minus 5 volt output which is remotely retrieved at the principal operating station.

The cylindrical to conical diffuser (8 degrees half angle) was equipped with static pressure taps longitudinally located along the wall, as shown in Figure 14.

The integrated centerbody and diffuser permitted wide variation in the flow area presented to the jet, including introduction of a variable second throat. Variation in flow area with axial position of the centerbody is shown in Figure 15.

D. ENGINES

Two sets of engines, Figure 16, were developed to model the F404 and the TF30 engines tested at NAPC. The engines were scaled to simulate the IRP and max A/B mode of testing. IRP represents Intermediate Rated Power which represents the highest power level without afterburner. This term is used synonymously with non-afterburning throughout the thesis. A/B refers to the maximum afterburning mode.

E. AIR SUPPLY

Compressed air from the Turbopropulsion Laboratory's Allis-Chalmers, twelve stage axial compressor, Figure 17, was utilized in all model testing. Maximum discharge pressure

of this machine was approximately 3.0 atmospheres at 15.0 lbm/sec mass flow rate.

Primary and secondary air, as previously shown in Figure 6a, were supplied to the engine model and test cell, respectively, through three inch I.D. piping. A six inch I.D. suction line was attached to the exhaust plenum to simulate the effect of the exhaust air pumps used in the full scale test facility. Primary and secondary air flows and exhaust plenum pressure were controlled by pneumatically operated valves set remotely by differential pressure transmitters.

F. INSTRUMENTATION

A forty-eight (48) port pressure scanner, a Scanivalve, shown in Figure 18, (with an automatic stepping feature) allowed using a single pressure transducer for sensing many system pressures. Geofarth, {Ref. 9}, documents the logic and associated hardware for this system. The Scanivalve was employed as a computer peripheral to permit near simultaneous logging of system pressures. Approximate sampling of one (1) pressure tap/second was representative of the acquisition rate. The Scanivalve measured the differential pressure between the nominated source and a known reference. One Scanivalve port was open to the atmosphere and zeroed against an input reference signal. All other pressures were referenced against this port to give a precise 'gage' measurement which becomes a transducer output for conditioning and subsequent

measurement by a digital voltmeter. Pressures were sampled across primary and secondary orifices for mass flow calculation, total pressure at engine inlet, engine throat, test cell plenum, fifteen (15) diffuser locations and the exhaust plenum. Atmospheric pressure was read from an absolute pressure Bourdon gage and manually recorded. Pressure taps were sized in accordance with Reference 10. Metering orifices, with $\beta = .7$ were utilized. In order to minimize the pressure drop in the primary flow system, the engine nozzles were calibrated using the flow rate indicated by the primary flow orifice. After calibration the orifice was removed.

Temperatures were measured using copper-constantan (Type T) thermocouples. An ice point reference was included in the design. Primary and secondary temperatures at 6 diameters downstream of the orifices were recorded. Temperature of the inlet air stream in the vicinity of the total pressure centerbody was also sampled. Thermocouple levels were input upon demand (computer controlled) to a Hewlett Packard 349A Scanner and relayed to a Hewlett Packard 3455 digital voltmeter for subsequent recording. Three portable digital voltmeters were employed in monitoring and modifying the controllable parameters.

G. DATA ACQUISITION

An integrated automatic data acquisition system was employed to record fluid properties. The Hewlett Packard HP-IB Interface Bus under the control of a Hewlett Packard

9830A calculator with HP9867B Mass Storage Unit and several peripheral options comprised the system. A computer program, Appendix H, adapted from the original work of Geopfarth {Ref. 9} controlled the data acquisition and storage process. Raw data were stored in mass memory with a hard copy backup. It was anticipated the data could be transferred to IBM 3033 for processing but communication problems necessitated that the data be hand input into the IBM files.

IV. EXPERIMENTAL PROCEDURES

Control over system operation was performed from a remote operating station, Figure 19. Three differential pressure transmitters (11), (12), (13), provided positive control over primary air, secondary air and exhaust pressure. These transmitters regulated a 0-15 psig signal to three remotely operated valves. Dedicated pressure transducers provided direct reading of nozzle total pressure, cell pressure and exhaust pressure and were remotely monitored on digital voltmeters (14), (15), (16). A preliminary check list for system checkout and an operating guide are provided in Appendix D. Output from the scanivalve controller (17) could be selectively monitored as desired. Total pressure regulation, once the primary valve was open fully, consisted of remotely manipulating the compressor air bypass.

Each engine and diffuser combination was tested over the entire range of deliverable pressures as mapped against exhaust pressures from atmospheric to full exhauster capacity. A matrix of total pressure versus exhaust pressure was generated prior to each run to optimize the time to record data and to identify the set points for each run. Typically, total nozzle pressure, PT8, was set at the prescribed value; exhaust plenum pressure, P14, was established; a manual code was input into the computer to order data acquisition. Back

pressure, P14, was then stepped a predetermined amount and the process repeated until exhauster limits were reached. Total pressure was then advanced and the cycle repeated. Setting the secondary air flow to a given fraction of the primary air flow required an iterative process of controlling both flows because of their common supply. This required an inordinate amount of time and was not done. Instead, the secondary flow was incremented when desired. If additional data was required a dedicated run for secondary flow was contemplated.

Repeatability of the data was challenged both on a random basis through the course of a test sequence and on separate dates to establish the limits of experimental uncertainty. Leakage checks were conducted prior to and during the course of each test.

V. DISCUSSION OF RESULTS

As established in response to the work definition provided by the sponsor, the goal of the study was to design, fabricate and test a cold flow model of the NAPC Test Facility for further utilization in testing alternative diffuser geometries. Detailed objectives were:

1. Model the NAPC test facility using Mach number similitude and scaled geometry.
2. Design/construct the model to allow for the greatest variation in test parameters.
3. Model a representative set of engines spanning the operating extremes of the actual test cells being studied.
4. Establish a data base against which alternative geometries may be compared and provide a basis of comparison.
5. Quantify and interpret the controlling parameters which influence diffuser efficiency as a prelude to alternate geometry proposals.
6. Provide a conceptual model(s) from which the second phase of the study may proceed.
7. Specifically evaluate cross sectional variations in the straight tube diffuser to improve range and/or efficiency when testing the F404 engine.
8. Explore overall systems efficiency considerations in the context of new design initiatives.

A. MODEL DESIGN/CONSTRUCTION

The model was designed as detailed in Appendix A. The success of the design/construction process is measured only in subjective terms. The parent facility as detailed in Appendix C did not possess the scope of instrumentation to provide a characteristic mapping which would allow a direct comparison. The operating variables, exhaust pressure/cell pressure ratio and nozzle total pressure/cell pressure ratio as shown in Figures 20 and 21, did, however, follow theory and closely match the general shape and bounds of model data provided by NAPC. The full scale facility performance will be different from that of the model due to thermal variations, leakage, working gas, surface roughness and machinery support structure. Having satisfied Mach number and geometric similitude it was reasonable to assume any substantive improvements in performance observed from model studies should translate well to the parent facility.

The maximum altitude achievable by the design was approximately 45,000 feet. The total pressure limitation of the Allis Chalmers was the dominant factor in this regard. Figures 21a and 22 show started operation of the ejector-diffuser only with the TF30 and F404 in the afterburning mode. This altitude limitation also derives from the need to scale according to the largest engine. This limitation will obviously preclude a full determination of the useable feasible range of new geometries. This limitation may also mask some benefits of new geometries thus resulting in a

more conservative estimate of performance than what might occur in practice.

B. ENGINE DESIGN

The test engines chosen were the TF30 and F404 whose characteristics were noted in Appendix C. The afterburning mode of the TF30 was utilized as the set point for the match with the compressor. A top end mass flow, with the TF30 in A/B, of 1.863 lbm/sec was expected and a maximum of 1.75 lbm/sec was observed. Precise measurements of the final nozzle diameters indicates an error of less than \pm to 1 percent in the area ratios between planning estimates and the machined product. The engine design should thus provide over 95% coverage of the operating range of the parent facility.

C. DATA BASE

The 2.71 inch scaled straight ejector-diffuser was established as the baseline diffuser against which alternative geometries may be contrasted. A non dimensional graphical representation was chosen as a preliminary method to interpret the test results. A gross survey of ejector-diffuser performance, under the influence of a parametric change relative to the baseline, can be readily observed. A detailed investigation may then be ordered to quantify any observable improvements in ejector-diffuser performance. Ideally, a real time performance map versus the baseline should be incorporated into the data acquisition package to

allow an interactive optimization during new geometry testing. Figures 23 and 24 are categorized as the baseline for each engine tested. Improved performance will be evidenced by a relative displacement of any new curve vertically up and/or horizontally to the left. This equates to operating with higher pressure recovery for a given PT8/PS9 which are the input specifications of any test program. The influence of parametric variations made during this study are presented in this manner for illustration. While conveying no additional information, an alternative representation of the operating characteristic by PS9/PT8 versus PT8/P14 is exemplified by Figure 25.

D. PARAMETRIC VARIATIONS

1. A_e/A*

This ratio is a naturally varying parameter when afterburning engines are tested due to their variable exhaust geometry. In the F404 the ratio varies from 1.21 at IRP to 1.58 at maximum A/B. In the TF30, this variation ranges from 1.03 to 1.20. It was anticipated that, as A_e/A^* increased for a given diffuser geometry and nozzle total to cell pressure ratio, (PT8/PS9), pressure recovery would increase. The higher Mach number at the diffuser entrance would govern the increase. Table 5.1 illustrates this fact for two runs with the F404; Figure 26 graphically conveys the same information.

Table 5.1

Engine	F404 Non A/B	F404 A/B
Run No.	24	29
PT8/PS9	11.84	11.85
P14/PS9	3.045	4.119

The operating envelope for any variable geometry engine necessitates that testing must span a broad range of power levels. As power is adjusted from IRP to maximum afterburner the exhaust to throat area ratio varies widely. Figure 23, for the F404, and Figure 24, for the TF30, illustrate that for a fixed nozzle total to cell pressure ratio, the exhauster requirements decrease in response to better pressure recovery. The proportion, in which the pressure recovery increase occurs, appears characteristic of the engine-ejector-diffuser match achieved by the design. The F404 full scale ejector diffuser combination shows less variation than the more closely matched TF30 full scale combination. Similarly, to maintain altitude while testing from IRP to max A/B the exhauster must also vary its operating set point to accommodate the varying demand. When a single test cell configuration must accommodate testing more than one class of engine, significant complications are introduced into achieving a near optimum design. Any retrofit of the parent facility must detail how the new geometry accommodates this parameter.

2. Secondary Flow

Secondary flow is injected into the test cell as a cooling medium for the engine. The added mass saps performance from the diffuser as a pressure recovery device. The diffuser entrains the additional low velocity, low energy flow with that of the high energy jet under complex flow conditions requiring greater exhaust work to sustain cell pressures. The postulate in the case of secondary flow is that, for a given nozzle total pressure and a given exhaust pressure, injection of secondary air increases the cell pressure. Secondary flow will result in a lowering of PT8/PS9 or, conversely, less efficient pressure recovery. The experimental results are strongly supportive of this statement. As shown in Figure 27, the operating curve shifts lower as losses increase at the price of mass ejection.

A detailed study of secondary effects, using the F404 in A/B with the 2/3 and full scale diffuser, was conducted as follows. Nozzle total to cell pressure ratio (PT8/PS9) was fixed while secondary flow was gradually increased. Table 5.2 for the full scale shows only minor variation in pressure recovery for typical amounts of secondary flow. Large amounts of secondary flow have a more adverse impact but this is purely of academic interest as 8 percent secondary represents an upper bound on practical cooling requirements. In marked contrast, the performance of the F404 and the two-thirds diffuser suffers a significant penalty in pressure recovery. Table 5.3 and Figure 28 detail this observation.

Table 5.2

Engine	F404 A/B	F404 A/B
% \dot{m}_s	0	8
Run	47	46
PT8/PS9	7.58	7.56
P14/PS9	1.951	1.939

Table 5.3

Engine	F404 A/B	F404 A/B
% \dot{m}_s	0	4
Run	30	2
PT8/PS9	12.71	12.75
P14/PS9	4.265	3.257

Expenditure of exhauster power will be required to achieve the same pressure in the presence of the added mass. A nonlinear variation in the loss of PT8/PS9 is anticipated due to the complex nature of mixing subsonic and supersonic streams. The two-thirds diffuser, having an L/D which more nearly matches the optimum suggested in the literature, more efficiently recovers pressure. This suggests that secondary flow effects become more prominent as the diffuser design becomes more efficient. The penalties in power consumption due to secondary flow effects are not linear, and this

observation results in wide variations in systems efficiency as discussed in Section F.

3. AD/A*

In applying the Law of Continuity to the nozzle-cell-diffuser, a minimum diffuser area may be determined. The minimum area in a diffuser is specified by $A_d = A^* p_{oy}/p_{ox}$ where p_{oy}/p_{ox} is the stagnation pressure ratio for a shock diffuser entrance Mach number. Allowing for an expansion to Mach 3.0 in the diffuser, A_d (min) ranges from A^* to $3.04A^*$. Matching the engine to diffuser permits upward variation in A_d from $6.67 \text{ (in}^2\text{)}$ for the TF30 and $1.93 \text{ (in}^2\text{)}$ for the F404. The full scale A_d is $5.768 \text{ (in}^2\text{)}$ which is below the minimum for the TF30 but lower Mach numbers are experienced with this engine. Optimum performance for constant area diffusers, from original model studies reported by NAPC, ranges from $Ad/A^* = 3.5$ to 4.0 . Neither of the engine extremes approaches this ratio with the TF30 being more closely matched while the F404 is undersized. As Ad/A^* was varied from full scale to two-thirds, performance improved dramatically as can be seen in Figure 29. An Ad/A^* of $6 - 7.5$ appears to bound the gains in performance for the F404 A/B. An A_d of $2.5 \text{ (in}^2\text{)}$ for the F404 should result in near optimal performance. No conclusions may be drawn for the non A/B case since improved performance occurs at the limit of Ad/A^* tested. Static wall pressure profiles as shown in Figure 30 depict the observable changes as Ad/A^* is varied from full scale to two-thirds for a fixed driving potential.

E. F404 IMPROVEMENT

The foregoing discussions have alluded to improvements in the F404 performance with variation in diffuser cross section, A_d . An A_d/A^* between 6 and 7.5 appears optimal in that the two-thirds and five-sixths reductions improve pressure recovery at all power settings. These diffusers can also achieve lower altitudes than the full scale, if that is the objective. Full scale attains 25,800 feet while two-thirds and five-sixths achieve 40,250 and 43,400 feet, respectively. The two-thirds, as shown in Figure 31, is capable of fully started operation despite the constraints on driving potential observed in this test facility. The gain in efficiency should be significant as previously noted in Table 5.1. The exhauster can operate at higher pressures for the same cell pressure, an obvious advantage. A ceiling on the potential gains cannot be ascertained from the available data. As an example, the F404 in the non A/B mode for a PT8/PS9 of 6.6 would require a P14/PS9 of 1.5 for the full scale, 1.75 with the five-sixths and 2.05 for two-thirds. This permits a near doubling of exhaust pressure while maintaining cell pressure at test conditions. The F404 in the A/B mode for a near constant PT8/PS9 shows the same results. Figure 30 also shows recovery occurs earlier with fewer losses in the two-thirds diffuser. The five-sixths and full scale attain different levels of diffusion but clearly greater work must be performed with the full scale diffuser.

In the course of the detailed investigation, both the two-thirds and five-sixths configurations were terminated in an abrupt expansion to maintain a near equivalence in L/D. Two additional tests were conducted with tapered afterbodies, Figures 9a and 9b, to capitalize on subsonic diffusion. Both modes of F404 operation were tested and as expected diffusion is improved, as shown in Figures 32 and 33. The improvement at lower PT8/PS9 is barely distinguishable but shows distinct gains at higher levels. Since the tests were conducted on different dates, precise quantification was not attempted. The use of some geometry to enhance subsonic diffusion, such as the taper afterbody, merits consideration in any retrofit proposal.

F. SYSTEMS EFFICIENCY

The complexity of the diffusion process makes the task of measuring the cost benefit of a design change a subtly challenging endeavor. The gains derived from a geometric change must be integrated over the test cycle for each engine. A typical jet engine test represents a non steady state problem where the time at a given power level becomes a significant factor when evaluating power consumption costs. Assuming testing only at discrete power settings, the cost of testing at each setting can be placed on a cost/unit time basis and total cost summed by integrating over the time interval for the test.

The efficiency of the system includes not only the ejector-diffuser but must reflect the efficiency aspects of the exhaust heat exchanger, the exhaust control valves and exhausters themselves. It is postulated that only one match of test conditions and these system components exists. A shift off design as prompted by new flow conditions such as higher power or secondary flow will dramatically influence overall power consumption since it is in direct proportion to the individual efficiencies of each component. An illustration, utilizing a much simplified model for the generalized case of testing with secondary flow and, making an allowance for auxiliary exhaustion of the secondary, provides a simple cost basing example. The test set up is as shown in Figure 36. An energy balance across a simple fan is utilized in this case for illustration only. The total work done by the fan per pound of working substance is H_t where

$$H_t = \frac{P_2}{\rho} - \frac{P_1}{\rho} + \frac{V_2^2}{2g_c} - \frac{V_1^2}{2g_c} + z_2 - z_1$$

which reduces for $\Delta Z = 0$ to

$$H_t = \frac{P_{02} - P_{01}}{\rho}$$

Fan total efficiency is often expressed as the ratio of the work done on the gas divided by the input shaft work or:

$$\eta_f = \frac{C \times \dot{m} \times H_t}{kw} ; (C = \text{constant for unit consistency})$$

Fan efficiency as a function of capacity follows a general variation as shown in Figure 35.

As operation shifts off design in either direction efficiency decreases substantially. Testing engines not properly matched must pay severe penalties in the cost of power consumption. Added mass alone provides a proportion increase as well. Capacity is observed to vary with the speed of a fan, static pressure with speed squared and required power with speed cubed.

The cost per lbm is equal to

$$\frac{Kw}{\dot{m}} = \frac{C \times (P_{02} - P_{01})}{\rho \eta_f}$$

An auxillary ejector employed solely to remove secondary flow must operate between cell pressure and something close to atmospheric. The cost per lbm for an auxiliary ejector would follow a similar discussion and may be described as

$$\frac{\text{Power (kw)}}{\dot{m}_s} = \frac{P_{atm} - P_{cell}}{\rho \eta_{aej}}$$

The combined work for the system to be more efficient must be less than the work of the original system without the auxiliary. Optimizing on a cost basis thus becomes quite

complex. As observed, with an oversized diffuser, the system pays little penalty in terms of pressure (PS9) for exhausting secondary flow. The added mass does, however, exact a direct cost from capacity considerations. A properly matched diffuser will cause a shift of the exhauster to an even less efficient setting and higher attendant costs. Similarly, the IRP testing setting pays a lower price in the presence of secondary flow than maximum A/B. The time factor then becomes crucial to assess total cost. An efficient auxiliary ejector could, coupled with a matched ejector-diffuser, markedly improve overall efficiency by eliminating extreme fluctuations in diffuser efficiency and in turn controlling the variations in the time the exhauster must spend off design.

In the absence of an auxiliary ejector, testing philosophy alone could be altered to improve efficiency. If the time intervals at a test condition (i.e., IRP) are of sufficient duration, consideration could be given to reconfiguring the cell for each major power level with a more closely matched diffuser. This could be accomplished by designing a series of pre-sized liners which could be inserted in the full scale diffuser.

VI. CONCLUSIONS AND RECOMMENDATIONS

A. CONCLUSIONS

1. The cold flow ejector diffuser model developed within the context of the study provides a versatile, although specifically tailored test bed, upon which geometric variations of the parent test facility may be experimentally evaluated.

2. A complex interdependency of geometric parameters which influence the pressure recovery mechanism exists. New designs should, therefore, attempt to incorporate as many degrees of freedom as practicable to allow optimization of the pressure recovery process.

3. When designing retrofits against a baseline model a real time graphical presentation of the performance curves, for old versus new, will enhance optimization by allowing the results to direct the conduct of the investigation.

4. Substantial improvements in pressure recovery when testing the F404 engine can be achieved through an alteration of the length to diameter ratio of the constant area ejector diffuser currently in use.

B. RECOMMENDATIONS

1. Upon successful resolution of the variable area diffuser vibration phenomenon, modify the test facility to accommodate the phenomenon and map the performance of that diffuser.

2. Using the results of the combined constant area and variable area studies, design, construct and test alternative geometries.

3. Modify the test facility by adapting the test cell for a separately driven ejector and evaluate in greater detail the added mass effect.

4. Modify the test facility to receive its secondary air input from an external source to preclude cross talk between primary and secondary flows.

5. Explore the possibility of including Schlierin photography to aid the investigative process and better document the geometric influences of new diffuser concepts. This would permit a realistic interpretation of the boundary layer interactions.

6. Data acquisition must be upgraded to accommodate data transfer to the in-house IBM 3033. A dedicated phone line with modem would be the first initiative warranted. A real time feedback to help focus the investigation is strongly recommended.

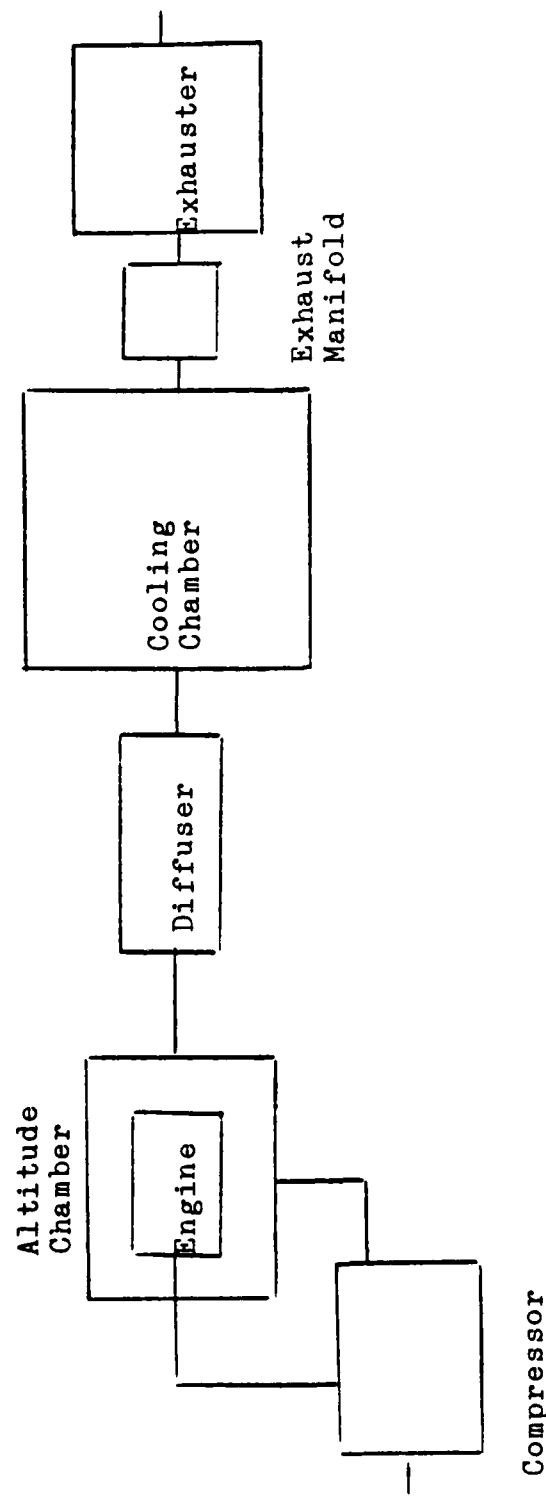


Figure 1. Typical Turbojet Test Cell

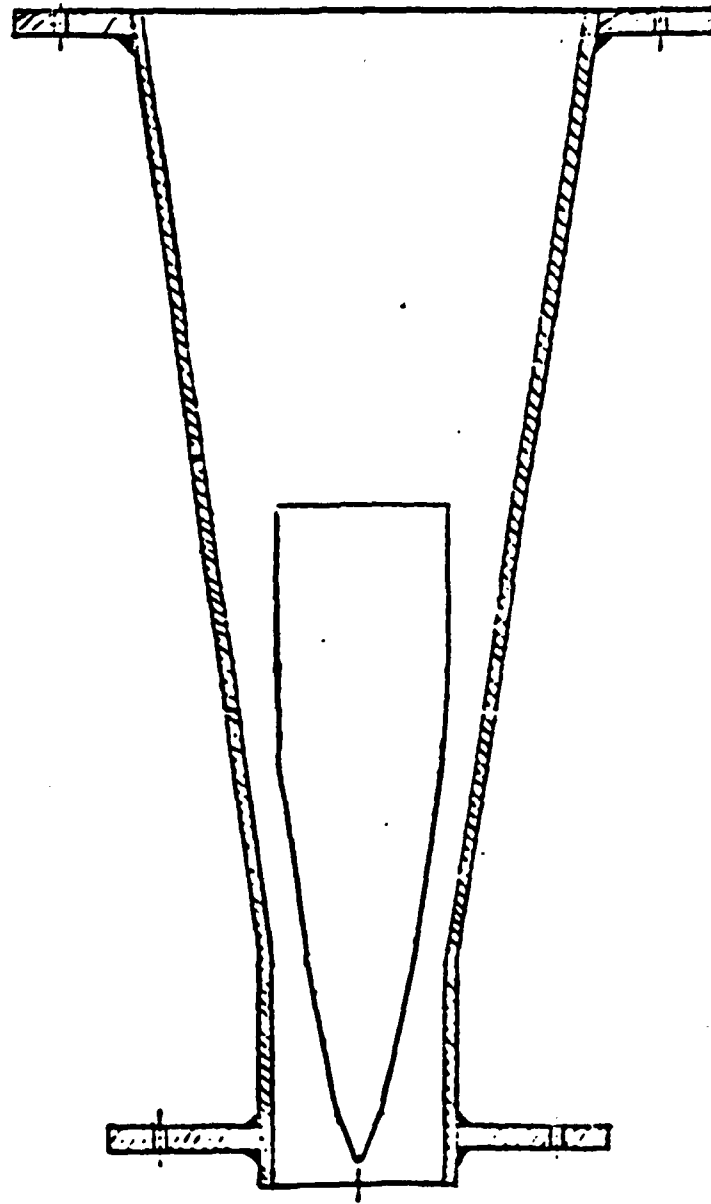


Figure 2. Variable Geometry Diffuser With Centerbody

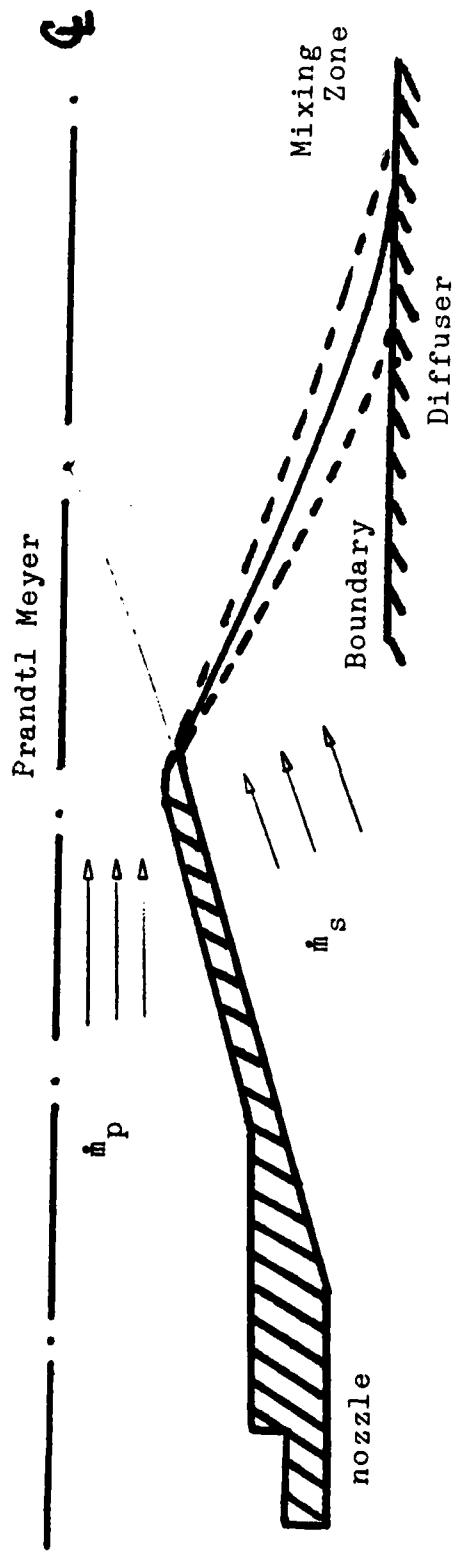


Figure 3. Generalized Flow Characterization of Expanding Jet with Secondary Flow

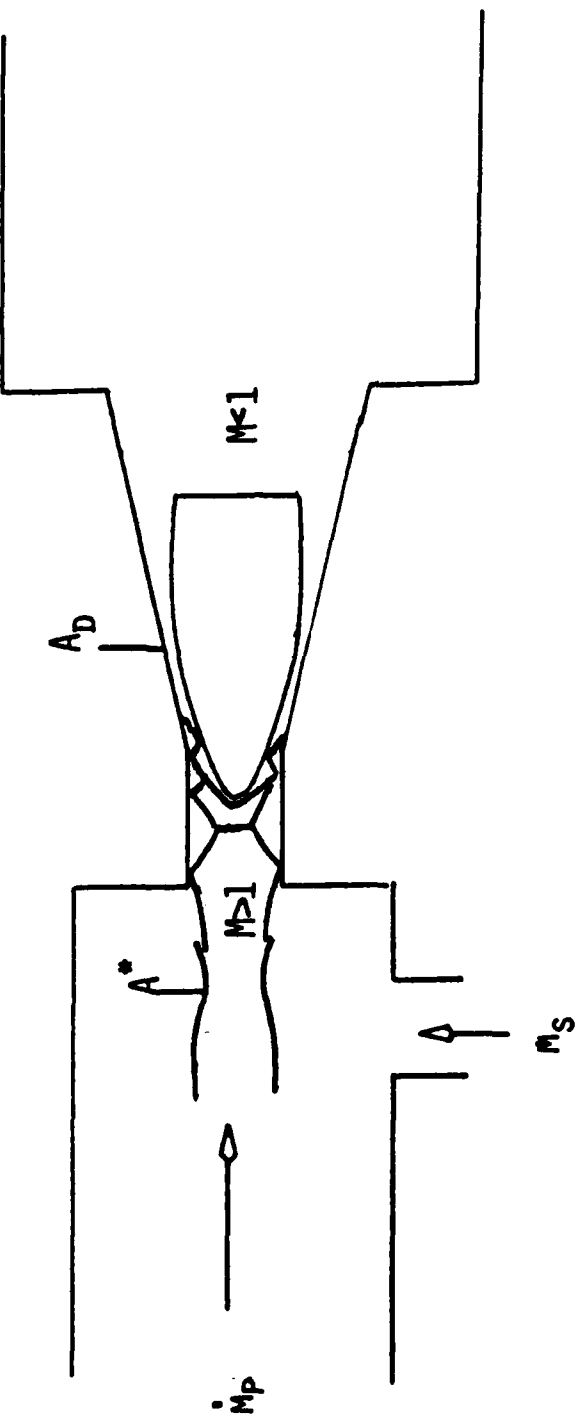


Figure 4. Simplified Test Cell

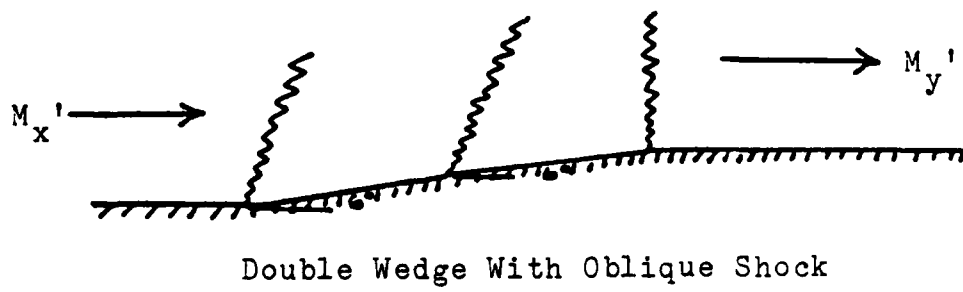
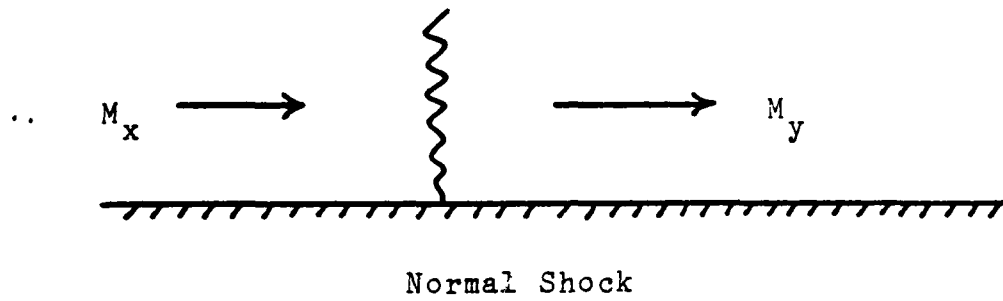


Figure 5. Shock Strength Model

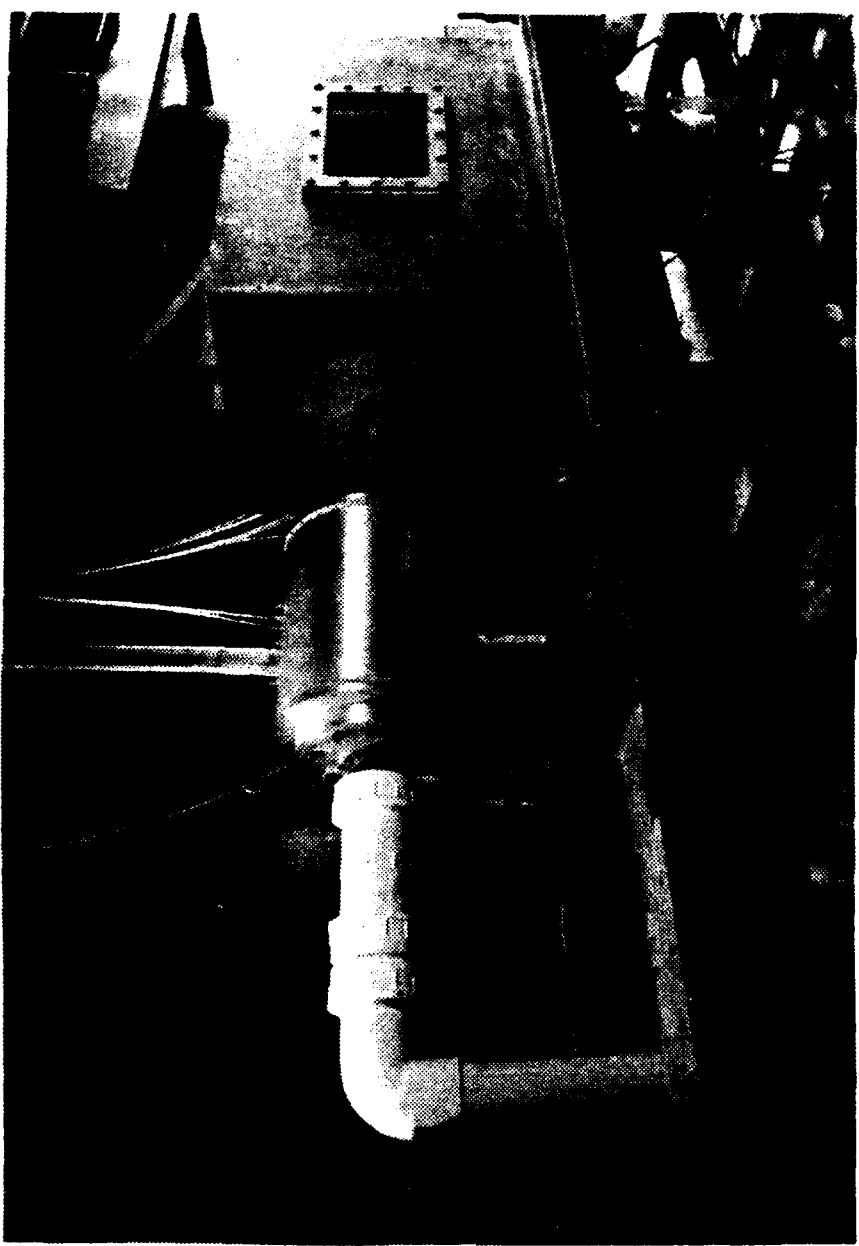


Figure 6. Scale Model Test Facility With Straight Tube Diffuser

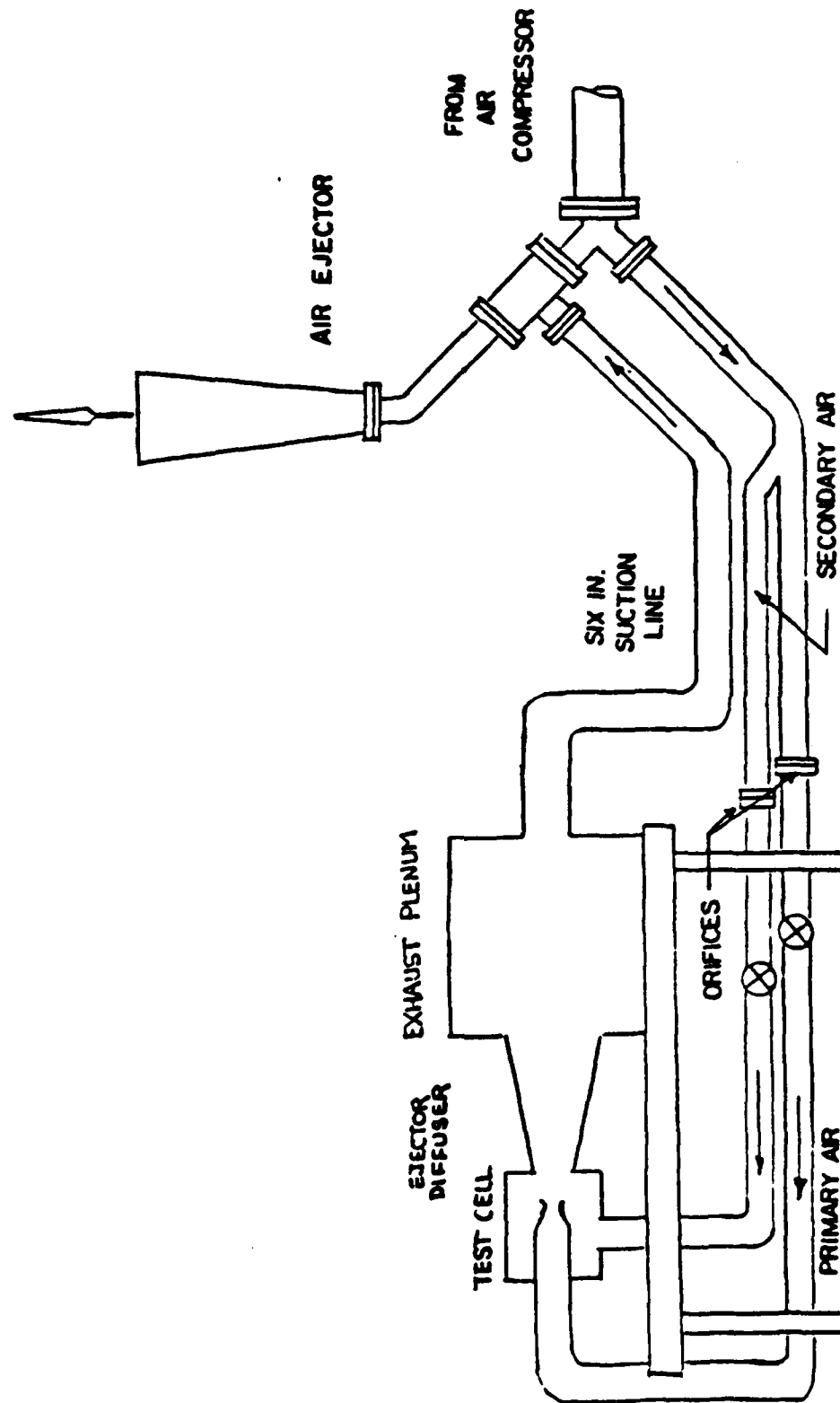


Figure 6a. Model Test Facility Schematic

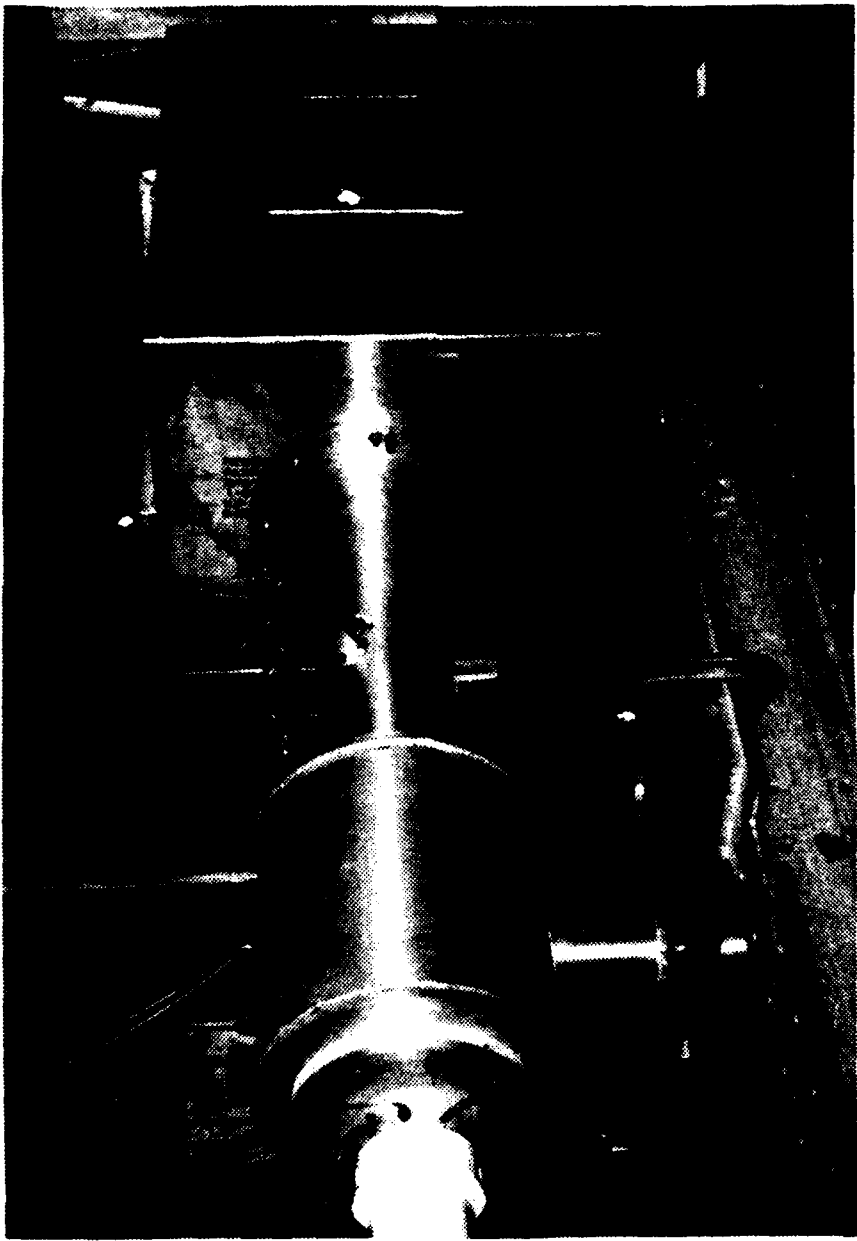


Figure 7. Scale Model Test Cell With Variable Area Diffuser

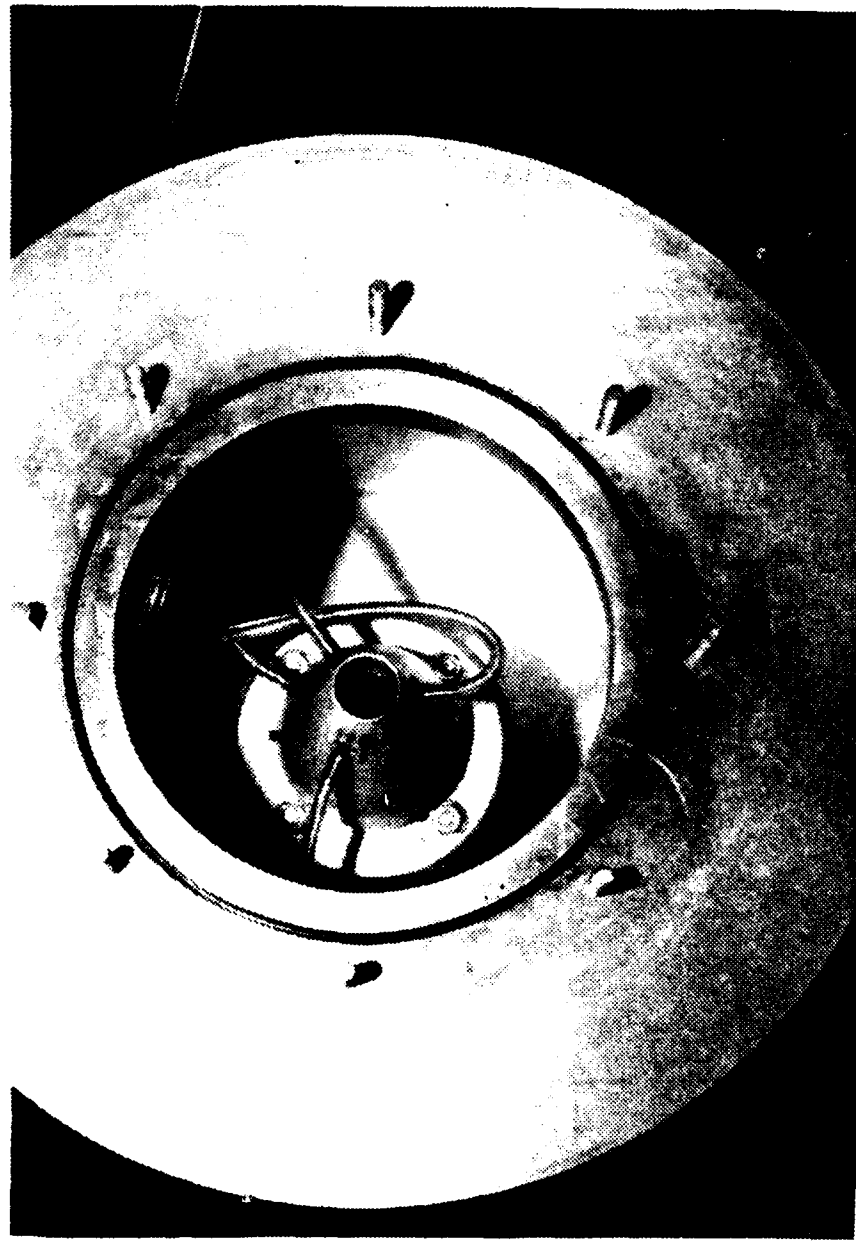


Figure 7a. F404 Engine Assembly

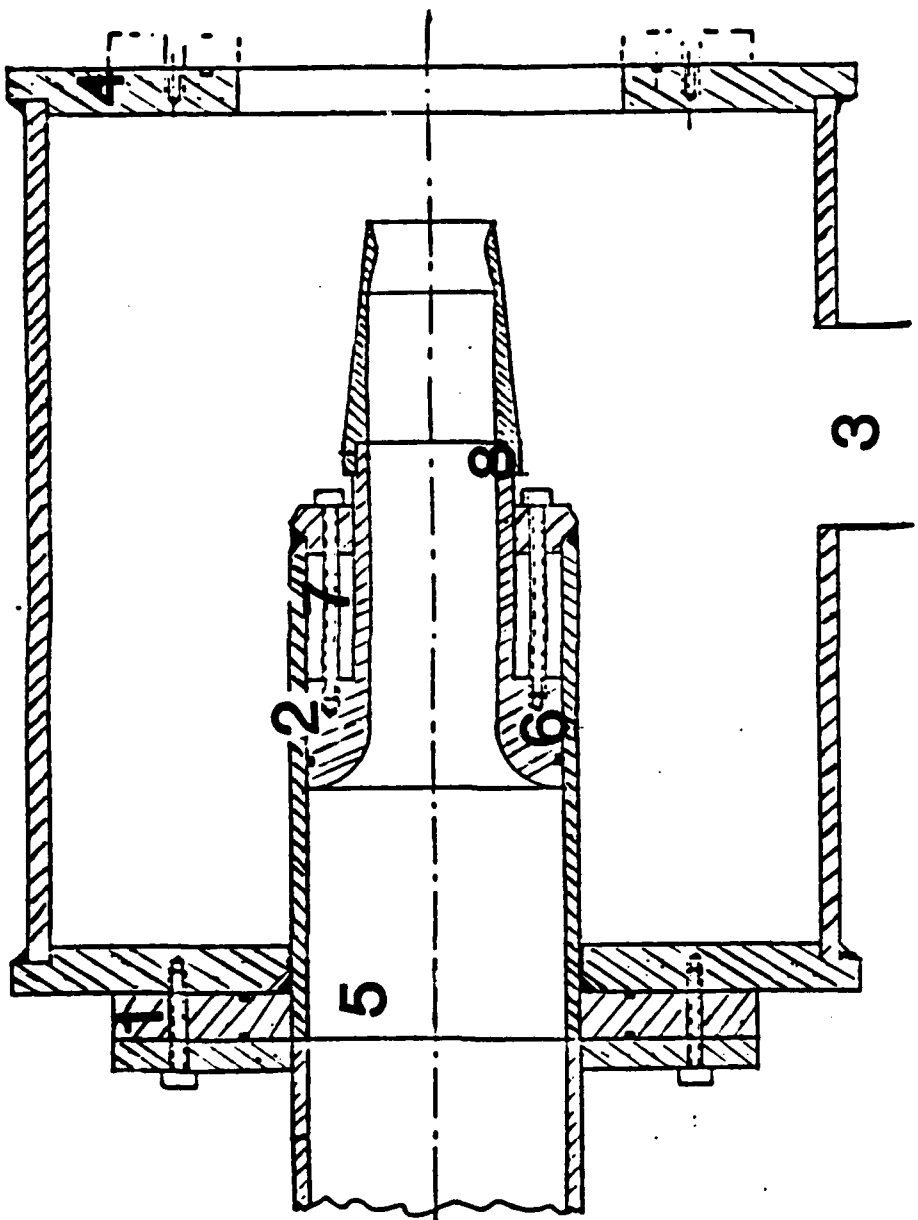


Figure 8. Test Cell Cross Section

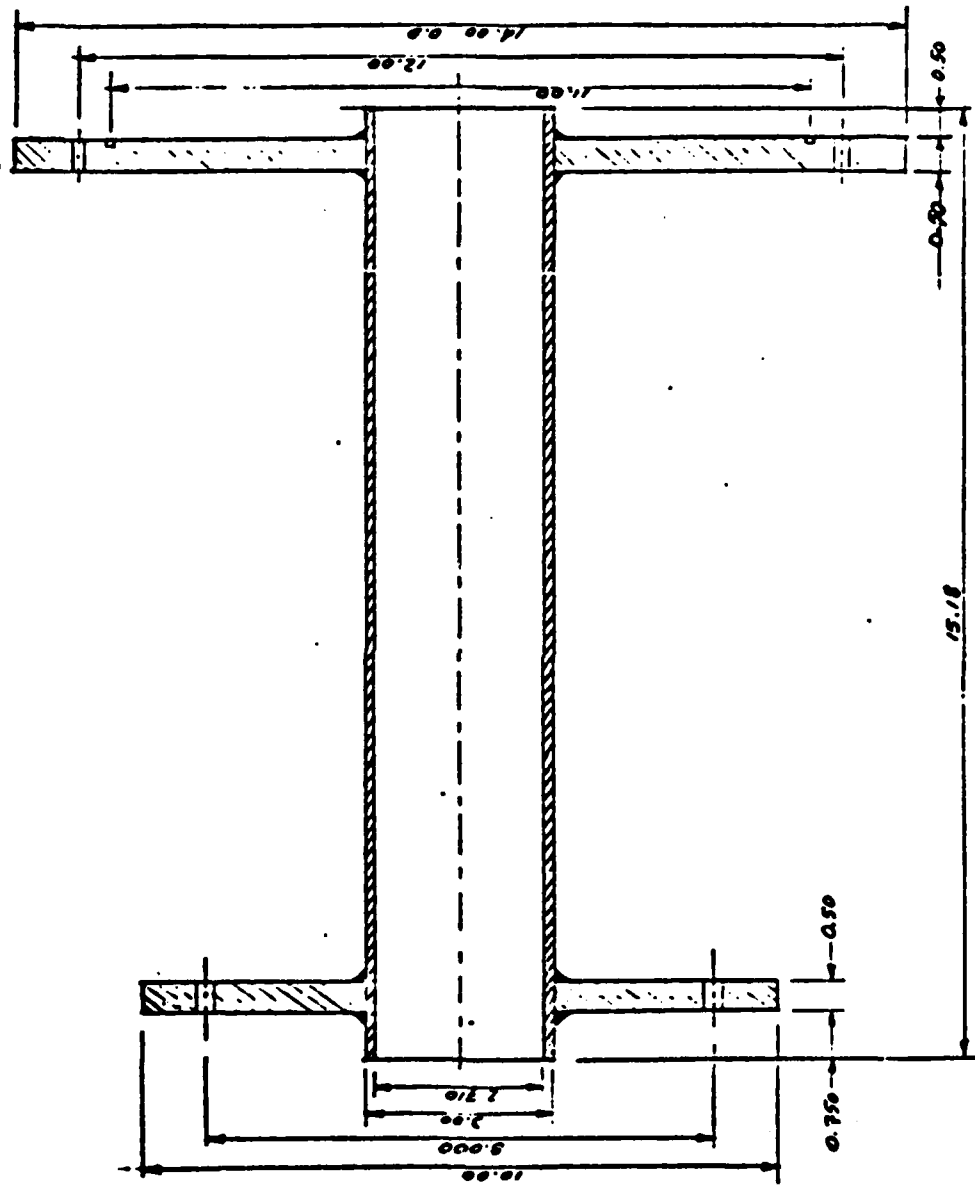


Figure 9. Straight Tube Diffuser (Full Scale)

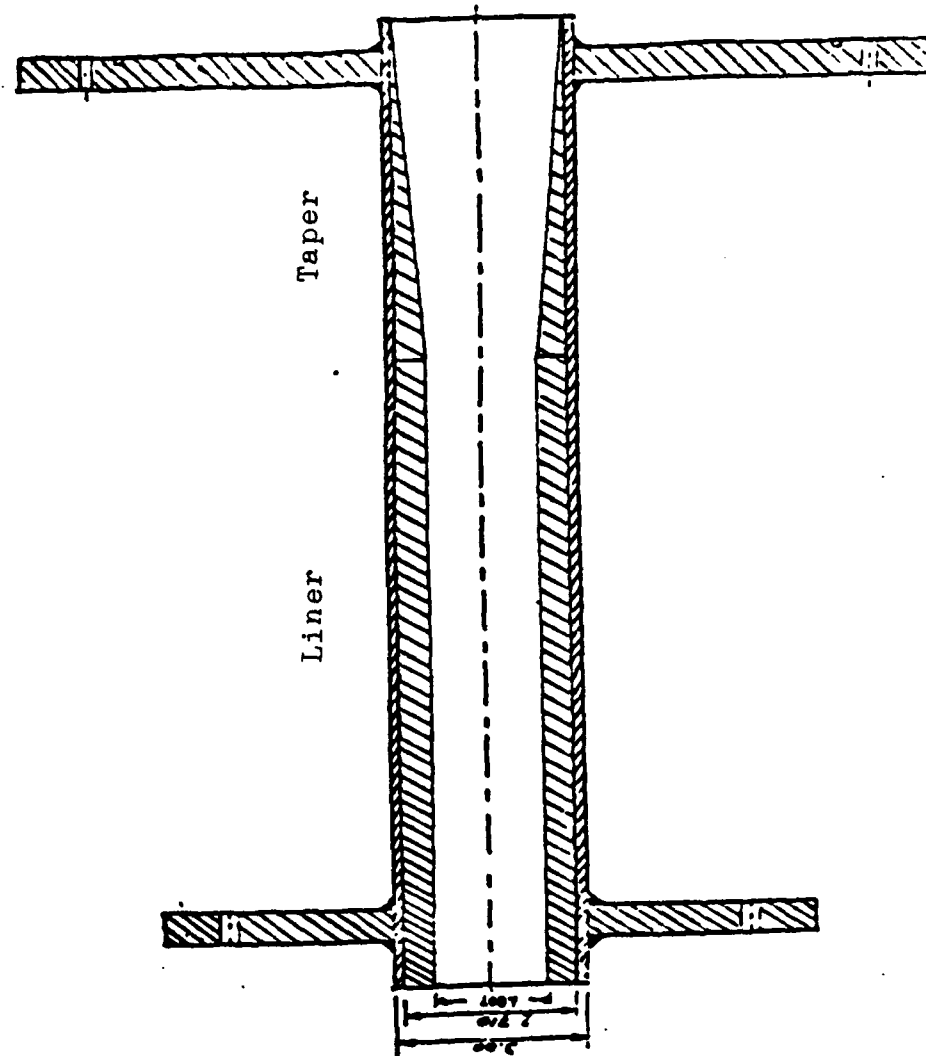


Figure 9a. Straight Tube Diffuser (Two-Thirds)

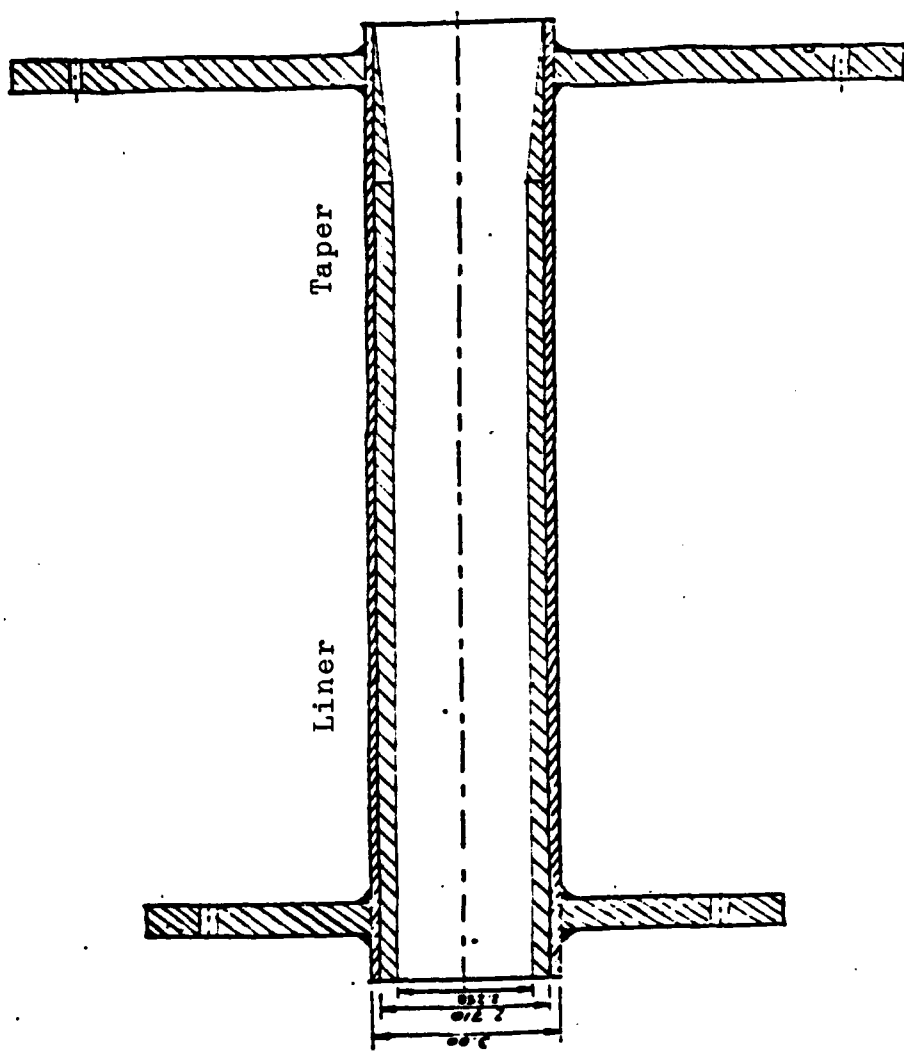


Figure 9b. Straight Tube Diffuser (Five Sixths)

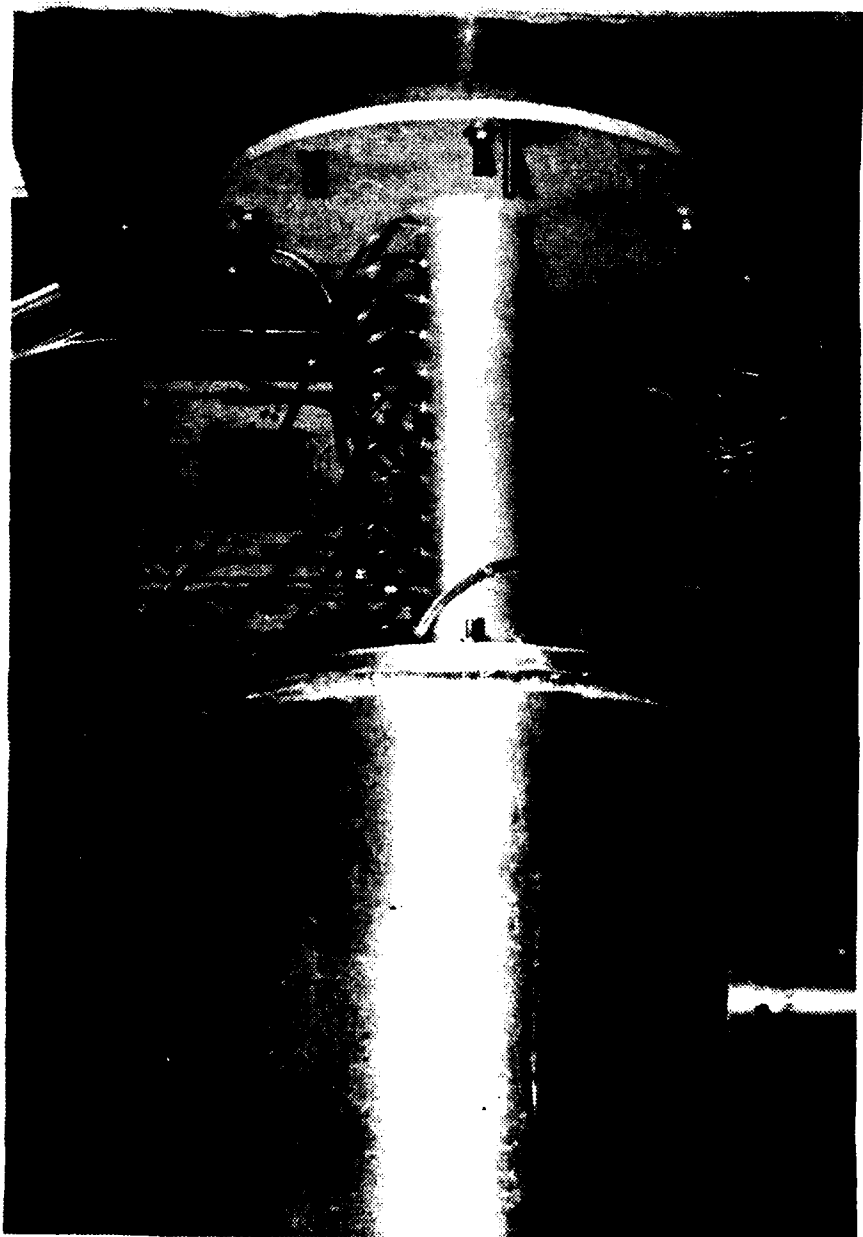


Figure 10. Pressure Tap Arrangement

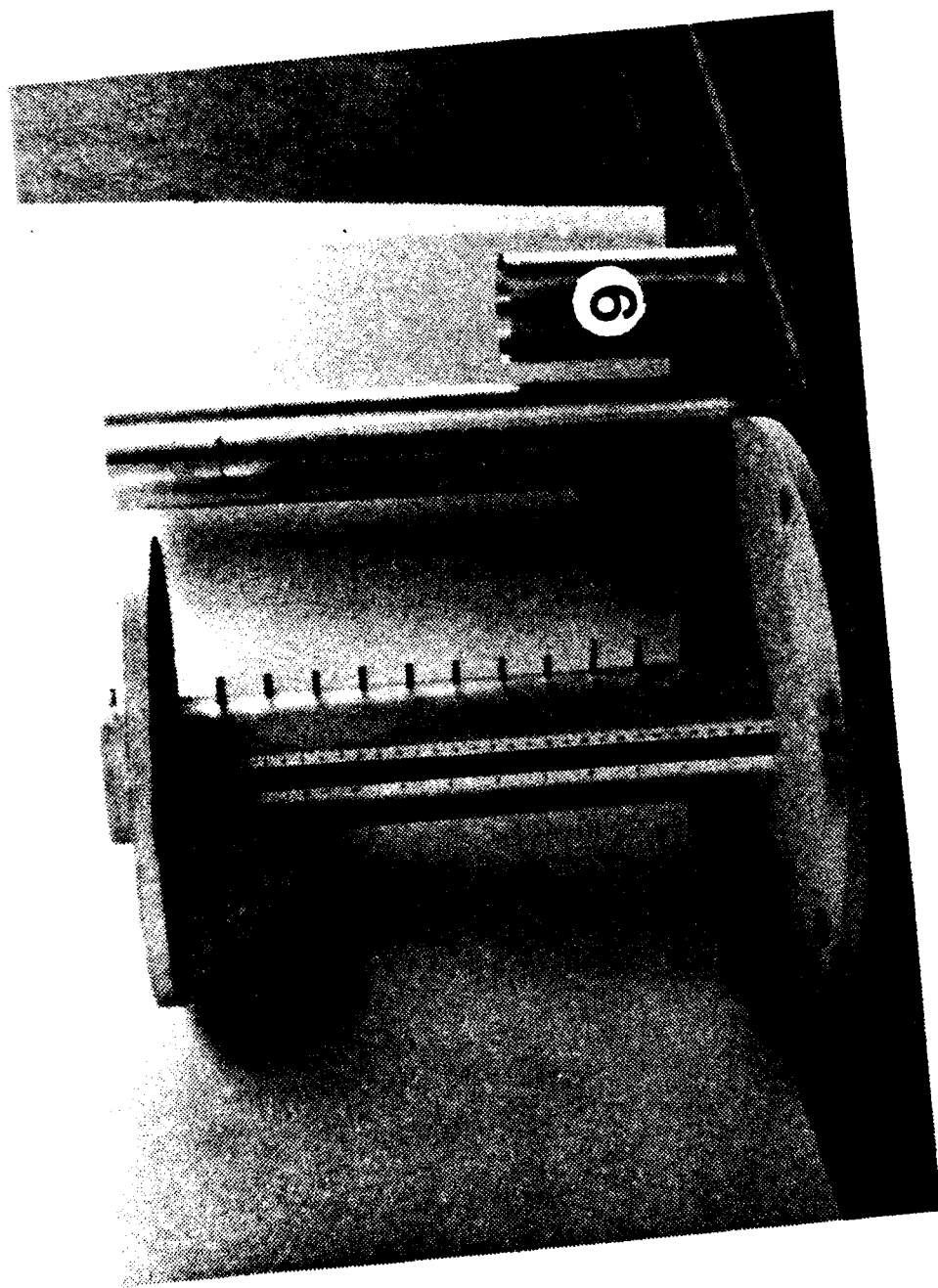


Figure 11. Constant Area Diffuser With Inserts



Figure 12. Variable Area Diffuser Exploded View



Figure 13. Remotedly Operated Drive Mechanism



Figure 14. Pressure Taps (Variable Area Diffuser)

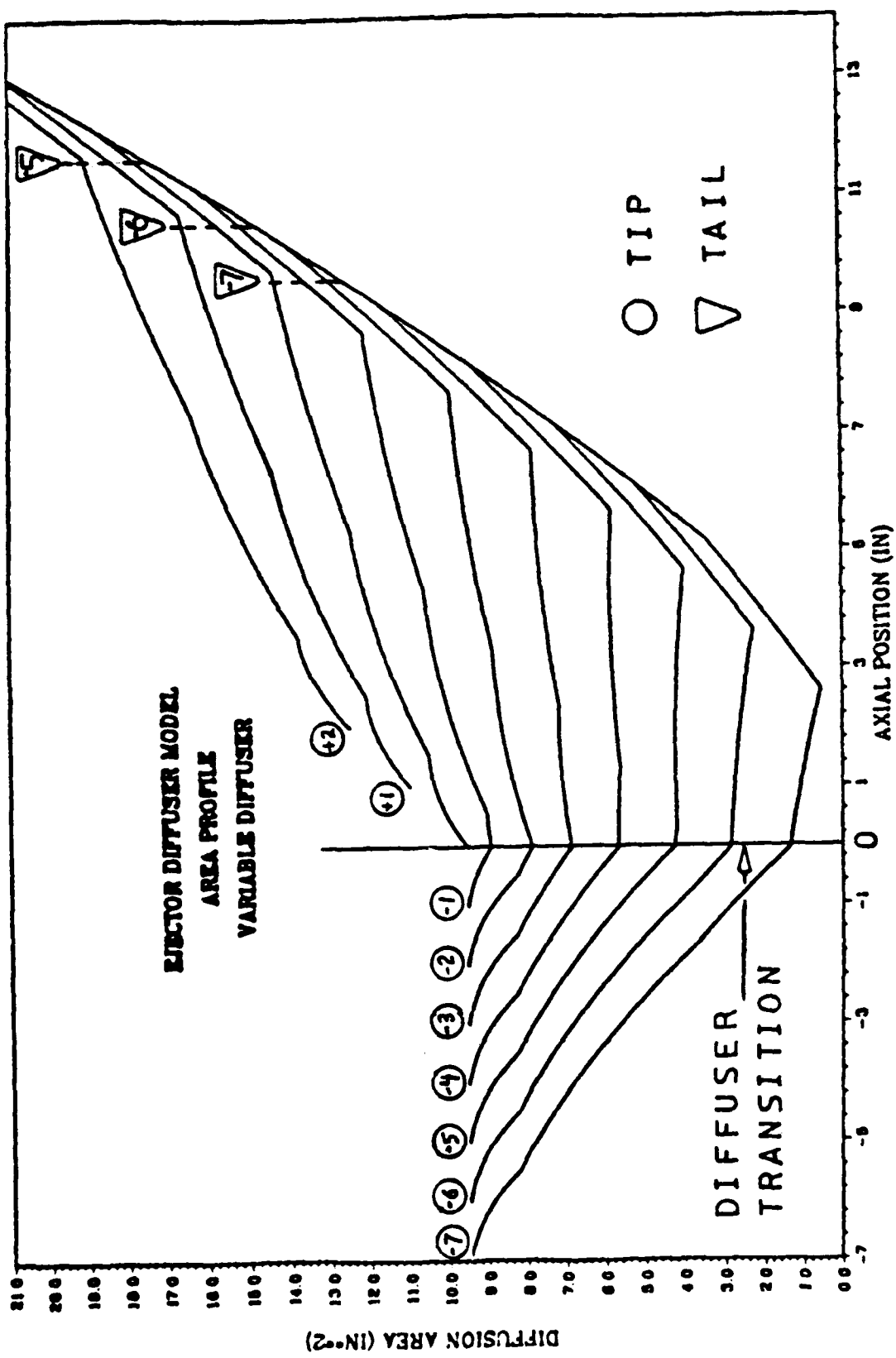


Figure 15. Variable Area Profile

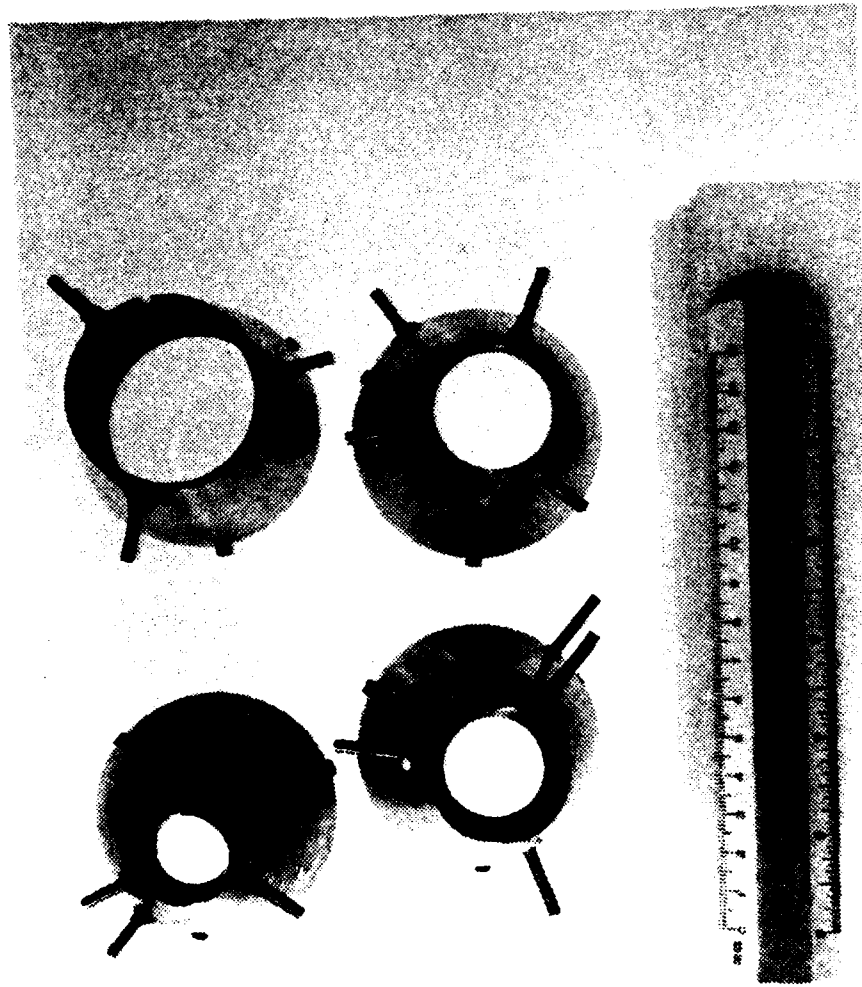


Figure 16. Test Engine Models

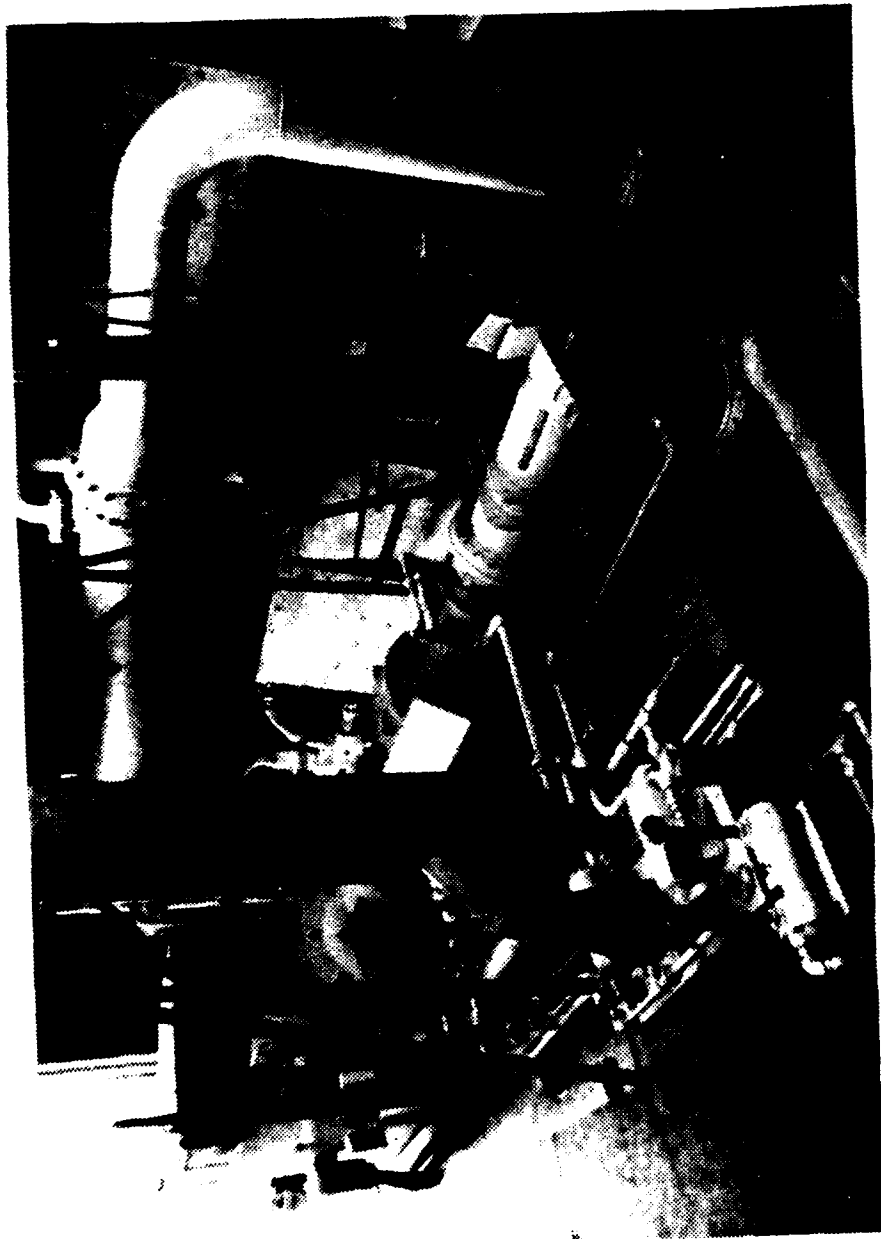


Figure 17. Allis Chalmers Twelve Stage Compressor

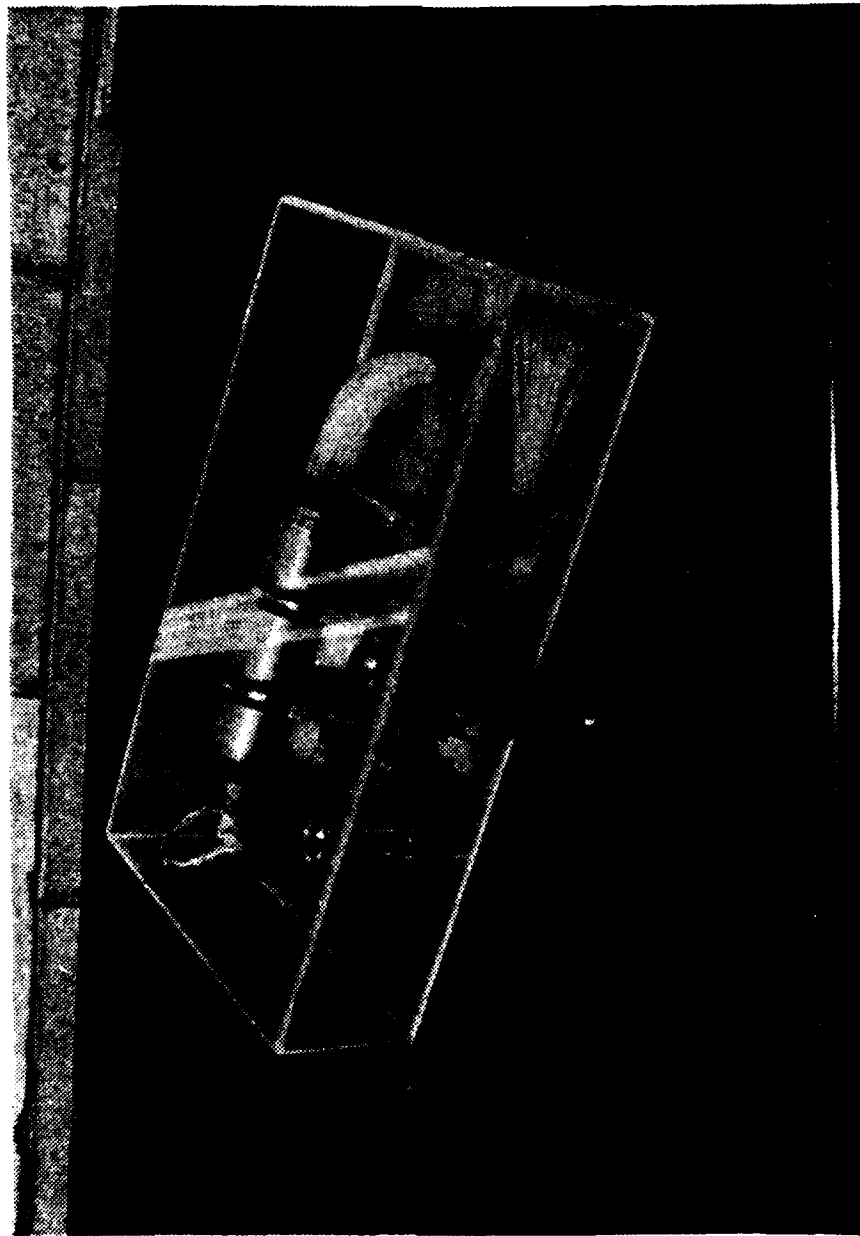


Figure 18. Scani valve pressure Scanner



Figure 19. Model Test Facility Remote Operating Station

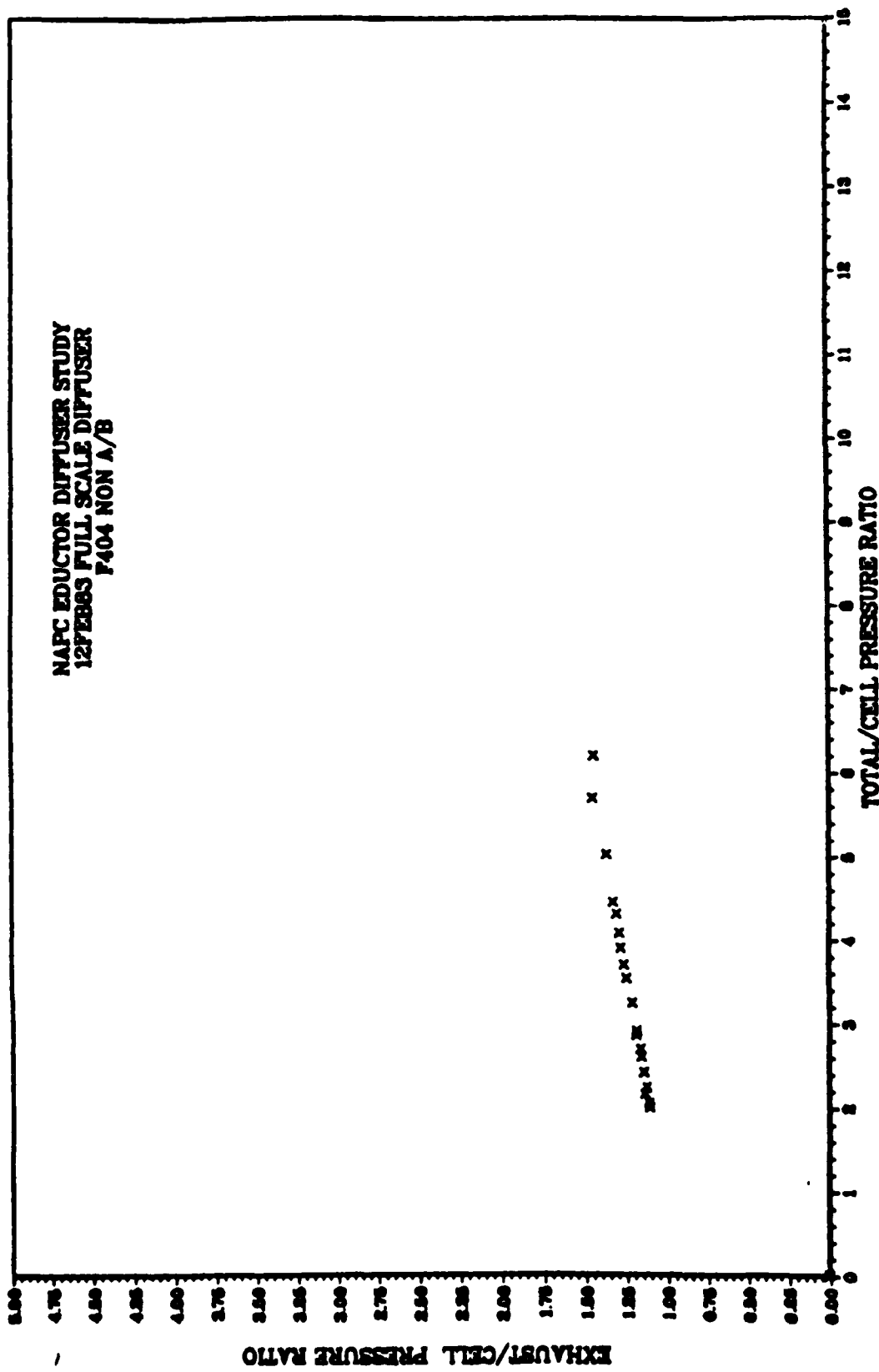


Figure 20. Operating Curve (F404 Non A/B)

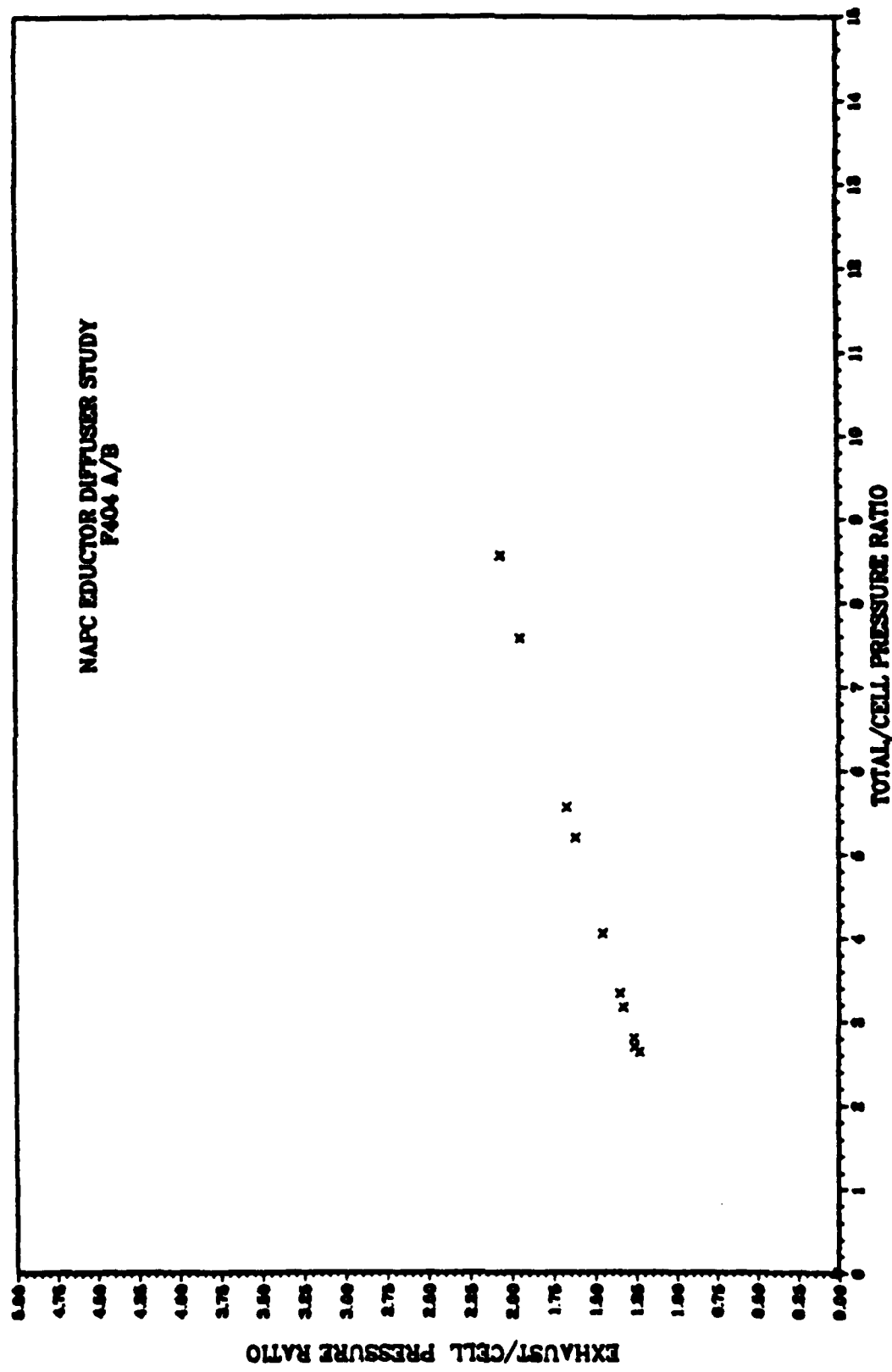


Figure 20a. Operating Curve (F404 A/B)

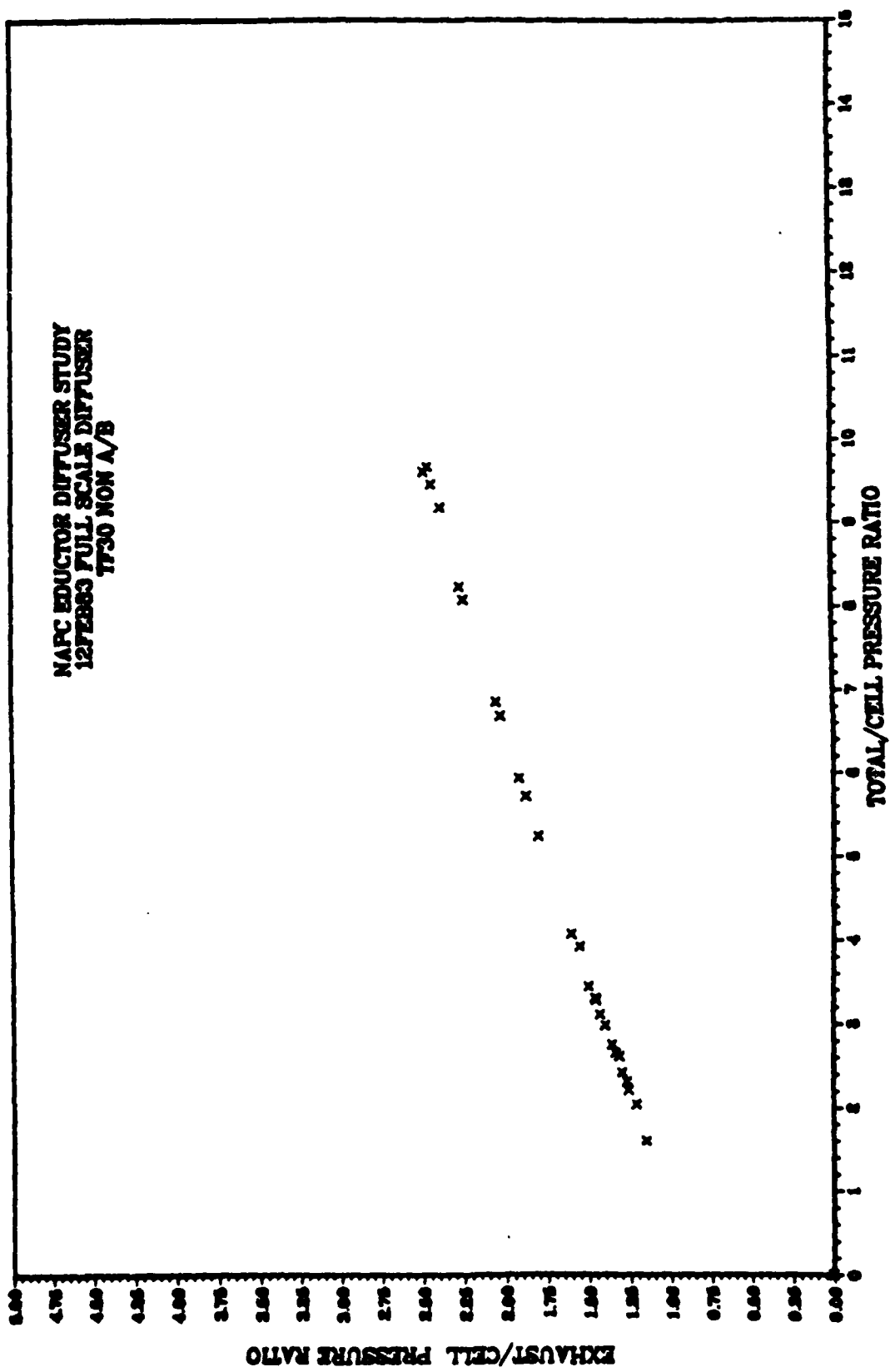


Figure 21. Operating Curve (TF30 Non A/B)

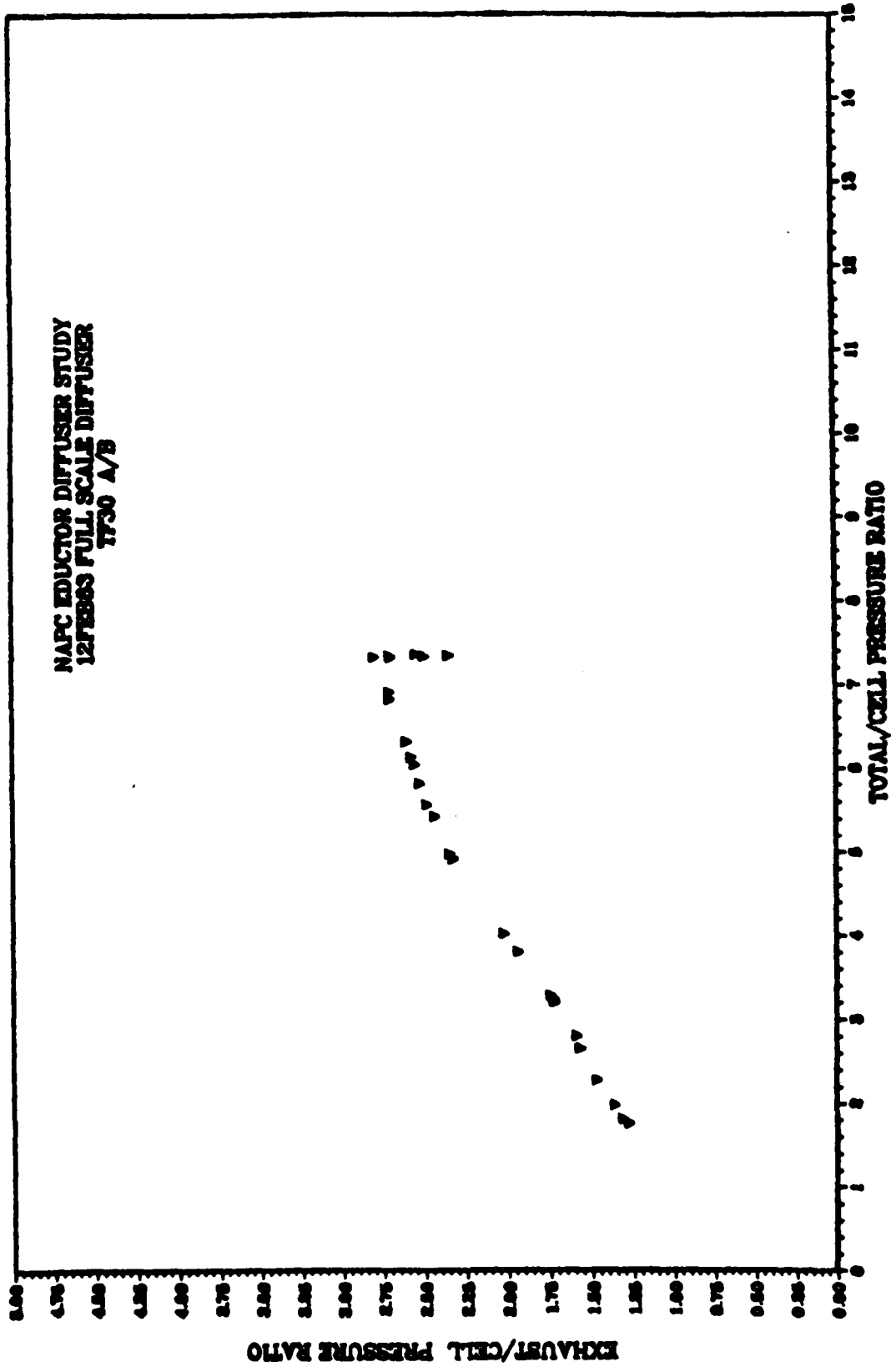


Figure 21a. Operating Curve (TF30 A/B)

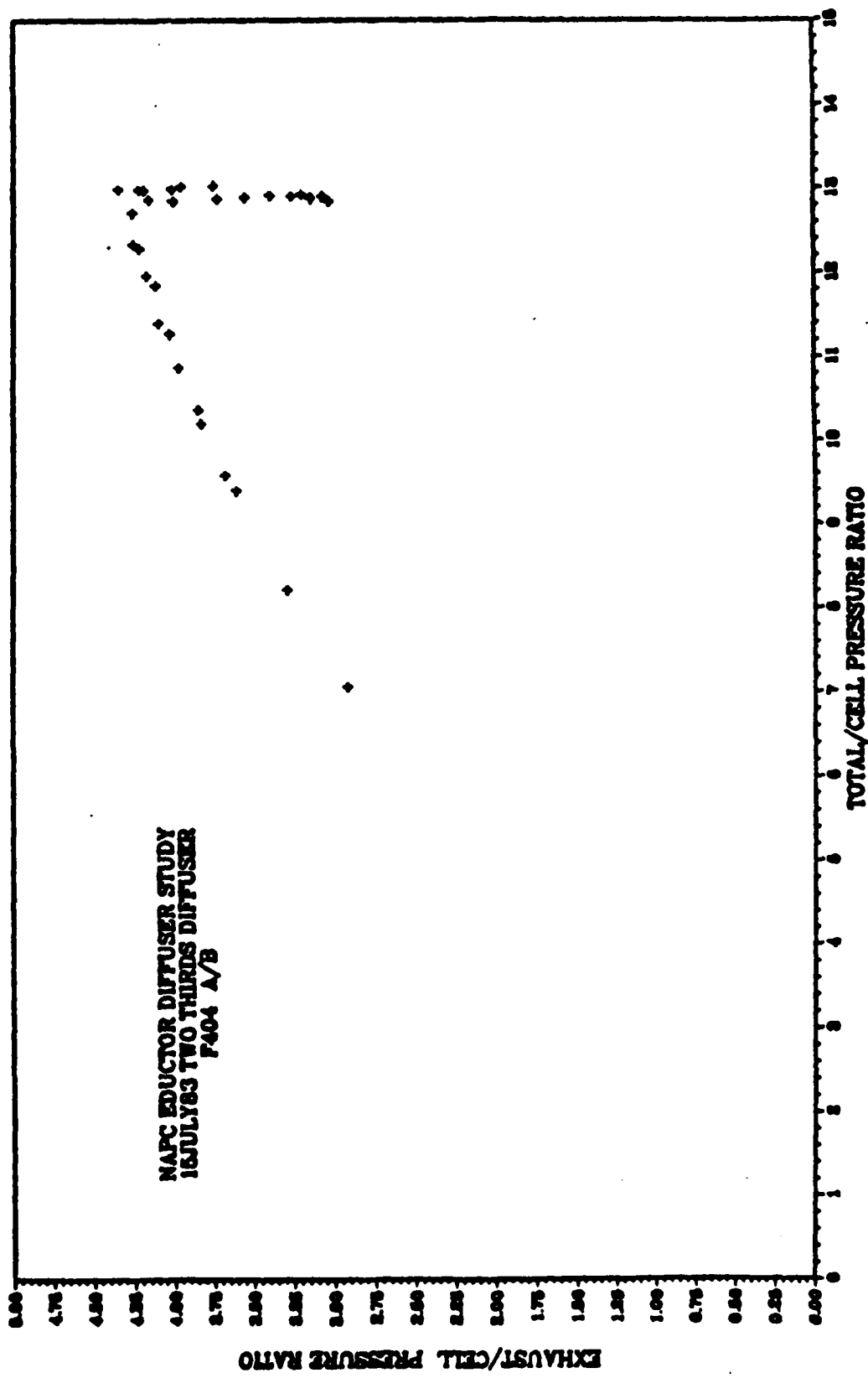


Figure 22. F404 Fully Started

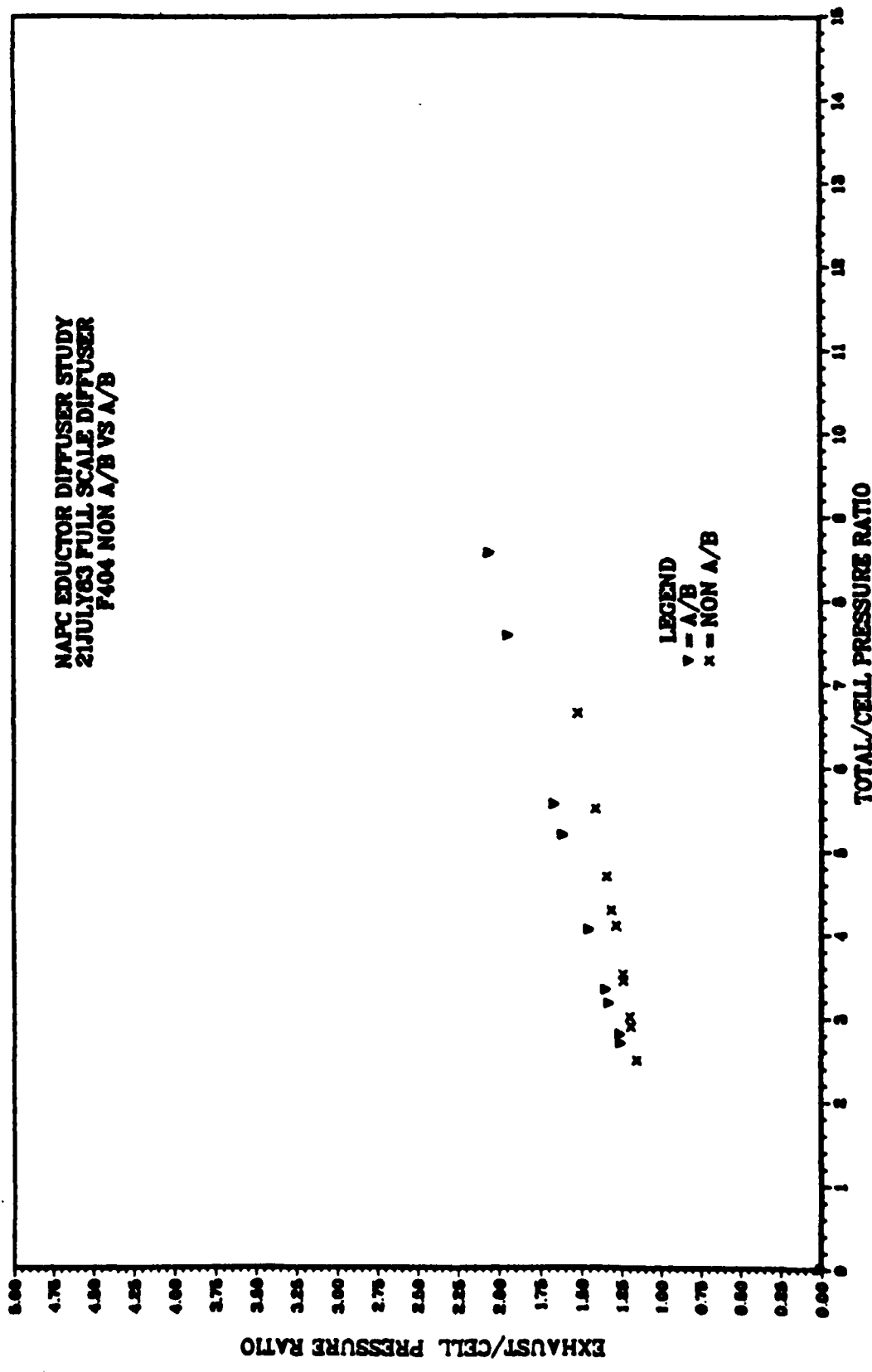


Figure 23. F404 Baseline

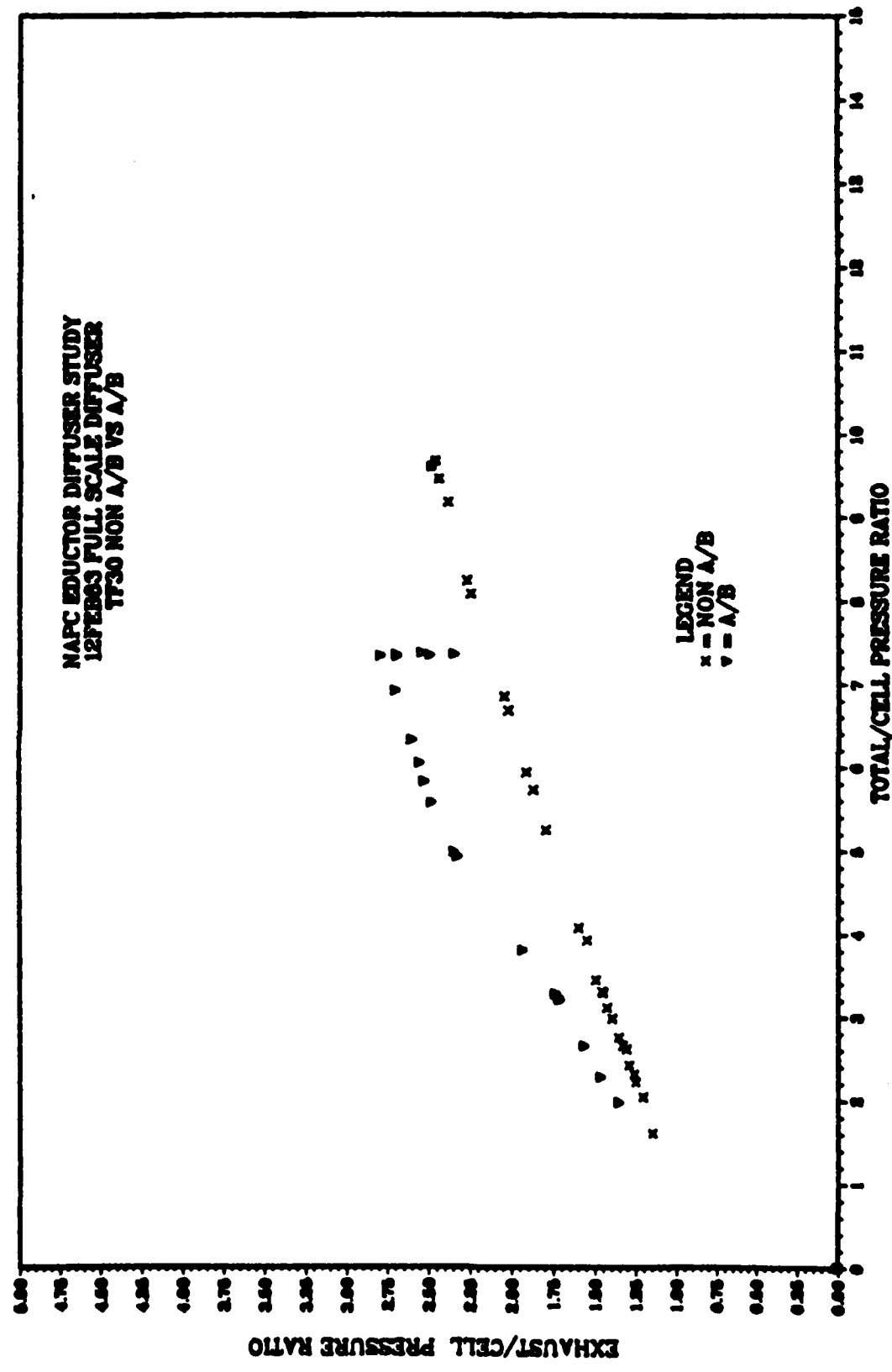


Figure 24. TF30 Baseline

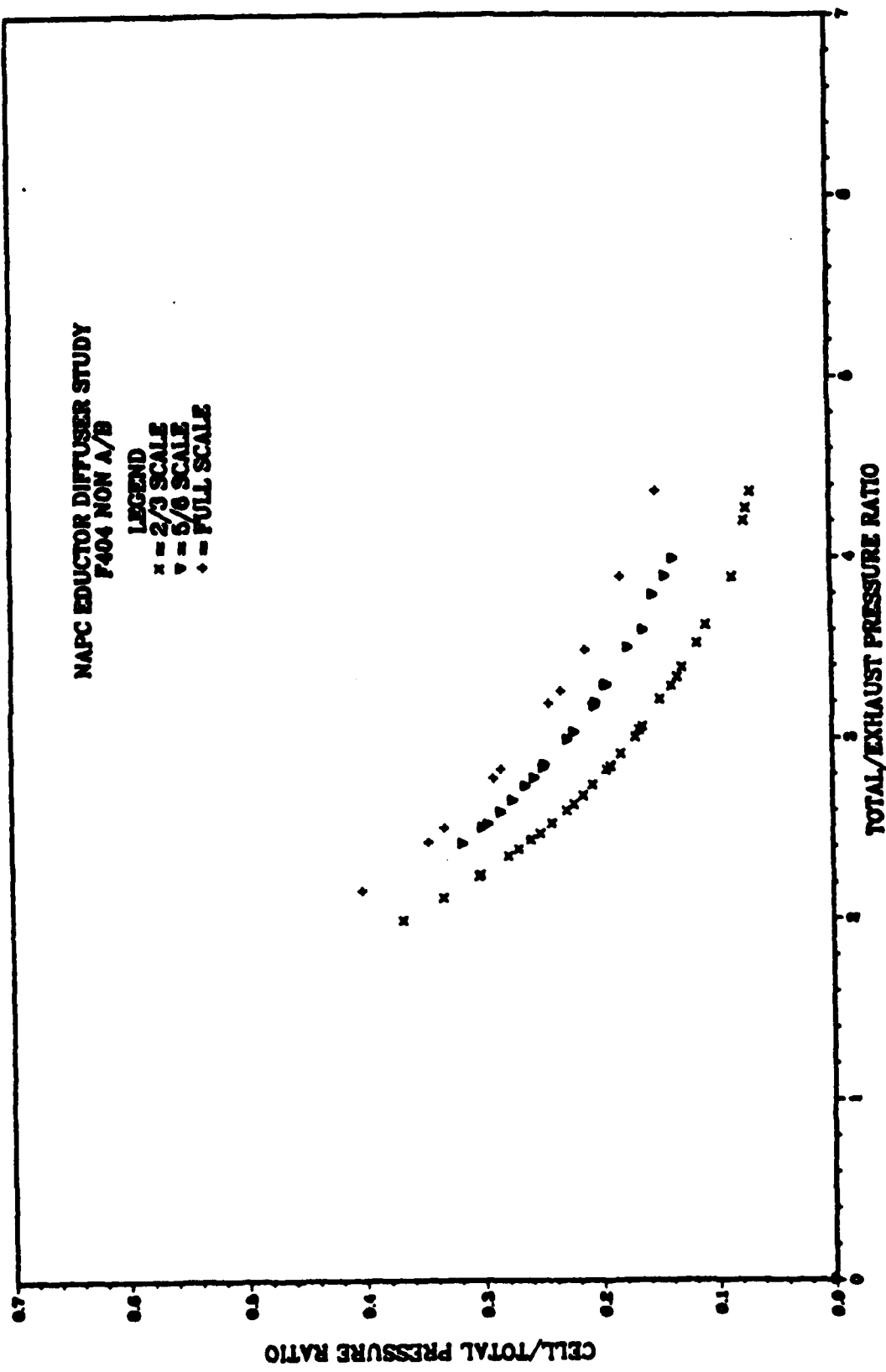


Figure 25. Optional Presentation of Operating Curves

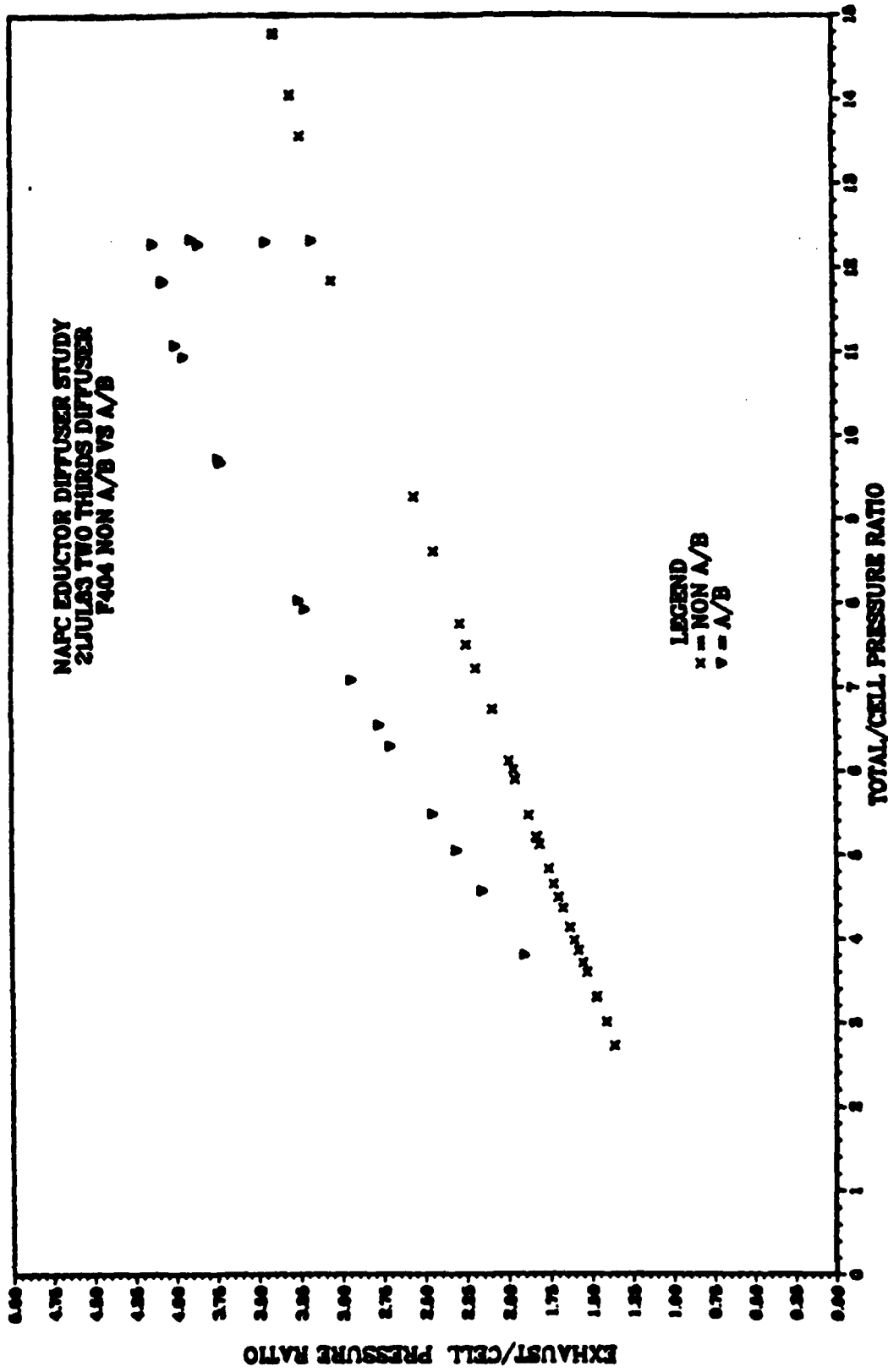


Figure 26. AE/A* Effects

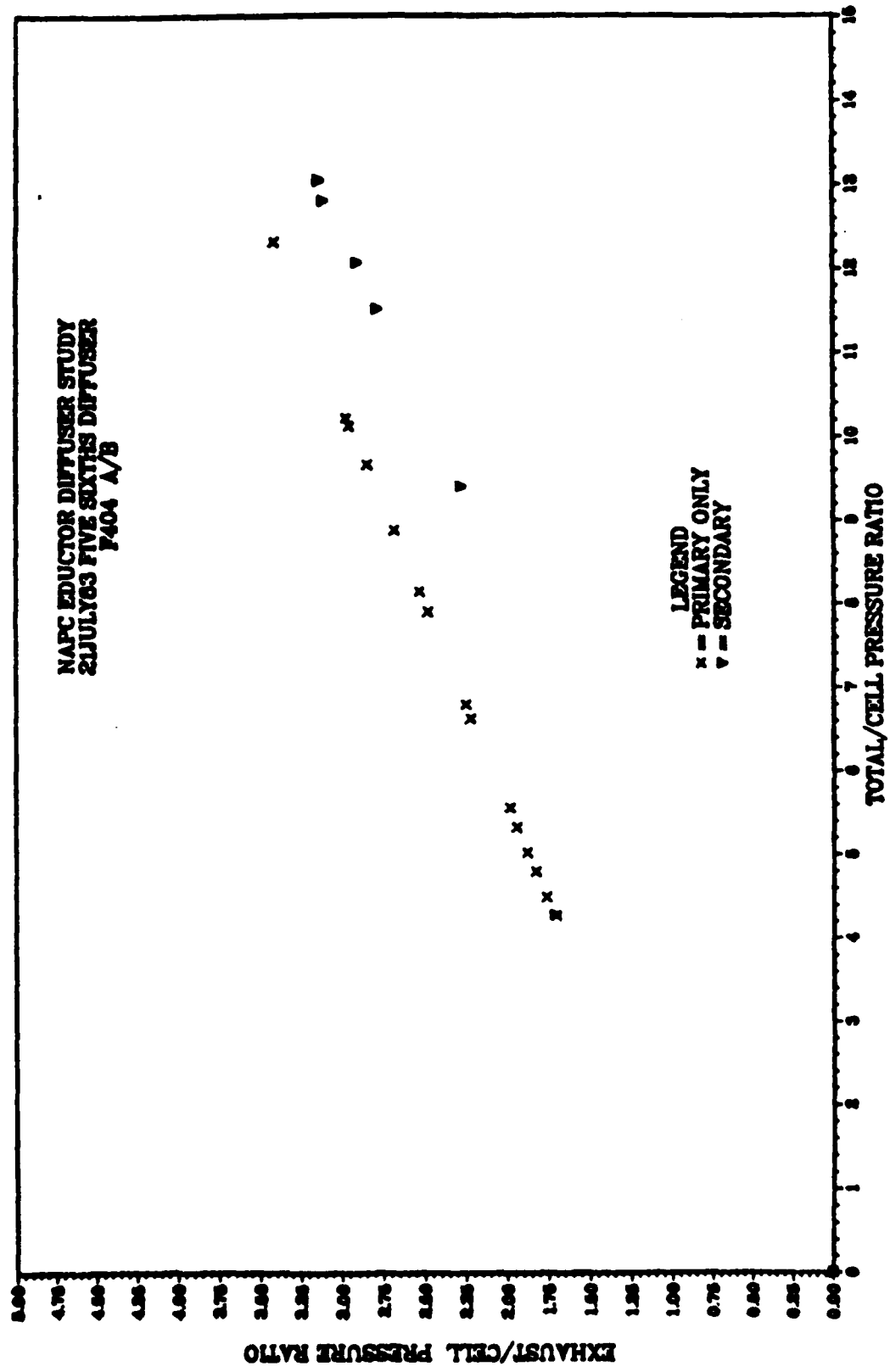


Figure 27. Secondary Flow Effects (Five-Sixths)

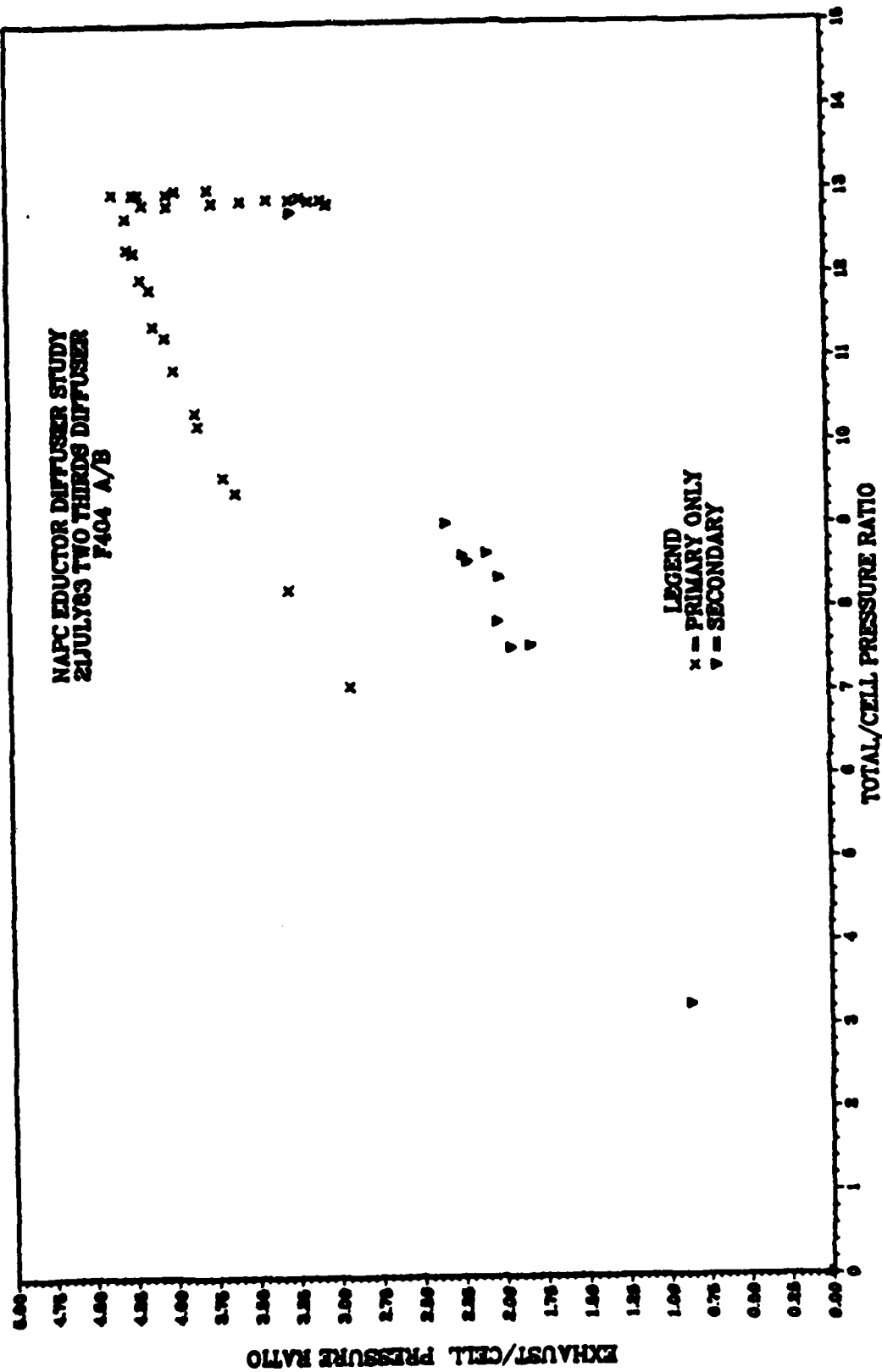


Figure 28. Secondary Flow Effects
 (Two-Thirds)

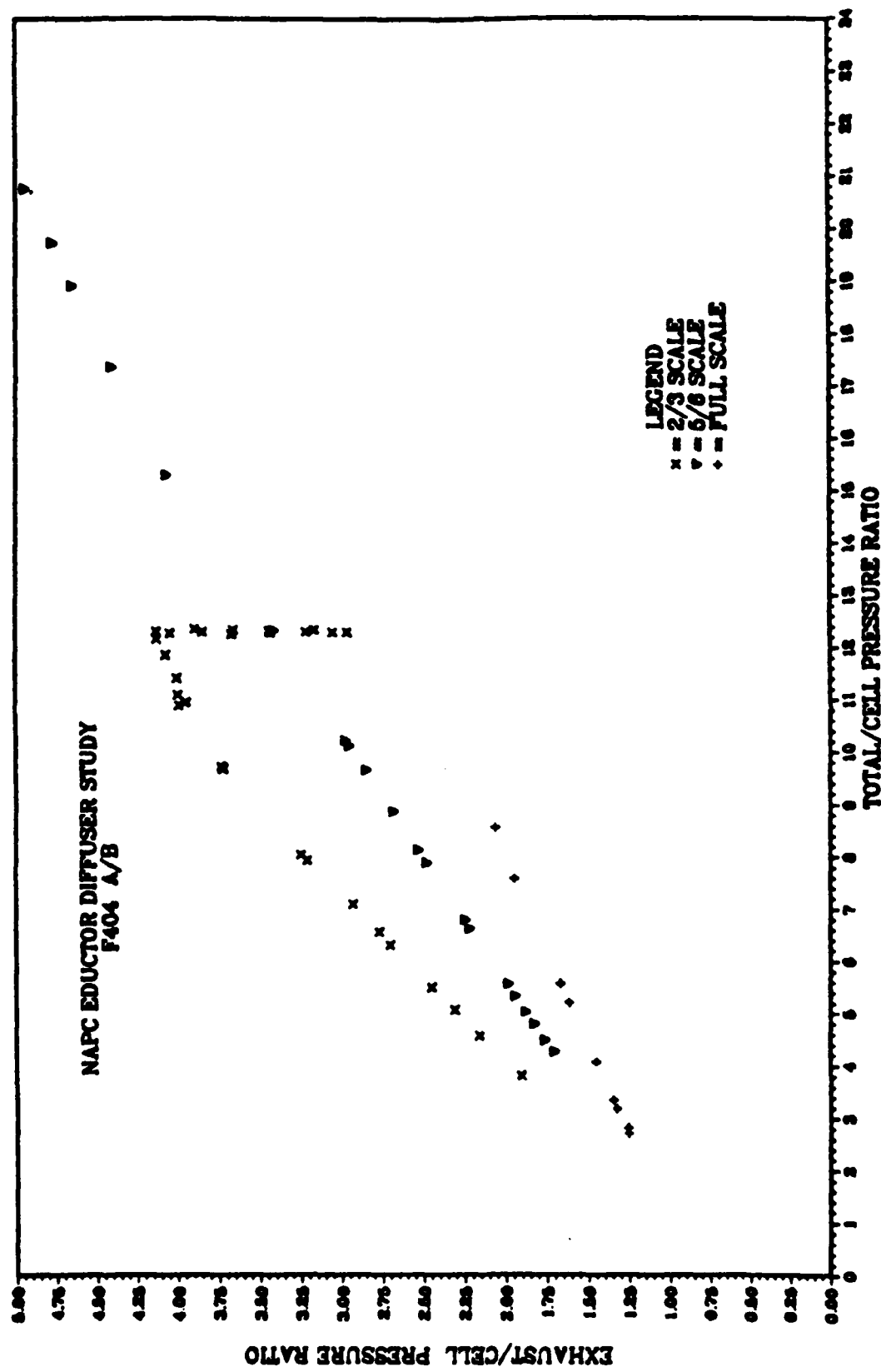


Figure 29. A/D/A* Effects

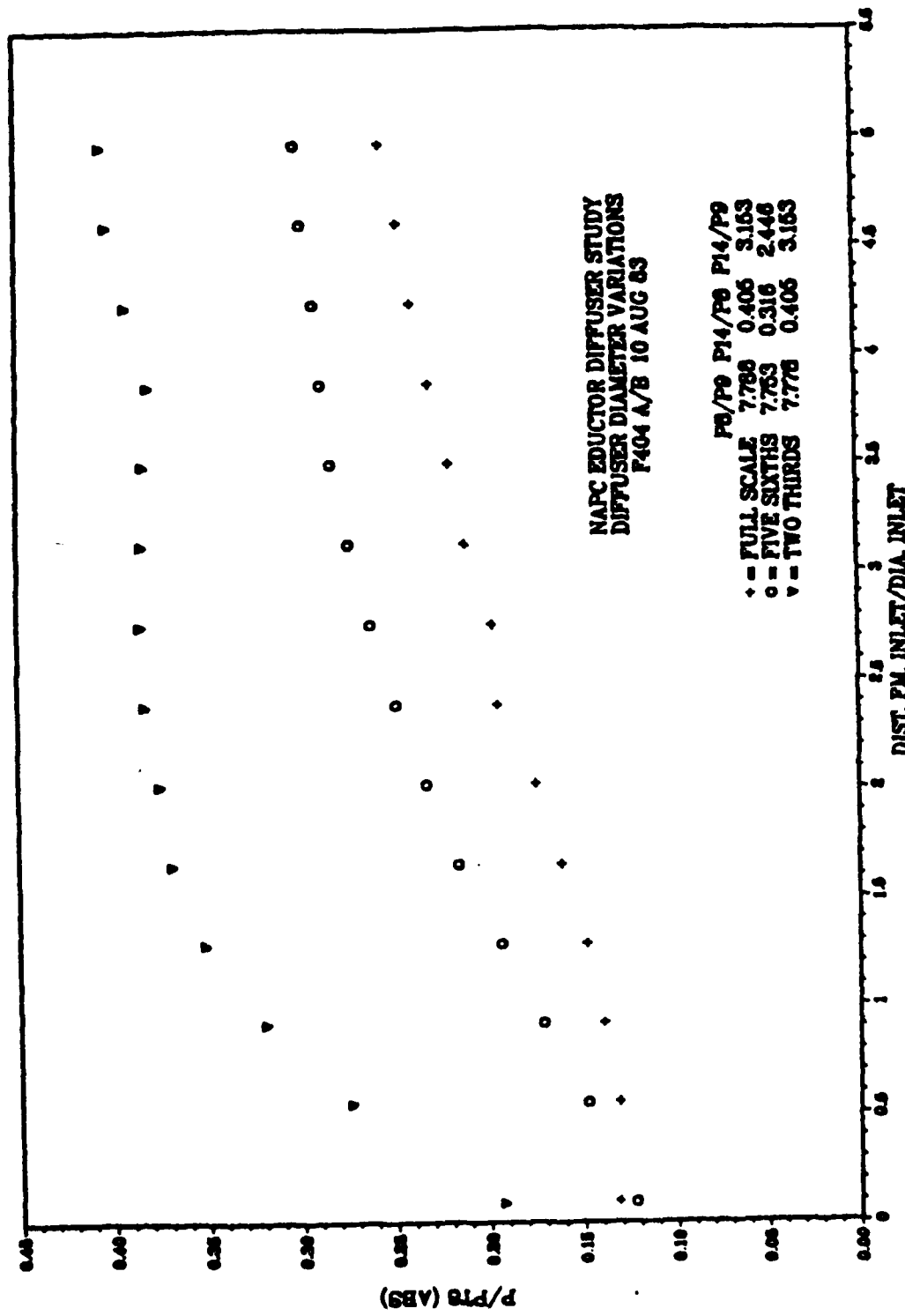


Figure 30. Static Pressure Profiles

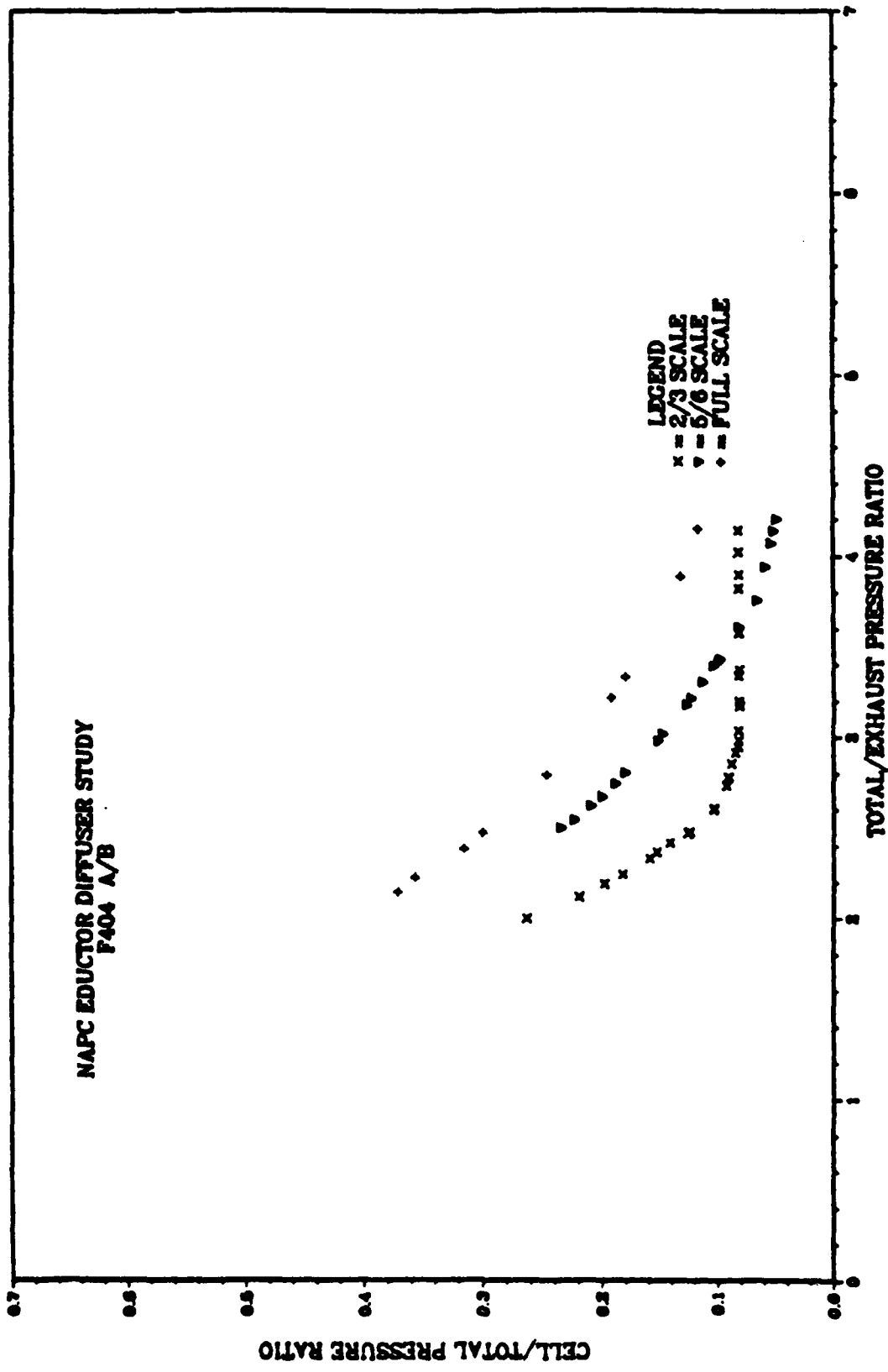


Figure 31. F404 Improvement Summary

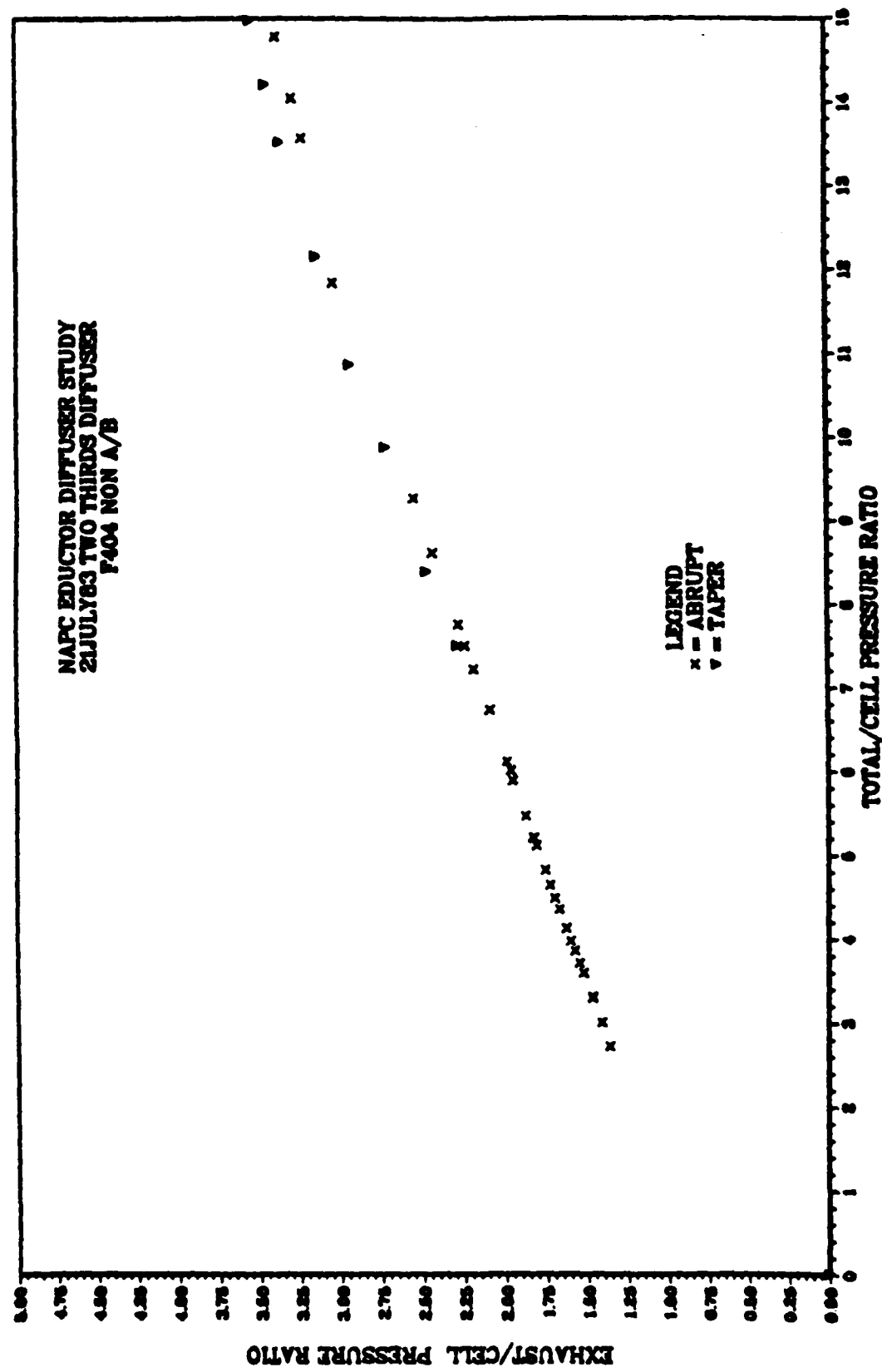


Figure 32. Taper Effects (F404 Non A/B)

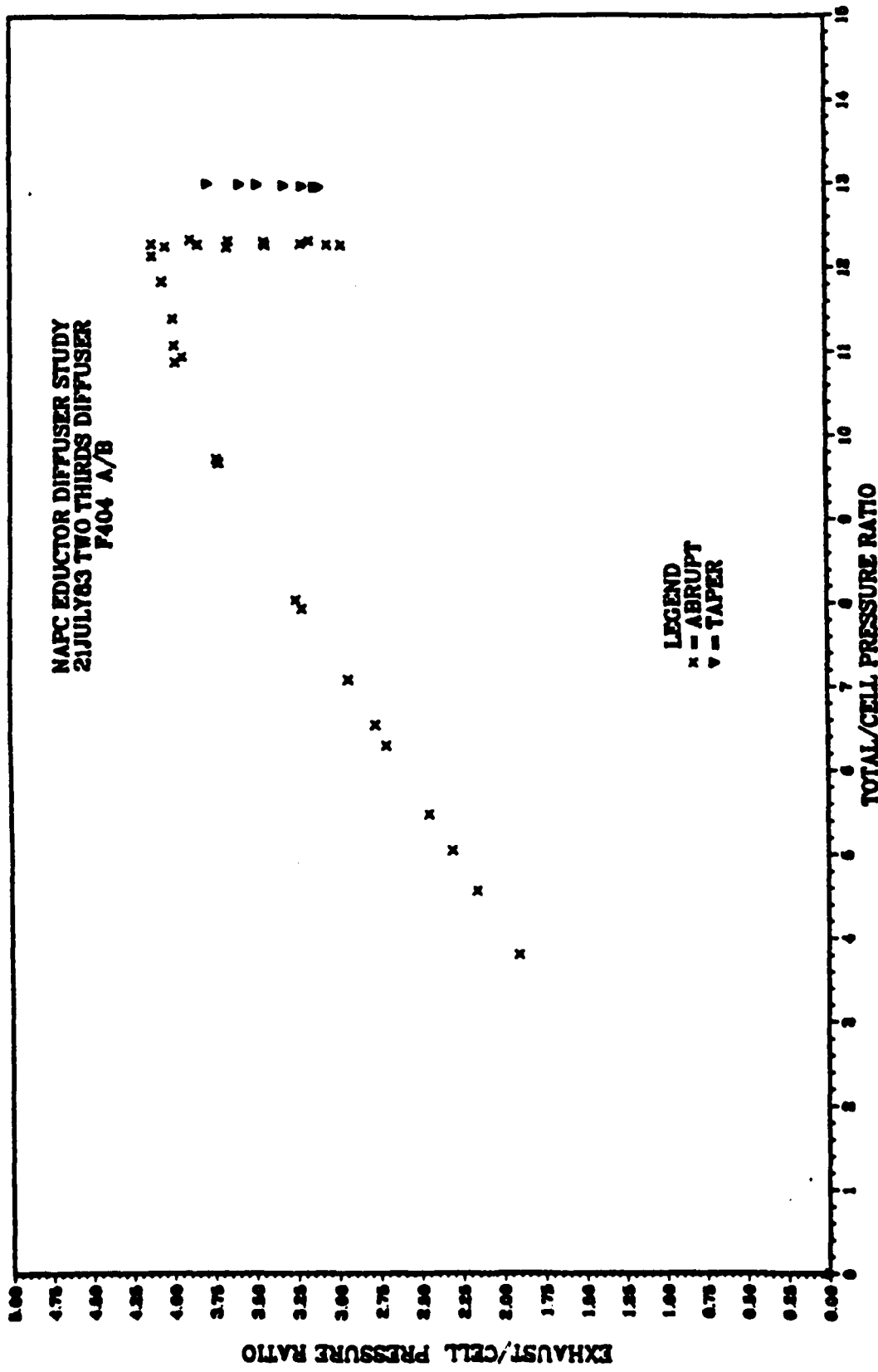


Figure 33. Taper Effects (F404 A/B)

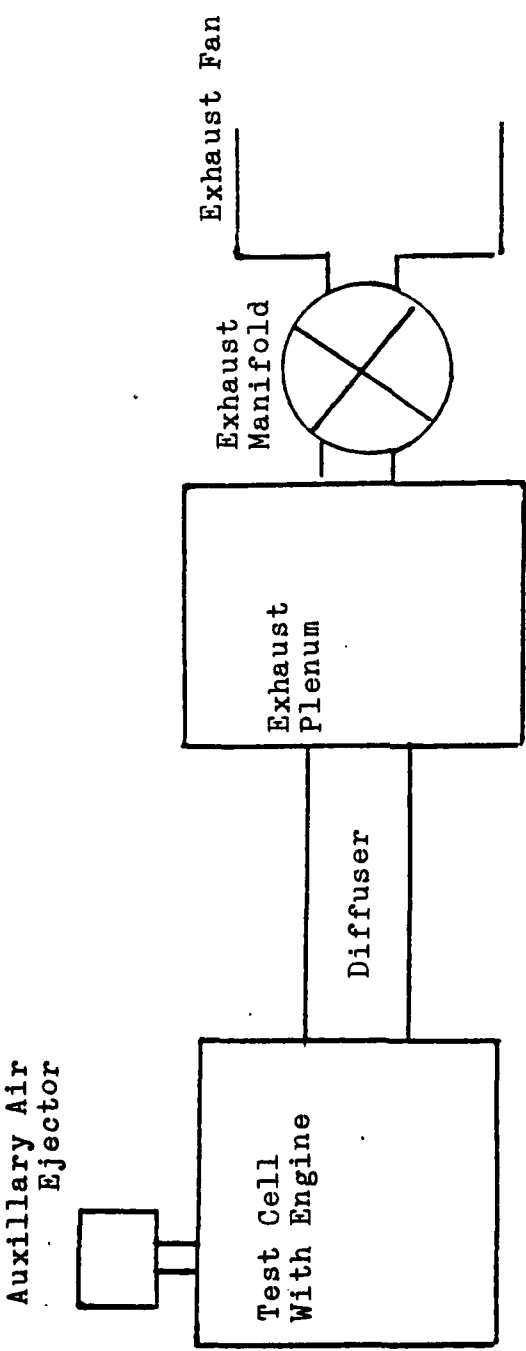


Figure 34. Test Facility Illustration

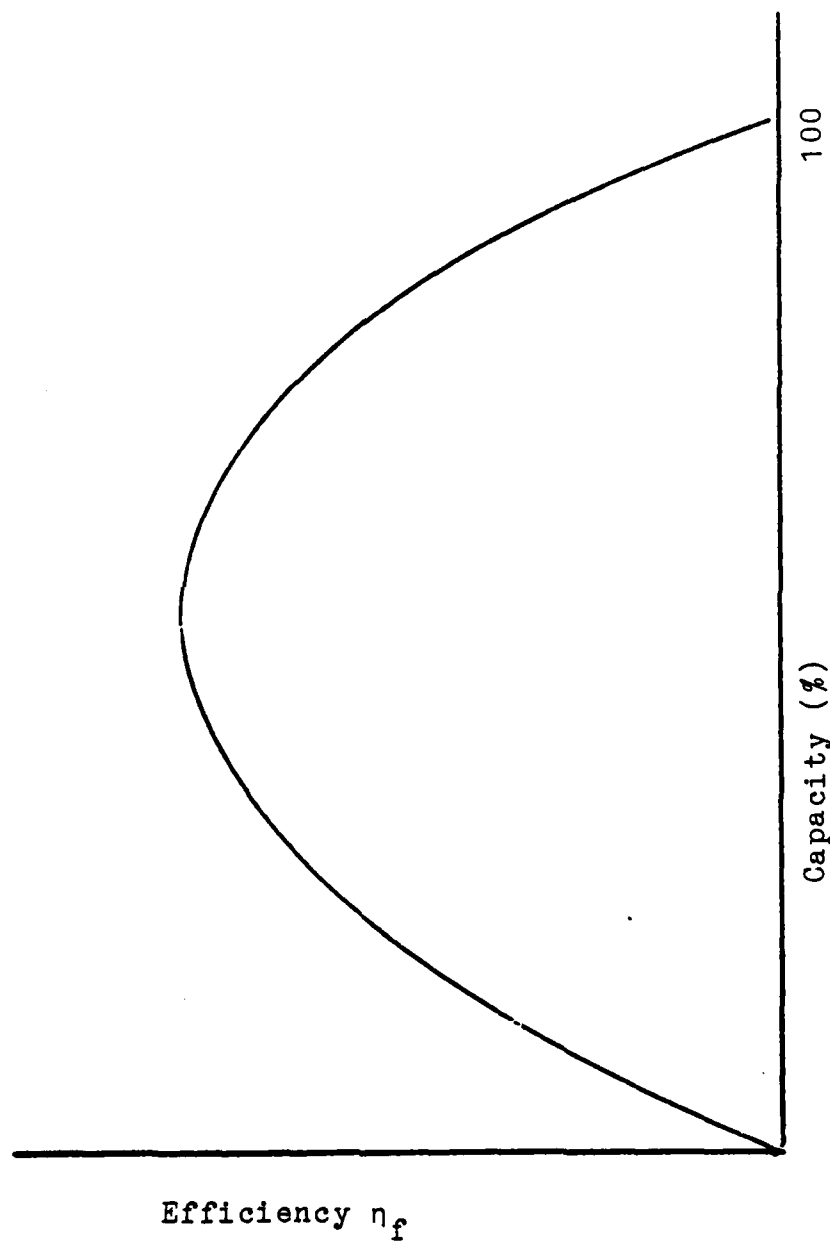


Figure 35. Generalized Exhaust Fan Efficiency

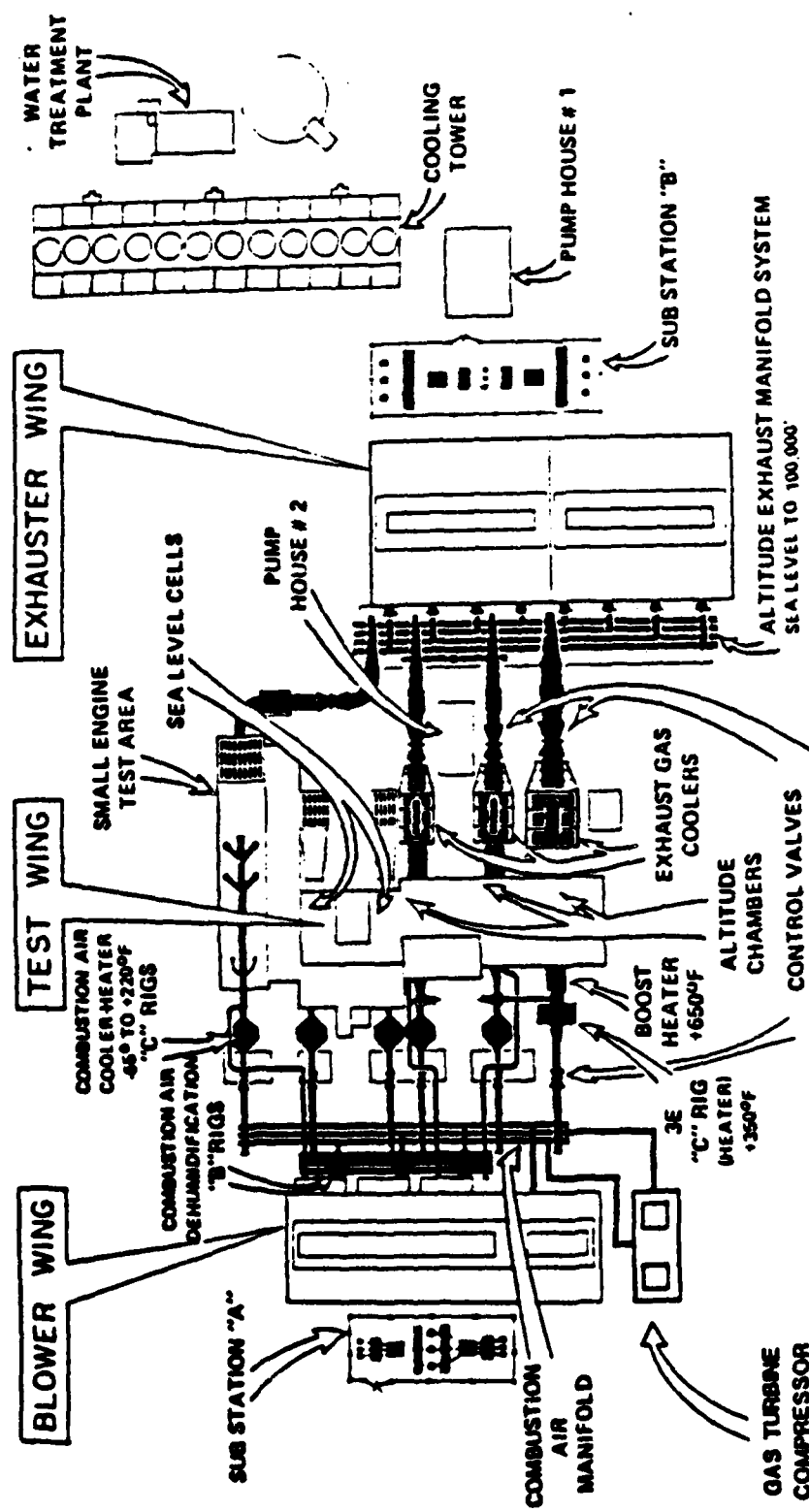


Figure 36. Engine Test Facilities

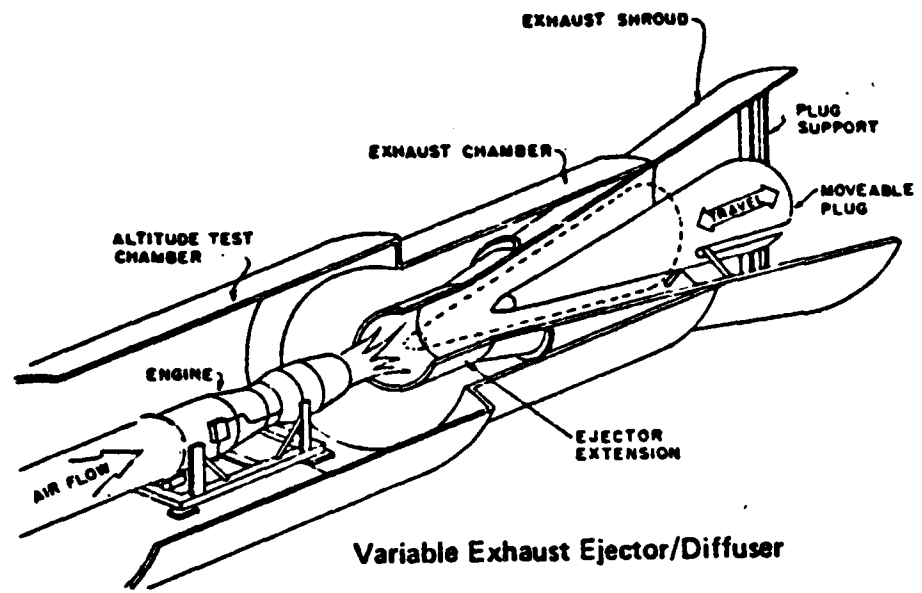


Figure 37. Variable Exhaust Ejector Diffuser

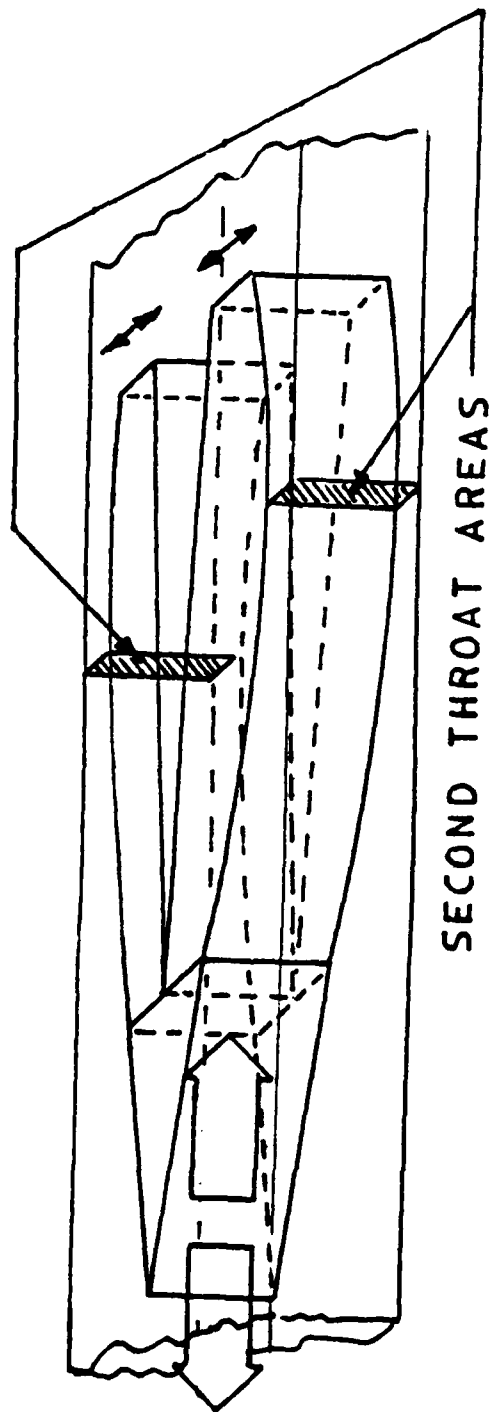


Figure 38. Conceptual Wedge Design

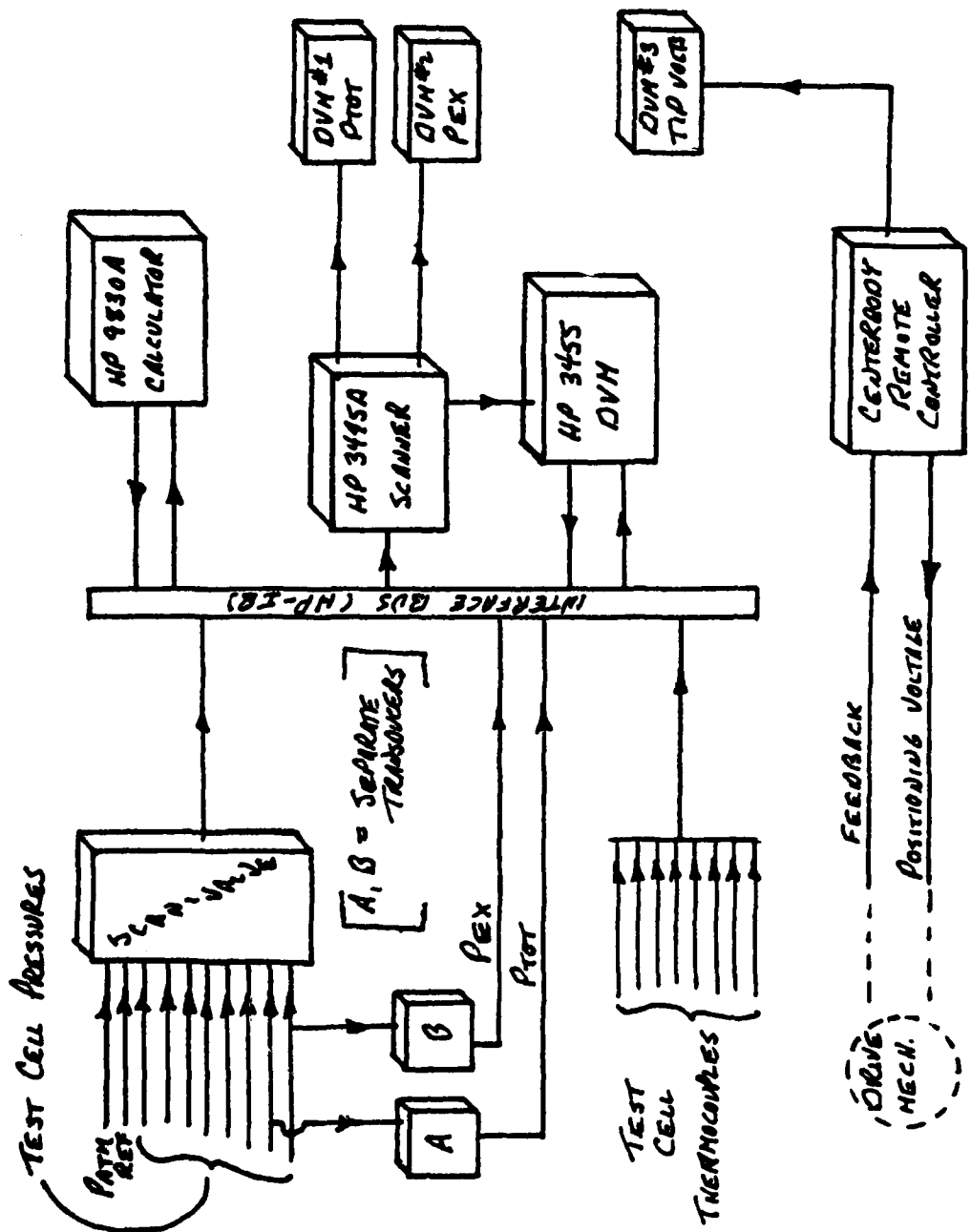


Figure 39. Instrumentation Schematic

APPENDIX A

DEVELOPMENT

Design of a subscale altitude test facility to approximate the salient features of the parent facility at the Naval Air Propulsion Center was governed by a multiplicity of interwoven factors. The underlayment for the design was the motive air supply; compressed air from an Allis Chalmers twelve-stage axial compressor (Figure 17). The dictates of the air supply qualified several engines from the family of engines tested by NAPC as candidates for scaled testing. The candidate engines elected, as listed in Table B.3 were, from a first cut, the most likely to give a broad representation of existing test frames suitable for comparative analysis with alternative ejector-diffuser geometries. Two afterburning engines were elected to span the operating range of the test facility from zero induced secondary flow to five (5) percent secondary flow. The choice of engines provided the vital ingredient upon which scaling of the facility could proceed.

Scaling. Scaling to achieve Mach number similitude was elected consistent with past studies by Merkli {Ref. 5} and Bevilaqua and Combs {Ref. 11}. The geometry of a scale model may easily match the prototype but simultaneous matching of Mach and Reynolds numbers is impossible. A match in

Mach number will present a model with a smaller Reynolds number. A match of Reynolds number induces a higher Mach number in the model. Noting that large Reynolds numbers, consistent with fully turbulent flow, are characteristic of the prototype, any variations in Reynold number would affect scaling only if a shift to less than fully turbulent flow was created. At a projected mass flow rate for the model of .5 lbm/sec, a simple calculation results in a Reynold number in excess of 1E6 thus relegating Reynolds effects to second order. It bears observation, however, that any flow phenomena which are sensitive to Reynolds number such as separation and reattachment will not result in agreement between model and prototype. Any improvement in diffusion which results from a geometric change must address this consideration.

Once Mach number had been established as the scaling parameter the cold flow model carried with it a significant scaling bonus. Mach number will ratio out any thermal effects since temperature appears as a dependent variable in both the stream and sonic velocities which comprise the ratio. In the context of this study, an order of magnitude difference between cold flow and hot flow temperatures will fail to elevate Reynolds effects beyond second order. At worst, an error within the range of computational accuracy is anticipated due to temperature extremes between model and prototype with the model outperforming the prototype. Work conducted by Welch {Ref. 16} with subsonic exhaust stack ejectors using Mach number scaling shows deviations of less than 1%

between hot and cold flow model test results. An order of magnitude in temperature variation occurred in these studies.

The TF30 in the afterburning mode, having the largest throat area, governed the compressor-engine match. One dimensional isentropic nozzle flow theory for choking requires that mass flow obey the following expression:

$$\dot{m} = \frac{A^* \times P_0}{\sqrt{T_0}}$$

The available air supply had the capacity to deliver 2.65 atmospheres and 12.0 lbm/sec at 600 degrees R. 2.65 atmospheres would be the maximum achievable ratio of total pressure to exhaust pressure under atmospheric conditions in the nozzle exit. This ratio was below the desired test range but could be boosted by utilizing an exhauster to lower exhaust pressure at the expense of air flow to drive the apparatus.

A survey of ejectors previously driven by this compressor revealed one design with a convergent-divergent nozzle, operating with half ($\frac{1}{2}$) an atmosphere back pressure, capable of pumping 2.0 lbm/sec with the exhauster drawing 8.85 lbm/sec. The total flow of 10.85 lbm/sec was well within the capability of the compressor and 2.0 lbm/sec was chosen as the design mass flow rate for an expected ratio of total pressure to exhaust pressure of 5.70. For 2.0 lbm/sec at 2.65 atmospheres and 600° R, a throat diameter (d^*) was computed to be 1.735 inches. Conservatively, a primary nozzle throat of 1.675

inches was chosen, which resulted in an $A^* = 2.204$ (in^2) and mass flow equal to 1.863 lbm/sec .

The TF30 has an actual throat area of 7.5 (ft^2) and diameter of 3.09 ft. Dividing this by the throat of the model, a scaling factor of 22.139 was derived. Full scale drawings of the test cell and diffuser assemblies to be modeled were scaled using this factor. License was taken to modify supports or stiffeners to accommodate fabrication and assembly. Detail drawings of the scaled model are included as Appendix F.

APPENDIX B

NAPC TEST FACILITY IMPROVEMENT PROGRAM

The Naval Air Propulsion Center is a major jet engine test facility, located in Trenton, New Jersey. It is the only facility in the nation capable at one site of testing turbojet/turbofan, turboprop/turboshaft engines under sea level, altitude and environmental conditions.

Engine Testing. The engine facility is composed of three major divisions: the Blower Wing, Test Wing and Exhauster Wing. A schematic is presented as Figure 36.

Blower Wing. The Blower Wing contains centrifugal air compressors and air conditioning systems which provide air to the test engine under the same conditions experienced by an aircraft in flight. Four 6,000 horsepower centrifugal blowers, one 30,000 horsepower gas turbine powered axial compressor, 5,000 tons of refrigeration, and an oil-fired indirect air heater are utilized to provide air flows up to 700 lbm/sec, at pressures up to five atmospheres and at air temperatures ranging from -65°F to +650°F. With these inlet conditions to the engine, the center can simulate flight velocities up to three times the speed of sound.

Test Wing. The Test Wing contains eleven test cells and their associated control rooms. Three of these cells are large altitude chambers, four are small altitude chambers for turboprop/turboshaft/auxiliary power unit testing, two

AD-A136 745

DESIGN AND TESTING OF SCALED EJECTOR-DIFFUSERS FOR JET
ENGINE TEST FACILITY APPLICATIONS (U) NAVAL POSTGRADUATE
SCHOOL MONTEREY CA J W MOLLOY SEP 83

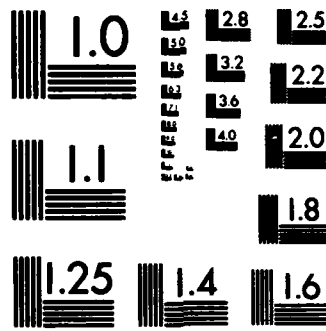
2/2

UNCLASSIFIED

F/G 14/2

NL





MICROCOPY RESOLUTION TEST CHART
NATIONAL BUREAU OF STANDARDS-1963-A

are large sea level test cells, one all purpose test tunnel and a helicopter transmission test facility. Test cell capabilities are summarized in Table B.1.

Exhauster Wing. The Exhauster Wing contains the air pumping machinery required to produce low pressure in the altitude test cells. Fourteen of these pumps with a combined power of 56,000 horsepower are utilized in conjunction with Test Chamber exhaust ejectors to simulate altitudes up to 100,000 feet. Table B.2 summarizes the performance parameters of ejector-diffuser (Figure 34) accompanies the large engine testing with straight tube diffusers accommodating smaller engines. Two of the engines which span the range of operation are the TF30 and the F404, whose characteristics are shown in Table B.3.

Facility Improvement Program. In January of 1982, an initiative to reduce the power consumption costs, directly related to engine testing, was proposed.

The stated objective was: Improve ejector-diffuser performance in NAPC altitude test cells to minimize exhauster power costs.

The approach proposed was:

Phase I. Survey the community for current advancements in ejector-diffuser performance, high-temperature materials applications and related functional fields. Examine alternate extended variable geometry ejector-diffuser concepts which will provide optimum performance by accommodating engine nozzle throat area variation.

TABLE B.1

CONDITIONS	3E	2E	1E	1W	2W	3W	4W	5W	6W
Airflow (lb./sec.)	700	430	430	350	350	100	100	100	100
Inlet Temp. (°F)	Cold	-65	-65	-65	-65	-65	-65	-65	-65
	Hot	+650	+390	+390	+220	+220	+220	+220	+220
Mach Number	3.0	2.4	2.4	1.1	1.1	1.1	1.1	1.1	1.1
Altitude (ft)	100,000	80,000	80,000	S.L.	S.L.	80,000	80,000	80,000	80,000
Test Area	Length (ft)	30	18	18	56	56	15	20	17
	Width/Diam. (ft)	17	14.5	14.5	23	23	8	10	10
	Height (ft)	-----	-----	-----	14	14	8	-----	10

Table B.2

MASS FLOW : 50 - 300 LB/SEC
 VELOCITY : SUPERSONIC AT ENGINE NOZZLE
 WITH OBLIQUE SHOCKING TO
 SUBSONIC IN DIFFUSER
 ENGINE NOZZLE EXHAUST TEMP : 1000°F - 3500°F (CORE)
 ENGINE NOZZLE PRESSURE RATIO : 3 - 14
 ENGINE NOZZLE AREA : 200 - 1200 in²
 OPTIMUM DIFFUSER AREA TO
 ENGINE NOZZLE THROAT AREA
 RATIO : 3½ - 4
 SECONDARY AIR TO PRIMARY
 AIR MASS FLOW RATIO : .08 - .15
 TEST CELL ALTITUDE PRESSURE : 1 - 14.7 psia
 SECONDARY AIR TEMPERATURE : 100°F - 200°F

Table B.3

<u>Engine</u>	<u>Max. Thrust</u>	<u>Stages</u>	<u>MDOT</u>	<u>CPR</u>
TF30	20,900	16	242	19.8:1
F404	16,000	3F,7C	140	25:1

Phase II. Select one or two of the most feasible concepts and evaluate performance with cold flow model testing. Select the optimum concept and confirm mechanical and aerodynamic performance with hot flow model testing. Analyze full-scale implementation cost versus potential power savings and determine payback period.

Phase III. Design, fabricate, install, test and evaluate a full-scale ejector-diffuser in one NAPC altitude test cell. Convert the remaining two NAPC test cells to full-scale ejector-diffuser.

APPENDIX C
DIFFUSER PROPOSALS

Proposals to modify the baseline diffuser geometries were developed with emphasis towards providing control over the shock mechanism. The design limitations were imposed by maintaining geometric similarity of the flow paths and the range of engines to be tested. Whereas simplicity would be incorporated where feasible, no constraints were imposed on the design with respect to strength, thermal effects, vibration or leakage.

Translating Wedge. A double hinged wedge in a rectangular duct was the first proposal considered. This assembly is shown in Figure 38. The two dimensional wedge was expected to provide more positive control over the strength of the shock system compared to the cone centerbody. All of the experimenters who have investigated a second throat diffuser have concurred that an optimum second throat size and axial position relative to the nozzle exit exist. The wedge would allow a finer control of the size versus axial position of the second throat than the cone assembly. The current centerbody notably couples the size of the second throat with the axial position of the centerbody. The translating wedge provides uncoupling of these variables with an expectation that the optimum can be approached by adjusting the second ramp to facilitate starting, then translating the wedge to move the

second throat to a position of lower Mach number, which should improve performance. The wedge would then be mapped against the baseline configurations for analysis. Current design techniques call for running a matrix at various settings, shutting down, reviewing the data, developing a new matrix based upon judgement and repeating the cycle. Cost and time consumption without achieving any guarantee of an optimum are a natural by-product of this process. As the number of independent variables increases, the test matrix becomes much more complex with the possible permutations following combinatorial theory. A simplified matrix of the test process as shown in Table C.1 leads one to recognize the merit of online evaluation. A real time mapping of pressure ratios would be prescribed for evaluating this model. This would permit detailed investigations when a point of significance was reached. Typically, once starting was confirmed, the wedge angles and/or their axial positions could be varied and the effect noted.

Auxiliary Mass Ejection. The deleterious effect of secondary flow gives rise to the possibility of equipping the test cell with an auxiliary ejector. This proposal, while not new, has oft been dismissed as being not cost effective. The recent cost spiral in exhauster power consumption opens the topic for renewed consideration. As observed in the baseline studies, the power setting of the engine has a dramatic effect on exhauster requirements and therefore, a direct bearing on power consumption costs. The

Table C.1

Optimization Goal	PT8	PS9	P14	Variable		m s
				Size A_d	Position A_d	
STARTING	H	V	A	H	H	H
STARTING	H	V	H	A	H	H
STARTING	H	V	H	H	A	H
STARTING	H	V	H	A	A	H
STARTING	H	V	A	A	H	H
PRESSURE RECOVERY	H	H	A	H	H	H
PRESSURE RECOVERY	H	H	H	A	H	H
PRESSURE RECOVERY	H	H	H	H	A	H
PRESSURE RECOVERY	H	H	H	A	A	H
PRESSURE RECOVERY	H	H	A	A	H	H
PRESSURE RECOVERY	H	H	A	H	A	H

H = HOLD CONSTANT

V = LET VARY

A = ADJUST

efficiency of the exhauster, when operating at off-design conditions, will be less, and the blend of an efficient auxiliary ejector to allow the prime exhauster to function at or near design should enhance overall efficiency. The ramifications of this approach are detailed in the discussion of results.

APPENDIX D
EXPERIMENTAL PROCEDURE

System Checkout. The Allis-Chalmers compressor is maintained and operated by TPL personnel. Twenty minutes of prelubrication is required on the compressor prior to start followed by approximately twenty minutes of warmup before the compressor is ready to assume the load of supplying air to the experimental apparatus. During this time it is prudent to accomplish the following checks and tasks:

1. Examine all pressure taps, tubing, and connections to Scanivalve port manifold and the two dedicated pressure transducers. Verify instrumentation is connected in accordance with Figure 39.
2. Turn on thermocouple ice point reference, and examine all thermocouples for broken wires or loose connections.
3. Hand test all PVC couplings for tightness and check to see that the primary and secondary root valves are open.
4. Turn on the HP-9830A Calculator and printer, HP-9867B Mass Memory Storage Unit, Scanivalve Multiplexer (S/V MUX), PH-3495A Scanner, HP-3455 Digital Voltmeter, Scanivalve control power supply, and the three separate digital voltmeters used for monitoring centerbody drive voltage, engine test cell pressure, and exhaust chamber pressure.

5. Load the program "VIBTEM" (Table I) into the memory of the HP-9830A calculator. Run the program once to ensure there are no anomalous readings from any thermocouple or pressure tap.

6. Read and record atmospheric pressure from the Wallace and Tiernan gage.

Procedure to Conduct Data Runs. Control of the experiment is exercised at the remote operating station. (Figure 19). *****WARNING***** FAILURE TO OPEN THE EXHAUST VALVE FIRST CAN RESULT IN OVERPRESSURIZATION OF THE SYSTEM. The system is brought on line by opening the exhaust valve fully and then the primary air may be cut into the system. Monitoring of total and exhaust pressure on the digital voltmeters allows setting of test point pressures in accordance with the test matrix.

APPENDIX E
SECOND THROAT DIFFUSERS

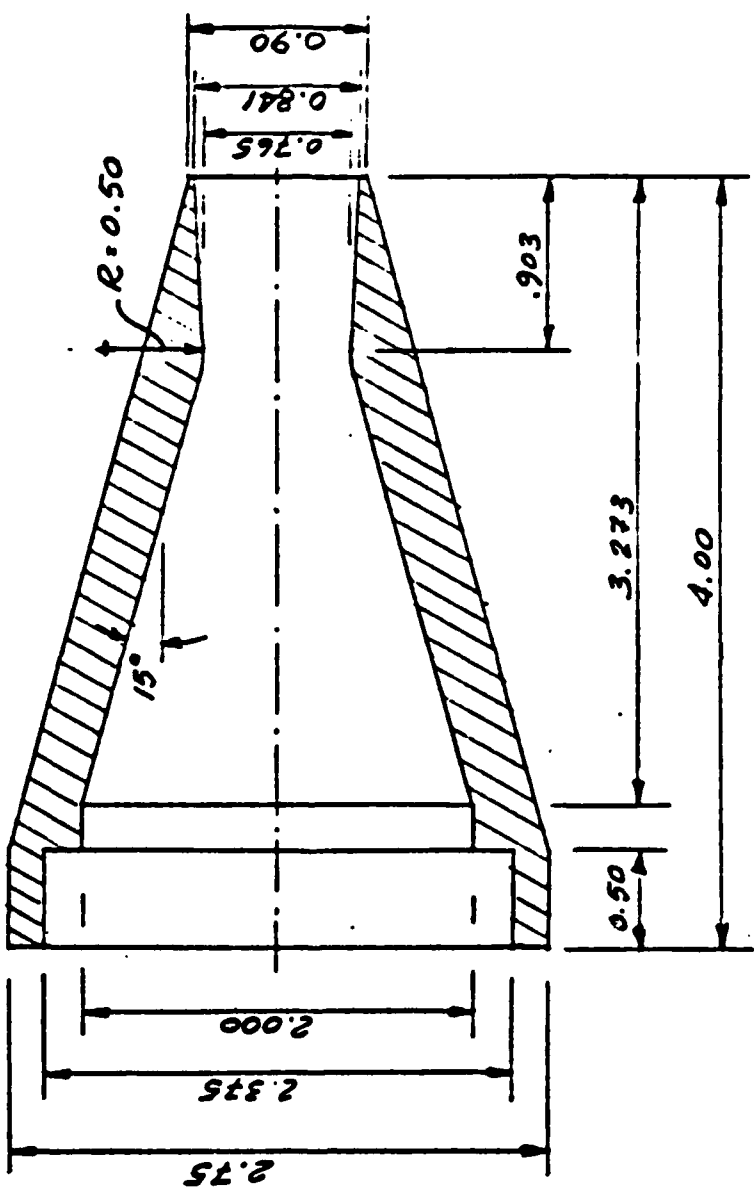
Second throat ejector-diffusers have had wide acceptance in gas turbine engine testing due to their ability to provide systems flexibility to cope with the variabilities involved in altitude testing. A variable area second throat geometry such as that shown in Figure 38 was developed when sizing and location of the optimum second throat was loosely defined. The idealization of the process is well understood, as detailed by Shapiro {Ref. 8} in his discussion of supersonic wind tunnels. The objective is to seek the maximum exhaust pressure at which the ejector-diffuser once started, can be maintained. A brief description of the operation permits an appreciation of the phenomenon involved. As mass flow through the nozzle is accelerated, the flow becomes supersonic and will cause a decrease in cell pressure by mixing. Exhaust pressure is lowered until a minimum cell pressure is attained with the ejector-diffuser then being considered "started." At this point, the shock stands upstream of the secondary throat and cell pressure becomes independent of exhauster pressure. Exhaust pressure may then be increased to the point where cell pressure begins to rise. This establishes the system's operating range. The variable geometry with a conical centerbody evolved to

accommodate the complex mix of parameters required to approach even near optimum operation. This concept, while attractive, couples a decrease in second throat area with a change in axial position of that throat, losing a degree of freedom which may be exploited for further gains. Although the goal of the design is to alter the second throat, the centerbody itself will influence the character of the shock system and, thus, may also be in direct competition with second throat effects as related to pressure recovery. Adding a degree of freedom here may also improve performance.

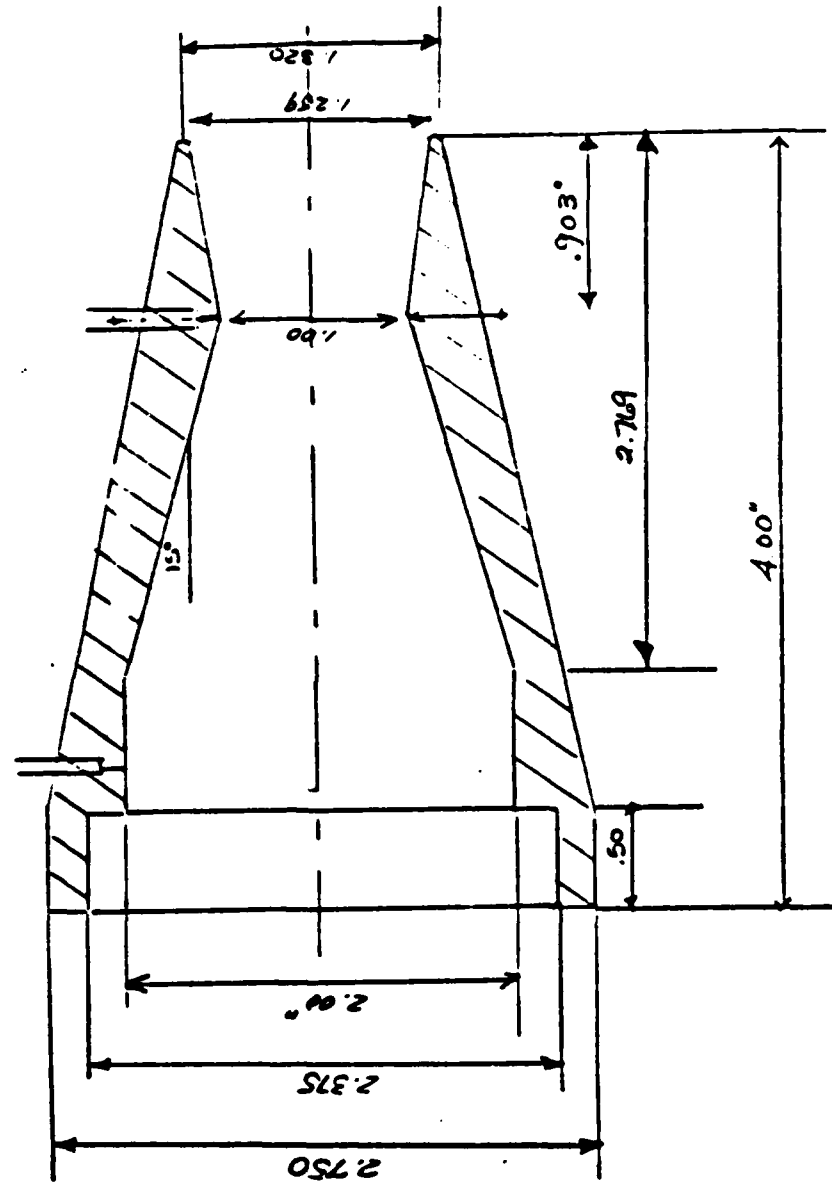
The final design of the variable diffuser utilized by NAPC was formulated in the early 60's, and the rationale behind the final geometry is not well defined. A best estimate is that the design was a compromise between model test studies and manufacturing ease and costs. The need to optimize the design for small percentage improvements in exhauster back pressure were likely secondary.

APPENDIX F
SCALED DRAWINGS

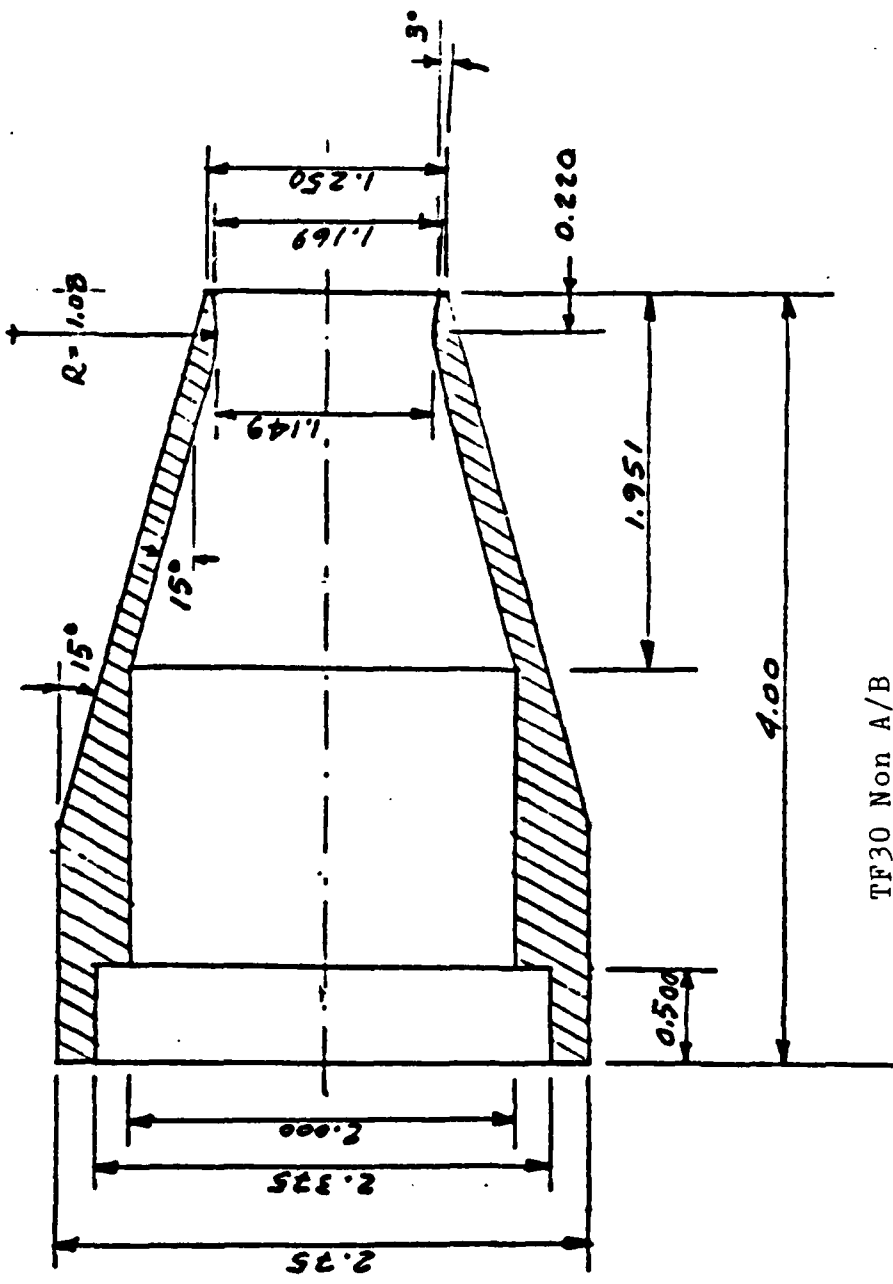
The scaled drawings in this Appendix represent the principal components of the design. All linear dimensions are in inches and angular measurements in degrees.

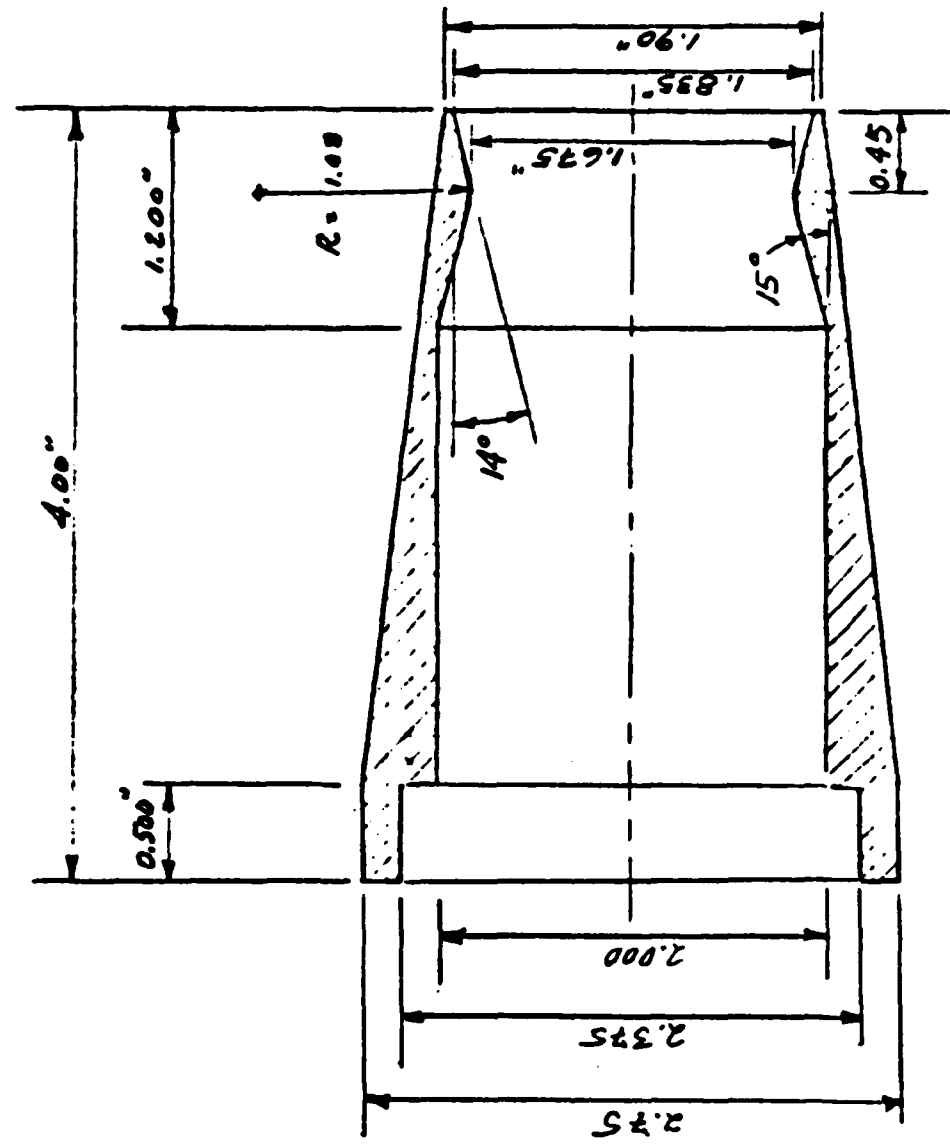


F404 Non A/B

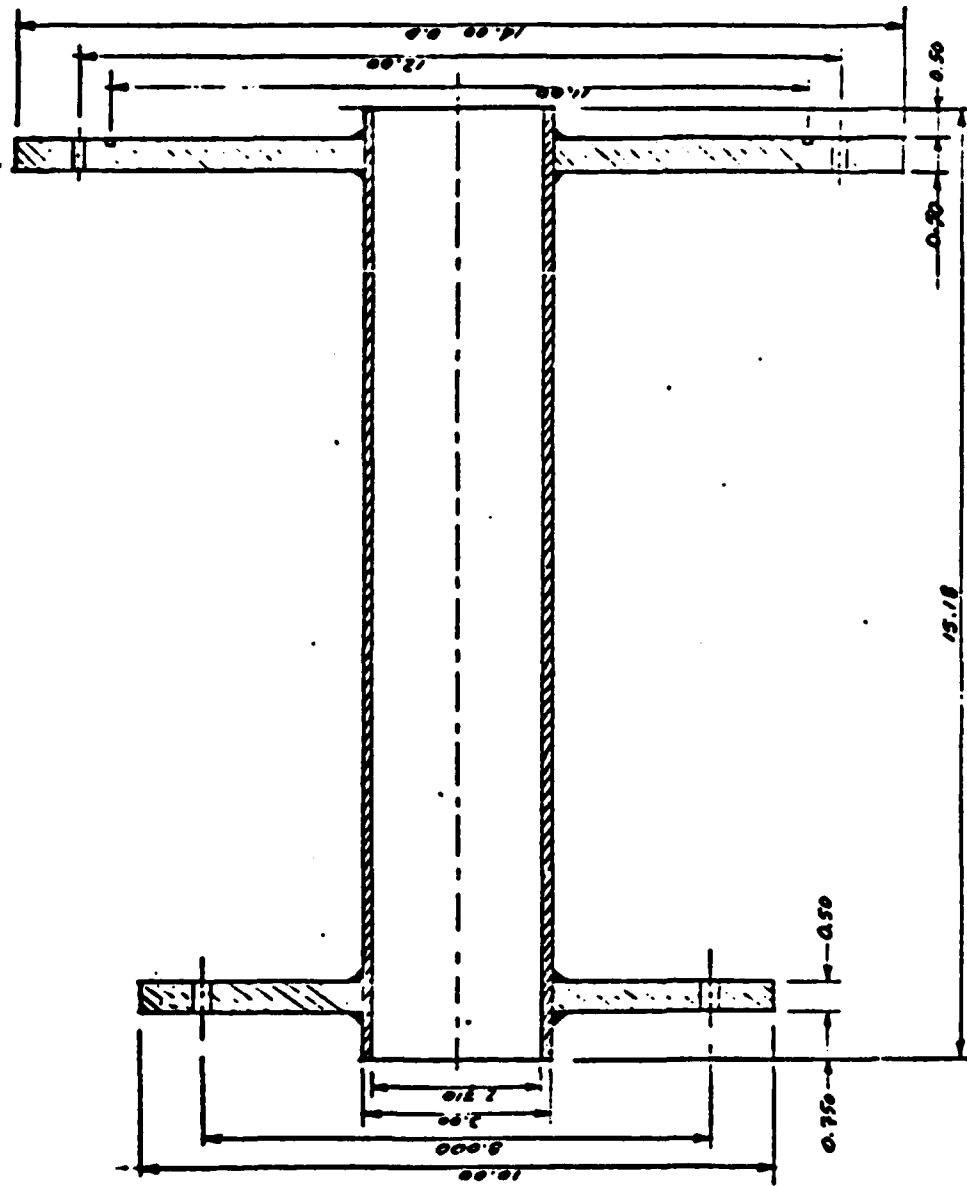


F404 A/B

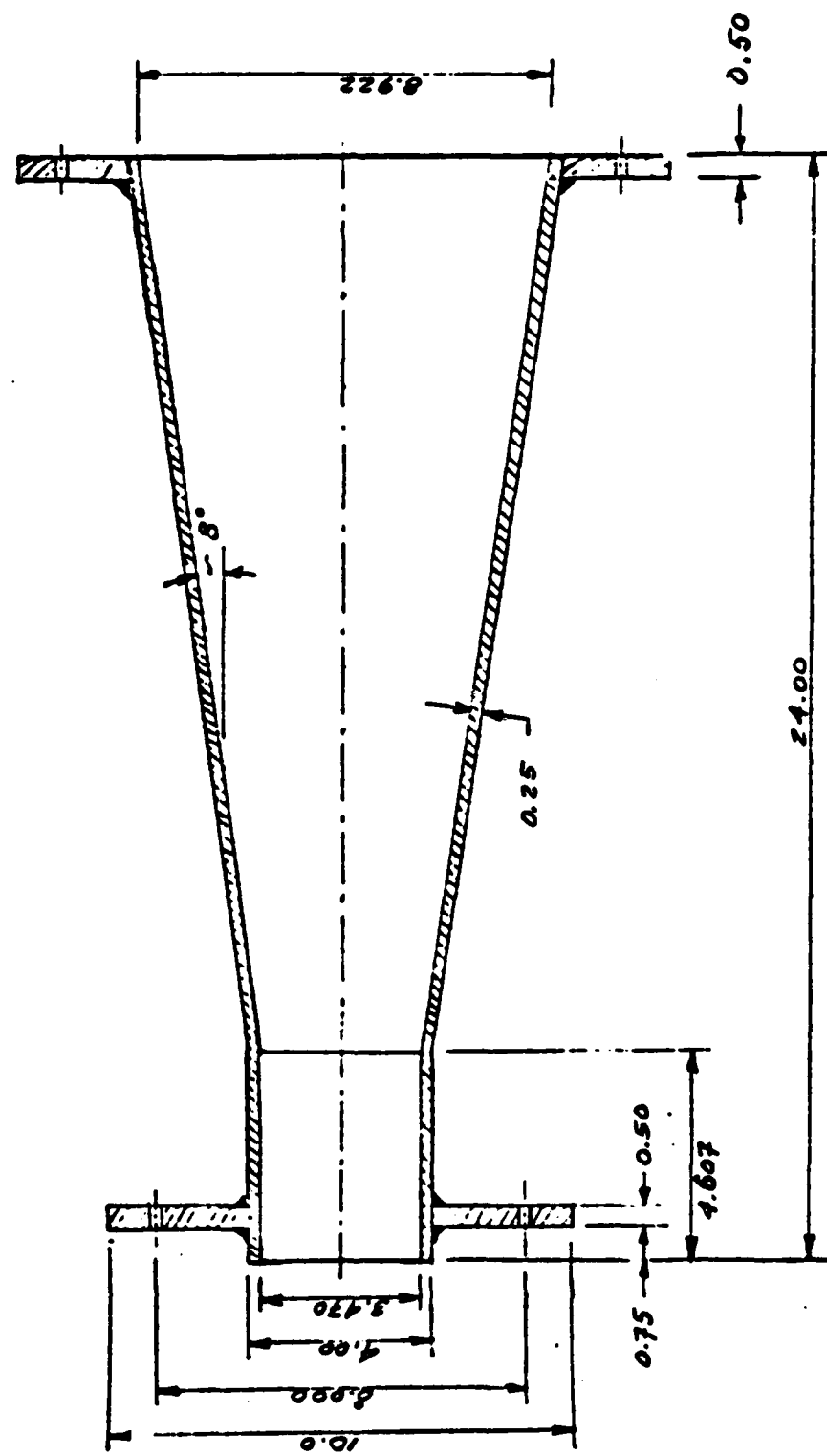




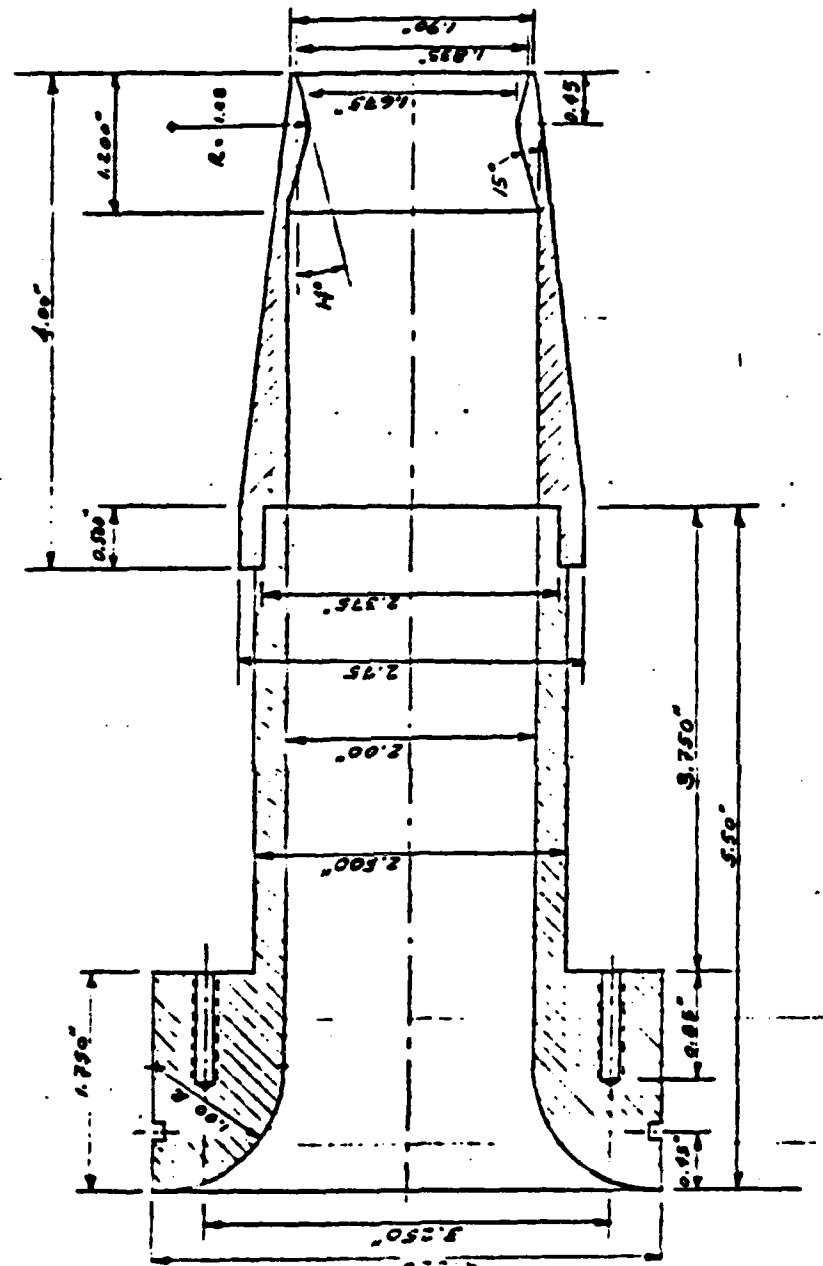
TF30 A/B



Constant Area Diffuser



Variable Area Diffuser



Engine Mounting

APPENDIX G

DATA TABLES

This appendix summarizes the reduced data collected during the course of this study. One set of raw data is included to summarize the details of the data acquisition process. The following abbreviations and units refer only to the data contained herein.

Abbreviations and Units

P ATM	Atmospheric Pressure (in. Hg)
P 01S	Secondary Orifice Pressures Upstream (in. H ₂ O)
P 02S	
P 03S	Secondary Orifice Pressures Downstream (in. H ₂ O)
P 04S	
P 01P	Primary Orifice Pressures Upstream (in. H ₂ O)
P 02P	
P 03P	Primary Orifice Pressures Downstream (in. H ₂ O)
P 04P	
P TOT	Total Pressure - PT8 (in. H ₂ O)
P TST	Inlet Static Pressure (in. H ₂ O)
P CEL	Cell Pressure - PS9 (in. H ₂ O)
P THS	Nozzle Entrance Pressure (in. H ₂ O)
P THT	Nozzle Throat Pressure (in. H ₂ O)
P D#_	Diffuser Wall Pressures (in. H ₂ O)
P EXH	Exhaust Pressure - P14 (in. H ₂ O)
T PRI	Primary Orifice Temperature (R)
T SEC	Secondary Orifice Temperature (R)

T TOT Total Temperature (R)
MASS FLOW (lbm/sec)
P STAG (in. H₂O abs.)
T STAG (Degrees R)

DATE OF RUNNED
7/15/1984
DIVISOR TESTED
2/1 SCALING
REFERENCE DATA FILE
BURNER

	RUN NUMBER									
	1	2	3	4	5	6	7	8	9	10
P ATM	29.78	29.78	29.78	29.78	29.78	29.78	29.78	29.78	29.78	29.78
P 015	-12.60	-12.30	-12.00	-11.00	-11.00	-11.00	-11.00	-11.00	-11.00	-14.00
P 025	-12.60	-12.30	-12.00	-11.00	-11.00	-11.00	-11.00	-11.00	-11.00	-14.00
P 035	-12.60	-12.30	-12.00	-11.00	-11.00	-11.00	-11.00	-11.00	-11.00	-14.00
P 045	-12.60	-12.30	-12.00	-11.00	-11.00	-11.00	-11.00	-11.00	-11.00	-14.00
P 01P	756.00	704.00	655.90	603.10	553.80	506.30	453.30	403.70	401.70	452.70
P 02P	756.70	703.80	655.50	601.80	553.60	508.20	454.20	401.50	401.70	452.80
P 03P	763.20	711.50	649.50	597.50	548.70	502.80	446.00	398.80	398.20	449.70
P 04P	763.20	711.50	649.50	597.50	548.70	502.80	446.00	398.80	398.20	449.70
P TOT	749.20	698.60	650.70	599.40	550.10	506.60	450.00	400.30	398.60	449.60
P TST	750.20	698.50	650.40	598.80	549.50	504.80	448.20	399.70	397.20	448.50
P CBL	-186.00	-178.70	-165.30	-154.50	-161.10	-131.60	-121.80	-110.20	-162.80	-176.60
P TUS	739.60	688.10	640.90	591.00	541.50	499.10	443.40	391.60	393.50	443.70
P THR	2.70	-15.20	-31.50	-49.10	-66.30	-81.80	-101.10	-118.70	-119.70	-102.10
P THR	1.50	-16.10	-32.60	-50.60	-67.90	-84.20	-103.50	-121.30	-121.70	-103.70
P D01	-163.40	-154.90	-147.10	-145.00	-115.49	-109.50	-103.50	-87.90	-157.00	-170.20
P D02	-110.70	-105.50	-96.80	-95.10	-92.50	-90.20	-86.60	-87.70	-124.90	-127.80
P D03	-79.70	-74.70	-64.70	-56.10	-49.30	-42.40	-36.40	-21.10	-15.90	-101.30
P D04	-56.80	-52.80	-43.80	-36.90	-28.80	-10.70	-10.20	-8.40	-81.00	-78.70
P D05	-36.10	-36.80	-27.60	-22.50	-7.80	-8.70	-9.00	-7.20	-6.80	-65.00
P D06	-28.70	-24.20	-18.30	-14.60	-7.20	-7.70	-6.60	-7.80	-59.70	-60.60
P D07	-16.60	-17.70	-12.30	-10.50	-5.80	-6.80	-7.80	-6.80	-54.80	-56.80
P D08	-13.80	-18.40	-10.50	-9.60	-6.70	-7.40	-8.20	-6.80	-53.40	-56.20
P D09	-11.80	-12.90	9.20	-8.80	-3.50	-5.20	-7.70	-6.80	-53.10	-55.30
P D011	-11.30	-13.20	-9.80	-9.20	-7.10	-8.10	-8.80	-7.20	-52.80	-55.80
P D012	-12.80	-16.50	-11.30	-10.80	-8.80	-9.50	-9.60	-7.80	-53.90	-56.70
P D013	-5.40	-7.50	-5.00	-5.10	-5.60	-5.30	-5.50	-4.50	-49.80	-52.10
P D014	-2.40	-4.80	-2.20	-2.30	-1.30	-2.80	-3.90	-2.90	-48.10	-49.60
P D015	-2.40	-2.30	-2.60	-2.40	-2.40	-2.80	-2.40	-2.70	-2.90	-3.00
P E04	-0.40	-6.30	-0.90	-0.80	-0.40	-1.50	-2.90	-2.10	-47.30	-48.90
T P01	569.10	568.10	566.20	566.70	565.90	566.70	567.30	567.80	569.00	
T SEC	528.80	529.70	528.30	528.80	528.80	528.70	528.70	528.70	528.70	
T TOT	560.30	559.40	556.40	557.90	558.40	558.40	558.40	558.40	558.40	

DATE OF RUN		RUN NUMBER									
DIFFUSION TESTED		NUMBER									
REFERENCE DATA FILE		NUMBER									
P ATM	29.78	29.78	29.78	29.78	29.78	29.78	29.78	29.78	29.78	29.78	29.78
P 015	-15.00	-15.00	-16.00	-16.00	-16.00	-16.00	-16.00	-15.00	-15.00	-17.00	-17.00
P 025	-15.00	-15.00	-16.00	-16.00	-16.00	-16.00	-16.00	-15.00	-15.00	-17.00	-17.00
P 035	-15.00	-15.00	-16.00	-16.00	-16.00	-16.00	-16.00	-15.00	-15.00	-17.00	-17.00
P 045	-15.00	-15.00	-16.00	-16.00	-16.00	-16.00	-16.00	-15.00	-15.00	-17.00	-17.00
P 01P	501.30	553.50	602.40	654.30	705.00	755.90	761.90	760.20	760.00	819.00	819.00
P 02P	502.30	553.30	601.60	653.90	702.90	760.10	761.10	761.00	778.00	819.70	819.70
P 03P	498.00	549.00	596.00	648.20	698.00	752.30	775.80	775.40	773.50	812.30	812.30
P 04P	498.00	549.00	596.00	648.20	698.30	752.30	775.80	775.40	773.50	812.30	812.30
P 05P	498.20	550.40	597.60	649.10	699.32	752.70	774.10	774.80	771.20	810.70	810.70
P TST	497.00	550.40	596.60	649.60	697.90	754.90	776.20	776.00	775.50	813.60	813.60
P CEL	-188.50	-201.60	-211.60	-232.00	-243.50	-253.20	-255.50	-323.70	-192.00	-201.10	-201.10
P TWS	490.70	541.60	587.10	637.80	687.50	741.30	764.20	766.50	765.00	803.70	803.70
P THR	-85.40	-67.30	-51.30	-33.20	-16.30	2.30	9.90	8.20	11.30	28.60	28.60
P THT	-86.30	-66.00	-51.60	-33.40	-16.13	2.40	10.10	10.40	9.80	23.40	23.40
P D01	-181.10	-184.90	-193.60	-212.50	-226.50	-230.90	-232.70	-237.40	-169.80	-177.40	-177.40
P D02	-139.50	-142.80	-149.00	-163.00	-174.32	-172.60	-172.00	-209.30	-114.70	-117.70	-117.70
P D83	-103.90	-117.10	-122.30	-135.70	-143.30	-138.60	-137.40	-165.00	-79.20	-82.20	-82.20
P D84	-81.10	-95.50	-98.80	-106.00	-119.00	-110.70	-111.20	-186.90	-50.80	-53.30	-53.30
P D05	-68.60	-78.30	-83.40	-86.10	-101.00	-93.50	-91.60	-143.30	-30.10	-29.30	-29.30
P D06	-61.90	-68.90	-73.20	-79.10	-87.60	-81.90	-83.20	-143.10	-22.60	-22.30	-22.30
P D07	-59.00	-63.00	-64.60	-72.20	-77.53	-76.40	-76.00	-147.60	-17.50	-16.30	-16.30
P D08	-57.90	-60.60	-62.30	-70.90	-77.20	-73.70	-73.30	-146.90	-16.50	-16.40	-16.40
P D09	-57.00	-59.40	-61.30	-70.80	-74.70	-73.20	-71.30	-144.90	-13.40	-14.30	-14.30
P D011	-57.20	-59.40	-61.00	-71.50	-74.10	-73.50	-72.60	-143.90	-13.60	-14.50	-14.50
P D012	-58.60	-60.40	-62.30	-73.60	-76.30	-74.80	-73.50	-145.90	-15.10	-16.10	-16.10
P D013	-53.40	-58.20	-56.00	-66.30	-68.80	-67.10	-65.30	-142.00	-7.83	-8.63	-8.63
P D014	-51.10	-52.20	-53.00	-62.10	-66.50	-62.80	-61.50	-135.10	-4.10	-4.03	-4.03
P D015	-3.00	-2.90	-3.10	-2.90	-2.83	-3.20	-3.00	-2.90	-2.40	-2.50	-2.50
P T SEC	-49.80	-50.60	-51.80	-61.00	-63.32	-60.10	-59.30	-130.80	-2.30	-2.40	-2.40
T PRI	570.00	571.70	572.10	573.00	573.10	572.80	572.50	571.90	571.10	569.60	569.60
T T SEC	528.70	529.10	529.30	529.20	529.10	529.00	528.90	528.90	528.90	562.10	562.10
T T T	560.60	562.80	564.10	564.00	564.10	564.00	564.00	564.00	564.00	563.70	563.70

DATE OF RUN 1/15/1981
 ENGINEERED TESTED NO/47728 808928
 INDEPENDENCE DATA FILE
 BIAS SCAL2
 BIAS SC

	BON NUMBER									
	21	22	23	24	25	26	27	28	29	30
P ATM	29.78	29.78	29.78	29.78	29.78	29.78	29.78	29.78	29.78	29.78
P 013	-18.00	-17.00	-17.00	-16.00	-16.00	-16.00	-15.00	-15.00	-15.00	-8.00
P 023	-18.00	-17.00	-17.00	-16.00	-16.00	-16.00	-15.00	-15.00	-15.00	-8.00
P 035	-18.00	-17.00	-17.00	-16.00	-16.00	-16.00	-15.00	-15.00	-15.00	-8.00
P 045	-18.00	-17.00	-17.00	-16.00	-16.00	-16.00	-15.00	-15.00	-15.00	-8.00
P 019	818.10	817.50	756.40	704.40	656.50	606.90	554.40	505.60	453.90	402.00
P 029	817.80	816.50	757.40	706.00	657.30	607.10	555.30	505.40	454.60	402.00
P 039	811.00	810.30	751.10	699.00	649.90	601.70	550.10	500.50	450.70	399.30
P 049	811.00	810.30	751.10	699.00	649.90	601.70	550.10	500.50	450.70	399.30
P ROT	810.30	808.70	751.80	700.00	650.60	602.70	551.30	501.10	451.10	399.30
P TST	813.60	810.20	751.90	700.20	650.10	602.20	550.70	500.50	450.80	399.60
P CEL	-266.40	-325.60	-322.40	-314.30	-293.53	-267.90	-251.00	-233.30	-216.50	-198.30
P IHS	603.30	802.30	745.20	692.10	642.63	596.30	546.30	494.80	445.40	395.20
P THT	22.30	20.10	-0.30	-17.60	-33.10	-48.30	-66.00	-83.80	-101.30	-118.30
P THT	23.40	23.50	4.90	-12.90	-30.20	-45.80	-64.30	-84.40	-98.60	-116.70
P D01	-238.00	-227.60	-238.10	-266.10	-267.20	-248.80	-235.40	-219.40	-202.10	-191.20
P D02	-162.90	-213.90	-197.40	-202.40	-207.60	-200.60	-189.10	-174.80	-164.90	-149.90
P D03	-126.80	-175.50	-156.00	-176.50	-176.20	-165.70	-156.20	-151.70	-140.60	-126.10
P D04	-103.00	-151.10	-187.70	-181.90	-151.40	-145.00	-133.50	-131.50	-121.60	-106.20
P D05	-39.20	-151.40	-143.50	-151.10	-143.90	-130.50	-122.33	-117.10	-107.00	-94.20
P D06	-83.10	-151.70	-145.30	-147.30	-134.10	-120.50	-112.80	-105.90	-98.40	-87.00
P D07	-77.70	-149.50	-148.20	-141.80	-129.20	-114.60	-106.90	-99.39	-92.20	-83.20
P D08	-75.50	-145.20	-143.60	-142.50	-127.80	-113.50	-103.70	-97.60	-89.90	-82.10
P D09	-76.70	-146.40	-146.00	-137.00	-128.30	-111.20	-101.00	-96.10	-90.20	-82.70
P D11	-76.60	-147.50	-143.60	-140.00	-127.50	-111.90	-104.30	-97.60	-90.00	-82.20
P D12	-79.00	-148.80	-144.20	-144.80	-131.60	-112.53	-103.00	-97.10	-90.50	-83.00
P D13	-70.40	-142.30	-140.70	-135.50	-121.90	-106.30	-99.80	-91.80	-84.60	-78.40
P D14	-68.80	-135.70	-136.50	-127.40	-117.80	-100.70	-96.10	-89.60	-83.30	-77.20
P D15	-2.40	-2.30	-1.90	-2.20	-2.60	-2.30	-2.50	-2.40	-2.00	-1.80
P RXH	-62.80	-128.80	-131.73	-122.90	-115.93	-100.60	-94.60	-88.30	-81.80	-76.80
T PBI	568.40	567.00	563.50	561.30	560.90	558.70	557.00	556.20	554.90	551.50
T SEC	528.90	528.70	528.60	528.50	528.30	528.00	528.70	529.00	528.70	528.70
T TOT	560.30	559.10	555.50	554.20	552.60	550.90	549.80	548.20	547.10	543.00

DATE OF RUN	7/15/1983		PT14/PS9
ENGINE TESTED	MODEL F404		PS 14 / PT8
DIFFUSER TESTED	2/3 SCALE		PS 14 / PS9
REFERENCE DATA FILES			PT8/PS4
RUNS	MASS FLOW	PRI SEC	STAGNATION
1	1157	0.82	560. 10
2	1106	0.582	559. 10
3	1058	0.282	557. 200
4	912	0.982	556. 200
5	857	0.882	555. 200
6	808	0.482	554. 200
7	806	0.482	553. 200
8	805	0.482	552. 200
9	955	0.482	551. 200
10	958	0.482	550. 200
11	956	0.482	549. 200
12	954	0.482	548. 200
13	952	0.482	547. 200
14	950	0.482	546. 200
15	948	0.482	545. 200
16	946	0.482	544. 200
17	944	0.482	543. 200
18	942	0.482	542. 200
19	940	0.482	541. 200
20	938	0.482	540. 200
21	936	0.482	539. 200
22	934	0.482	538. 200
23	932	0.482	537. 200
24	930	0.482	536. 200
25	928	0.482	535. 200
26	926	0.482	534. 200
27	924	0.482	533. 200
28	922	0.482	532. 200
29	920	0.482	531. 200
30	918	0.482	530. 200
31	916	0.482	529. 200
32	914	0.482	528. 200
33	912	0.482	527. 200
34	910	0.482	526. 200
35	908	0.482	525. 200
36	906	0.482	524. 200
37	904	0.482	523. 200
38	902	0.482	522. 200
39	900	0.482	521. 200
40	898	0.482	520. 200
41	896	0.482	519. 200
42	894	0.482	518. 200
43	892	0.482	517. 200
44	890	0.482	516. 200
45	888	0.482	515. 200
46	886	0.482	514. 200
47	884	0.482	513. 200
48	882	0.482	512. 200
49	880	0.482	511. 200
50	878	0.482	510. 200
51	876	0.482	509. 200
52	874	0.482	508. 200
53	872	0.482	507. 200
54	870	0.482	506. 200
55	868	0.482	505. 200
56	866	0.482	504. 200
57	864	0.482	503. 200
58	862	0.482	502. 200
59	860	0.482	501. 200
60	858	0.482	500. 200
61	856	0.482	499. 200
62	854	0.482	498. 200
63	852	0.482	497. 200
64	850	0.482	496. 200
65	848	0.482	495. 200
66	846	0.482	494. 200
67	844	0.482	493. 200
68	842	0.482	492. 200
69	840	0.482	491. 200
70	838	0.482	490. 200
71	836	0.482	489. 200
72	834	0.482	488. 200
73	832	0.482	487. 200
74	830	0.482	486. 200
75	828	0.482	485. 200
76	826	0.482	484. 200
77	824	0.482	483. 200
78	822	0.482	482. 200
79	820	0.482	481. 200
80	818	0.482	480. 200
81	816	0.482	479. 200
82	814	0.482	478. 200
83	812	0.482	477. 200
84	810	0.482	476. 200
85	808	0.482	475. 200
86	806	0.482	474. 200
87	804	0.482	473. 200
88	802	0.482	472. 200
89	800	0.482	471. 200
90	798	0.482	470. 200
91	796	0.482	469. 200
92	794	0.482	468. 200
93	792	0.482	467. 200
94	790	0.482	466. 200
95	788	0.482	465. 200
96	786	0.482	464. 200
97	784	0.482	463. 200
98	782	0.482	462. 200
99	780	0.482	461. 200
100	778	0.482	460. 200
101	776	0.482	459. 200
102	774	0.482	458. 200
103	772	0.482	457. 200
104	770	0.482	456. 200
105	768	0.482	455. 200
106	766	0.482	454. 200
107	764	0.482	453. 200
108	762	0.482	452. 200
109	760	0.482	451. 200
110	758	0.482	450. 200
111	756	0.482	449. 200
112	754	0.482	448. 200
113	752	0.482	447. 200
114	750	0.482	446. 200
115	748	0.482	445. 200
116	746	0.482	444. 200
117	744	0.482	443. 200
118	742	0.482	442. 200
119	740	0.482	441. 200
120	738	0.482	440. 200
121	736	0.482	439. 200
122	734	0.482	438. 200
123	732	0.482	437. 200
124	730	0.482	436. 200
125	728	0.482	435. 200
126	726	0.482	434. 200
127	724	0.482	433. 200
128	722	0.482	432. 200
129	720	0.482	431. 200
130	718	0.482	430. 200
131	716	0.482	429. 200
132	714	0.482	428. 200
133	712	0.482	427. 200
134	710	0.482	426. 200
135	708	0.482	425. 200
136	706	0.482	424. 200
137	704	0.482	423. 200
138	702	0.482	422. 200
139	700	0.482	421. 200
140	698	0.482	420. 200
141	696	0.482	419. 200
142	694	0.482	418. 200
143	692	0.482	417. 200
144	690	0.482	416. 200
145	688	0.482	415. 200
146	686	0.482	414. 200
147	684	0.482	413. 200
148	682	0.482	412. 200
149	680	0.482	411. 200
150	678	0.482	410. 200
151	676	0.482	409. 200
152	674	0.482	408. 200
153	672	0.482	407. 200
154	670	0.482	406. 200
155	668	0.482	405. 200
156	666	0.482	404. 200
157	664	0.482	403. 200
158	662	0.482	402. 200
159	660	0.482	401. 200
160	658	0.482	400. 200
161	656	0.482	399. 200
162	654	0.482	398. 200
163	652	0.482	397. 200
164	650	0.482	396. 200
165	648	0.482	395. 200
166	646	0.482	394. 200
167	644	0.482	393. 200
168	642	0.482	392. 200
169	640	0.482	391. 200
170	638	0.482	390. 200
171	636	0.482	389. 200
172	634	0.482	388. 200
173	632	0.482	387. 200
174	630	0.482	386. 200
175	628	0.482	385. 200
176	626	0.482	384. 200
177	624	0.482	383. 200
178	622	0.482	382. 200
179	620	0.482	381. 200
180	618	0.482	380. 200
181	616	0.482	379. 200
182	614	0.482	378. 200
183	612	0.482	377. 200
184	610	0.482	376. 200
185	608	0.482	375. 200
186	606	0.482	374. 200
187	604	0.482	373. 200
188	602	0.482	372. 200
189	600	0.482	371. 200
190	598	0.482	370. 200
191	596	0.482	369. 200
192	594	0.482	368. 200
193	592	0.482	367. 200
194	590	0.482	366. 200
195	588	0.482	365. 200
196	586	0.482	364. 200
197	584	0.482	363. 200
198	582	0.482	362. 200
199	580	0.482	361. 200
200	578	0.482	360. 200
201	576	0.482	359. 200
202	574	0.482	358. 200
203	572	0.482	357. 200
204	570	0.482	356. 200
205	568	0.482	355. 200
206	566	0.482	354. 200
207	564	0.482	353. 200
208	562	0.482	352. 200
209	560	0.482	351. 200
210	558	0.482	350. 200
211	556	0.482	349. 200
212	554	0.482	348. 200
213	552	0.482	347. 200
214	550	0.482	346. 200
215	548	0.482	345. 200
216	546	0.482	344. 200
217	544	0.482	343. 200
218	542	0.482	342. 200
219	540	0.482	341. 200
220	538	0.482	340. 200
221	536	0.482	339. 200
222	534	0.482	338. 200
223	532	0.482	337. 200
224	530	0.482	336. 200
225	528	0.482	335. 200
226	526	0.482	334. 200
227	524	0.482	333. 200
228	522	0.482	332. 200
229	520	0.482	331. 200
230	518	0.482	330. 200
231	516	0.482	329. 200
232	514	0.482	328. 200
233	512	0.482	327. 200
234	510	0.482	326. 200
235	508	0.482	325. 200
236	506	0.482	324. 200
237	504	0.482	323. 200
238	502	0.482	322. 200
239	500	0.482	321. 200
240	498	0.482	320. 200
241	496	0.482	319. 200
242	494	0.482	318. 200
243	492	0.482	317. 200
244	490	0.482	316. 200
245	488	0.482	315. 200
246	486	0.482	314. 200
247	484	0.482	313. 200
248	482	0.482	312. 200
249	480	0.482	311. 200
250	478	0.482	310. 200
251	476	0.482	309. 200
252	474	0.482	308. 200
253	472	0.482	307. 200
254	470	0.482	306. 200
255	468	0.482	305. 200
256	466	0.482	304. 200
257	464	0.482	303. 200
258	462	0.482	302. 200
259	460	0.482	301. 200
260	458	0.482	300. 200
261	456	0.482	299. 200
262	454	0.482	298. 200
263	452	0.482	297. 200
264	450	0.482	296. 200
265	448	0.482	295. 200
266	446	0.482	294. 200
267	444	0.482	293. 200
268	442	0.482	292. 200
269	440	0.482	291. 200
270	438	0.482	290. 200
271	436	0.482	289. 200
272	434	0.482	288. 200
273	432	0.482	287. 200
274	430	0.482	286. 200
275	428	0.482	285. 200
276	426	0.482	284. 200
277	424	0.482	283. 200
278			

DATE OF RUN 7/21/1983
DYNAMIC TESTED
DYNAMIC TESTED
PRESSURE DATA FILES
RUN 9
5/6 SCALP
MODEL P04
DC/APTER BURNER

DATE OF RUN 7/27/1983
ENGINE TESTED MODEL P404
DIFFUSER TESTED 5/6 SCALE

REFERENCE DATA FILES						RUN12
RUN NO.	MASS FLUX PRI SEC	MASS FLOW SEC	STAGNATION P	STAGNATION T	STAGNATION N	PS9/PT8
						PS14/PT8

תְּבִדְלָה תְּבִדְלָה תְּבִדְלָה תְּבִדְלָה תְּבִדְלָה תְּבִדְלָה תְּבִדְלָה

DATE OF RUN 7/15/1983
 ENGINE TESTED MODEL P404 V/APTER BURNER
 DIFFUSER TESTED 2/3 SCALE
 DIFFERENCE DATA FILES
 RUN 6

DATE OF RUN

ENGINE TESTED

DIFFUSER TESTED

REFERENCE DATA FILES

7/18/1983
MODEL P404 W/AFTER BURNER
2/3 SCALE
RUN 7

RUN NO.	MASS FLOW PRI	MASS FLOW SEC	P STAGNATION	T STAGNATION	PS9 PS8/PS9	PS14/PS8 PT14/PS9
1	0.57149	0.28564	10.94467	5.711.80	3.226	0.270
2	0.57969	0.22132	11.10.067	5.711.70	12.013	0.233
3	0.57875	0.27583	11.08.267	5.711.60	19.026	0.235
4	0.57916	0.08329	11.11.167	5.711.72	8.650	0.222
5	0.58026	0.08140	11.11.09.967	5.711.70	7.82.0	0.222
6	0.58043	0.08179	11.11.09.767	5.711.70	7.541	0.222
7	0.58055	0.08179	11.11.09.767	5.711.70	8.354	0.222
8	0.58055	0.08179	11.11.09.767	5.711.70	8.653	0.222
9	0.58055	0.08179	11.11.09.767	5.711.70	8.638	0.222
10	0.58055	0.08179	11.11.09.767	5.711.70	8.638	0.222
11	0.58055	0.08179	11.11.09.767	5.711.70	8.638	0.222
12	0.58055	0.08179	11.11.09.767	5.711.70	8.638	0.222
13	0.58055	0.08179	11.11.09.767	5.711.70	8.638	0.222
14	0.58055	0.08179	11.11.09.767	5.711.70	8.638	0.222
15	0.58055	0.08179	11.11.09.767	5.711.70	8.638	0.222
16	0.58055	0.08179	11.11.09.767	5.711.70	8.638	0.222
17	0.58055	0.08179	11.11.09.767	5.711.70	8.638	0.222
18	0.58055	0.08179	11.11.09.767	5.711.70	8.638	0.222
19	0.58055	0.08179	11.11.09.767	5.711.70	8.638	0.222
20	0.58055	0.08179	11.11.09.767	5.711.70	8.638	0.222

RUN NO.	MASS FLOW PRI	MASS FLOW SEC	P STAGNATION	T STAGNATION	PS9 PS8/PS9	PS14/PS8 PT14/PS9
1	0.57149	0.28564	10.94467	5.711.80	3.226	0.270
2	0.57969	0.22132	11.10.067	5.711.70	12.013	0.233
3	0.57875	0.27583	11.08.267	5.711.60	19.026	0.235
4	0.57916	0.08329	11.11.167	5.711.72	8.650	0.222
5	0.58026	0.08140	11.11.09.967	5.711.70	7.82.0	0.222
6	0.58043	0.08179	11.11.09.767	5.711.70	7.541	0.222
7	0.58055	0.08179	11.11.09.767	5.711.70	8.354	0.222
8	0.58055	0.08179	11.11.09.767	5.711.70	8.653	0.222
9	0.58055	0.08179	11.11.09.767	5.711.70	8.638	0.222
10	0.58055	0.08179	11.11.09.767	5.711.70	8.638	0.222
11	0.58055	0.08179	11.11.09.767	5.711.70	8.638	0.222
12	0.58055	0.08179	11.11.09.767	5.711.70	8.638	0.222
13	0.58055	0.08179	11.11.09.767	5.711.70	8.638	0.222
14	0.58055	0.08179	11.11.09.767	5.711.70	8.638	0.222
15	0.58055	0.08179	11.11.09.767	5.711.70	8.638	0.222
16	0.58055	0.08179	11.11.09.767	5.711.70	8.638	0.222
17	0.58055	0.08179	11.11.09.767	5.711.70	8.638	0.222
18	0.58055	0.08179	11.11.09.767	5.711.70	8.638	0.222
19	0.58055	0.08179	11.11.09.767	5.711.70	8.638	0.222
20	0.58055	0.08179	11.11.09.767	5.711.70	8.638	0.222

DATE OF RUN 7/21/1983
 ENGINE TESTED MODEL P404 W/AFTER BURNER
 DIFFUSER TESTED 5/6 SCALE
 DIFFERENCE DATA FILES
 RUN 10

DATE OF RUN
ENGINE TESTED
DIFFUUSER TESTED
REFERENCE DATA FILES

7/27/1983
MODEL P404
5/6 SCALE
RUN 11
W/AFTER BURNER

DATE OF RUN
ENGINE TESTED
DIFFUSER TESTED
REFERENCE DATA FILES
RUN13

7/27/1983
MODEL F404 W/AFTER BURNER
FULL SCALE

RUN NO.	MASS FLOW PR	MASS FLOW SEC	P STAGNATION	T STAGNATION	PS8/PS9	PT8/PT8	PS14/PS9	PT14/PT8
1	3572060676000000	3234220976000000	332.80	334.70	1.331	1.258	1.236	1.228
2	3572060676000000	3234220976000000	335.70	337.60	1.336	1.234	1.216	1.216
3	3572060676000000	3234220976000000	336.70	338.60	1.337	1.237	1.217	1.217
4	3572060676000000	3234220976000000	337.70	339.60	1.338	1.238	1.218	1.218
5	3572060676000000	3234220976000000	338.70	339.60	1.339	1.239	1.219	1.219
6	3572060676000000	3234220976000000	339.70	340.60	1.340	1.240	1.220	1.220
7	3572060676000000	3234220976000000	340.70	341.60	1.341	1.241	1.221	1.221
8	3572060676000000	3234220976000000	341.70	342.60	1.342	1.242	1.222	1.222
9	3572060676000000	3234220976000000	342.70	343.60	1.343	1.243	1.223	1.223
10	3572060676000000	3234220976000000	343.70	344.60	1.344	1.244	1.224	1.224
11	3572060676000000	3234220976000000	344.70	345.60	1.345	1.245	1.225	1.225
12	3572060676000000	3234220976000000	345.70	346.60	1.346	1.246	1.226	1.226
13	3572060676000000	3234220976000000	346.70	347.60	1.347	1.247	1.227	1.227
14	3572060676000000	3234220976000000	347.70	348.60	1.348	1.248	1.228	1.228
15	3572060676000000	3234220976000000	348.70	349.60	1.349	1.249	1.229	1.229
16	3572060676000000	3234220976000000	349.70	350.60	1.350	1.250	1.230	1.230
17	3572060676000000	3234220976000000	350.70	351.60	1.351	1.251	1.231	1.231
18	3572060676000000	3234220976000000	351.70	352.60	1.352	1.252	1.232	1.232
19	3572060676000000	3234220976000000	352.70	353.60	1.353	1.253	1.233	1.233
20	3572060676000000	3234220976000000	353.70	354.60	1.354	1.254	1.234	1.234
21	3572060676000000	3234220976000000	354.70	355.60	1.355	1.255	1.235	1.235
22	3572060676000000	3234220976000000	355.70	356.60	1.356	1.256	1.236	1.236
23	3572060676000000	3234220976000000	356.70	357.60	1.357	1.257	1.237	1.237
24	3572060676000000	3234220976000000	357.70	358.60	1.358	1.258	1.238	1.238
25	3572060676000000	3234220976000000	358.70	359.60	1.359	1.259	1.239	1.239
26	3572060676000000	3234220976000000	359.70	360.60	1.360	1.260	1.240	1.240
27	3572060676000000	3234220976000000	360.70	361.60	1.361	1.261	1.241	1.241
28	3572060676000000	3234220976000000	361.70	362.60	1.362	1.262	1.242	1.242
29	3572060676000000	3234220976000000	362.70	363.60	1.363	1.263	1.243	1.243
30	3572060676000000	3234220976000000	363.70	364.60	1.364	1.264	1.244	1.244
31	3572060676000000	3234220976000000	364.70	365.60	1.365	1.265	1.245	1.245
32	3572060676000000	3234220976000000	365.70	366.60	1.366	1.266	1.246	1.246
33	3572060676000000	3234220976000000	366.70	367.60	1.367	1.267	1.247	1.247
34	3572060676000000	3234220976000000	367.70	368.60	1.368	1.268	1.248	1.248
35	3572060676000000	3234220976000000	368.70	369.60	1.369	1.269	1.249	1.249
36	3572060676000000	3234220976000000	369.70	370.60	1.370	1.270	1.250	1.250
37	3572060676000000	3234220976000000	370.70	371.60	1.371	1.271	1.251	1.251
38	3572060676000000	3234220976000000	371.70	372.60	1.372	1.272	1.252	1.252
39	3572060676000000	3234220976000000	372.70	373.60	1.373	1.273	1.253	1.253
40	3572060676000000	3234220976000000	373.70	374.60	1.374	1.274	1.254	1.254
41	3572060676000000	3234220976000000	374.70	375.60	1.375	1.275	1.255	1.255
42	3572060676000000	3234220976000000	375.70	376.60	1.376	1.276	1.256	1.256
43	3572060676000000	3234220976000000	376.70	377.60	1.377	1.277	1.257	1.257
44	3572060676000000	3234220976000000	377.70	378.60	1.378	1.278	1.258	1.258
45	3572060676000000	3234220976000000	378.70	379.60	1.379	1.279	1.259	1.259
46	3572060676000000	3234220976000000	379.70	380.60	1.380	1.280	1.260	1.260
47	3572060676000000	3234220976000000	380.70	381.60	1.381	1.281	1.261	1.261
48	3572060676000000	3234220976000000	381.70	382.60	1.382	1.282	1.262	1.262
49	3572060676000000	3234220976000000	382.70	383.60	1.383	1.283	1.263	1.263
50	3572060676000000	3234220976000000	383.70	384.60	1.384	1.284	1.264	1.264
51	3572060676000000	3234220976000000	384.70	385.60	1.385	1.285	1.265	1.265
52	3572060676000000	3234220976000000	385.70	386.60	1.386	1.286	1.266	1.266
53	3572060676000000	3234220976000000	386.70	387.60	1.387	1.287	1.267	1.267
54	3572060676000000	3234220976000000	387.70	388.60	1.388	1.288	1.268	1.268
55	3572060676000000	3234220976000000	388.70	389.60	1.389	1.289	1.269	1.269
56	3572060676000000	3234220976000000	389.70	390.60	1.390	1.290	1.270	1.270
57	3572060676000000	3234220976000000	390.70	391.60	1.391	1.291	1.271	1.271
58	3572060676000000	3234220976000000	391.70	392.60	1.392	1.292	1.272	1.272
59	3572060676000000	3234220976000000	392.70	393.60	1.393	1.293	1.273	1.273
60	3572060676000000	3234220976000000	393.70	394.60	1.394	1.294	1.274	1.274
61	3572060676000000	3234220976000000	394.70	395.60	1.395	1.295	1.275	1.275
62	3572060676000000	3234220976000000	395.70	396.60	1.396	1.296	1.276	1.276
63	3572060676000000	3234220976000000	396.70	397.60	1.397	1.297	1.277	1.277
64	3572060676000000	3234220976000000	397.70	398.60	1.398	1.298	1.278	1.278
65	3572060676000000	3234220976000000	398.70	399.60	1.399	1.299	1.279	1.279
66	3572060676000000	3234220976000000	399.70	400.60	1.400	1.300	1.280	1.280
67	3572060676000000	3234220976000000	400.70	401.60	1.401	1.301	1.281	1.281
68	3572060676000000	3234220976000000	401.70	402.60	1.402	1.302	1.282	1.282
69	3572060676000000	3234220976000000	402.70	403.60	1.403	1.303	1.283	1.283
70	3572060676000000	3234220976000000	403.70	404.60	1.404	1.304	1.284	1.284
71	3572060676000000	3234220976000000	404.70	405.60	1.405	1.305	1.285	1.285
72	3572060676000000	3234220976000000	405.70	406.60	1.406	1.306	1.286	1.286
73	3572060676000000	3234220976000000	406.70	407.60	1.407	1.307	1.287	1.287
74	3572060676000000	3234220976000000	407.70	408.60	1.408	1.308	1.288	1.288
75	3572060676000000	3234220976000000	408.70	409.60	1.409	1.309	1.289	1.289
76	3572060676000000	3234220976000000	409.70	410.60	1.410	1.310	1.290	1.290
77	3572060676000000	3234220976000000	410.70	411.60	1.411	1.311	1.291	1.291
78	3572060676000000	3234220976000000	411.70	412.60	1.412	1.312	1.292	1.292
79	3572060676000000	3234220976000000	412.70	413.60	1.413	1.313	1.293	1.293
80	3572060676000000	3234220976000000	413.70	414.60	1.414	1.314	1.294	1.294
81	3572060676000000	3234220976000000	414.70	415.60	1.415	1.315	1.295	1.295
82	3572060676000000	3234220976000000	415.70	416.60	1.416	1.316	1.296	1.296
83	3572060676000000	3234220976000000	416.70	417.60	1.417	1.317	1.297	1.297
84	3572060676000000	3234220976000000	417.70	418.60	1.418	1.318	1.298	1.298
85	3572060676000000	3234220976000000	418.70	419.60	1.419	1.319	1.299	1.299
86	3572060676000000	3234220976000000	419.70	420.60	1.420	1.320	1.300	1.300
87	3572060676000000	3234220976000000	420.70	421.60	1.421	1.321	1.301	1.301
88	3572060676000000	3234220976000000	421.70	422.60	1.422	1.322	1.302	1.302
89	3572060676000000	3234220976000000	422.70	423.60	1.423	1.323	1.303	1.303
90	3572060676000000	3234220976000000	423.70	424.60	1.424	1.324	1.304	1.304
91	3572060676000000	3234220976000000	424.70	425.60	1.425	1.325	1.305	1.305
92	3572060676000000	3234220976000000	425.70	426.60	1.426	1.326	1.306	1.306
93	3572060676000000	3234220976000000	426.70	427.60	1.427	1.327	1.307	1.307
94	3572060676000000	3234220976000000	427.70	428.60	1.428	1.328	1.308	1.308
95	3572060676000000	3234220976000000	428.70	429.60	1.429	1.329	1.309	1.309
96	3572060676000000	3234220976000000	429.70	430.60	1.43			

DATE OF RUN 7/27/1983
 ENGINE TESTED MODEL P404 W/ AFTER BURNER
 DIFFUSER TESTED PULL SCALE
 PREFERENCE DATA FILES RUN 13

DATE OF RUN
ENGINE TESTED
DIFPUSE TESTED
REFERENCE DATA FILES

7/27/1983
MODEL P404 HC/AFTB BURNER
FULL SCALE
RUN14

RUN NO.	MASS FLOW	MASS SEC	PRI	STAGNATION	STAGNATION	PT8/PS9	PS14/PT8	PT14/PS9
				517.40	518.50	2.889	4.134	1.190
				519.00	500.23	2.222	4.454	1.126
				520.00	500.23	2.222	4.454	1.123
				521.00	500.23	2.222	4.454	1.125
				522.00	500.23	2.222	4.454	1.124
				523.00	500.23	2.222	4.454	1.127
				524.00	500.23	2.222	4.454	1.128
				525.00	500.23	2.222	4.454	1.129
				526.00	500.23	2.222	4.454	1.130
				527.00	500.23	2.222	4.454	1.131
				528.00	500.23	2.222	4.454	1.132
				529.00	500.23	2.222	4.454	1.133
				530.00	500.23	2.222	4.454	1.134
				531.00	500.23	2.222	4.454	1.135
				532.00	500.23	2.222	4.454	1.136
				533.00	500.23	2.222	4.454	1.137
				534.00	500.23	2.222	4.454	1.138
				535.00	500.23	2.222	4.454	1.139
				536.00	500.23	2.222	4.454	1.140
				537.00	500.23	2.222	4.454	1.141
				538.00	500.23	2.222	4.454	1.142
				539.00	500.23	2.222	4.454	1.143
				540.00	500.23	2.222	4.454	1.144
				541.00	500.23	2.222	4.454	1.145
				542.00	500.23	2.222	4.454	1.146
				543.00	500.23	2.222	4.454	1.147
				544.00	500.23	2.222	4.454	1.148
				545.00	500.23	2.222	4.454	1.149
				546.00	500.23	2.222	4.454	1.150
				547.00	500.23	2.222	4.454	1.151
				548.00	500.23	2.222	4.454	1.152
				549.00	500.23	2.222	4.454	1.153
				550.00	500.23	2.222	4.454	1.154
				551.00	500.23	2.222	4.454	1.155
				552.00	500.23	2.222	4.454	1.156
				553.00	500.23	2.222	4.454	1.157
				554.00	500.23	2.222	4.454	1.158
				555.00	500.23	2.222	4.454	1.159
				556.00	500.23	2.222	4.454	1.160
				557.00	500.23	2.222	4.454	1.161
				558.00	500.23	2.222	4.454	1.162
				559.00	500.23	2.222	4.454	1.163
				560.00	500.23	2.222	4.454	1.164
				561.00	500.23	2.222	4.454	1.165
				562.00	500.23	2.222	4.454	1.166
				563.00	500.23	2.222	4.454	1.167
				564.00	500.23	2.222	4.454	1.168
				565.00	500.23	2.222	4.454	1.169
				566.00	500.23	2.222	4.454	1.170
				567.00	500.23	2.222	4.454	1.171
				568.00	500.23	2.222	4.454	1.172
				569.00	500.23	2.222	4.454	1.173
				570.00	500.23	2.222	4.454	1.174
				571.00	500.23	2.222	4.454	1.175
				572.00	500.23	2.222	4.454	1.176
				573.00	500.23	2.222	4.454	1.177
				574.00	500.23	2.222	4.454	1.178
				575.00	500.23	2.222	4.454	1.179
				576.00	500.23	2.222	4.454	1.180
				577.00	500.23	2.222	4.454	1.181
				578.00	500.23	2.222	4.454	1.182
				579.00	500.23	2.222	4.454	1.183
				580.00	500.23	2.222	4.454	1.184
				581.00	500.23	2.222	4.454	1.185
				582.00	500.23	2.222	4.454	1.186
				583.00	500.23	2.222	4.454	1.187
				584.00	500.23	2.222	4.454	1.188
				585.00	500.23	2.222	4.454	1.189
				586.00	500.23	2.222	4.454	1.190
				587.00	500.23	2.222	4.454	1.191
				588.00	500.23	2.222	4.454	1.192
				589.00	500.23	2.222	4.454	1.193
				590.00	500.23	2.222	4.454	1.194
				591.00	500.23	2.222	4.454	1.195
				592.00	500.23	2.222	4.454	1.196
				593.00	500.23	2.222	4.454	1.197
				594.00	500.23	2.222	4.454	1.198
				595.00	500.23	2.222	4.454	1.199
				596.00	500.23	2.222	4.454	1.200
				597.00	500.23	2.222	4.454	1.201
				598.00	500.23	2.222	4.454	1.202
				599.00	500.23	2.222	4.454	1.203
				600.00	500.23	2.222	4.454	1.204
				601.00	500.23	2.222	4.454	1.205
				602.00	500.23	2.222	4.454	1.206
				603.00	500.23	2.222	4.454	1.207
				604.00	500.23	2.222	4.454	1.208
				605.00	500.23	2.222	4.454	1.209
				606.00	500.23	2.222	4.454	1.210
				607.00	500.23	2.222	4.454	1.211
				608.00	500.23	2.222	4.454	1.212
				609.00	500.23	2.222	4.454	1.213
				610.00	500.23	2.222	4.454	1.214
				611.00	500.23	2.222	4.454	1.215
				612.00	500.23	2.222	4.454	1.216
				613.00	500.23	2.222	4.454	1.217
				614.00	500.23	2.222	4.454	1.218
				615.00	500.23	2.222	4.454	1.219
				616.00	500.23	2.222	4.454	1.220
				617.00	500.23	2.222	4.454	1.221
				618.00	500.23	2.222	4.454	1.222
				619.00	500.23	2.222	4.454	1.223
				620.00	500.23	2.222	4.454	1.224
				621.00	500.23	2.222	4.454	1.225
				622.00	500.23	2.222	4.454	1.226
				623.00	500.23	2.222	4.454	1.227
				624.00	500.23	2.222	4.454	1.228
				625.00	500.23	2.222	4.454	1.229
				626.00	500.23	2.222	4.454	1.230
				627.00	500.23	2.222	4.454	1.231
				628.00	500.23	2.222	4.454	1.232
				629.00	500.23	2.222	4.454	1.233
				630.00	500.23	2.222	4.454	1.234
				631.00	500.23	2.222	4.454	1.235
				632.00	500.23	2.222	4.454	1.236
				633.00	500.23	2.222	4.454	1.237
				634.00	500.23	2.222	4.454	1.238
				635.00	500.23	2.222	4.454	1.239
				636.00	500.23	2.222	4.454	1.240
				637.00	500.23	2.222	4.454	1.241
				638.00	500.23	2.222	4.454	1.242
				639.00	500.23	2.222	4.454	1.243
				640.00	500.23	2.222	4.454	1.244
				641.00	500.23	2.222	4.454	1.245
				642.00	500.23	2.222	4.454	1.246
				643.00	500.23	2.222	4.454	1.247
				644.00	500.23	2.222	4.454	1.248
				645.00	500.23	2.222	4.454	1.249
				646.00	500.23	2.222	4.454	1.250
				647.00	500.23	2.222	4.454	1.251
				648.00	500.23	2.222	4.454	1.252
				649.00	500.23	2.222	4.454	1.253
				650.00	500.23	2.222	4.454	1.254
				651.00	500.23	2.222	4.454	1.255
				652.00	500.23	2.222	4.454	1.256
				653.00	500.23	2.222	4.454	1.257
				654.00	500.23	2.222	4.454	1.258
				655.00	500.23	2.222	4.454	1.259
				656.00	500.23	2.222	4.454	1.260
				657.00	500.23	2.222	4.454	1.261
				658.00	500.23	2.222	4.454	1.262
				659.00	500.23	2.222	4.454	1.263
				660.00	500.23	2.222	4.454	1.264
				661.00	500.23	2.222	4.454	1.265
				662.00	500.23	2.222	4.454	1.266
				663.00	500.23	2.222	4.454	1.267
				664.00	500.23	2.222	4.454	1.268
				665.00	500.23	2.222	4.454	1.269
				666.00	500.23	2.222	4.454	1.270
				667.00	500.23	2.222	4.454	1.271
	</							

DATE OF RUN
ENGINE TESTED
DIPUSER TESTED
REFERENCE DATA FILES

7/27/1983 WO/AFPER BURNER
MODEL P404 FULL SCALE RUN 14

APPENDIX H
DATA ACQUISITION PROGRAM

A computer program which details the data acquisition process is included in this Appendix. VIBTEM was executed on a Hewlett Packard 9830 and is written in BASIC.

10 REM
 20 REM
 30 REM **DESCRIPTION:**
 40 REM THIS PROGRAM PERFORMS SEQUENTIAL SCANNING
 50 REM OF SCANIVALE '5' BETWEEN PORT ADDRESSES 1-42 IN STEPS OF ONE.
 60 REM IT ALSO PERFORMS TEMPERATURE MEASUREMENTS ON SRC '2, BETWEEN
 70 REM CHANNELS 1-19

80 REM
 90 REM
 100 REM **VARIABLES FOR S/V SECTION.**
 110 REM V = DESIRED S/V
 110 REM A1 = LOW PORT
 120 REM A2 = HIGH PORT
 130 REM P = PRESENT S/V PORT
 140 REM S = STEP SIZE
 150 REM **VARIABLES FOR TEMPERATURE SECTION.**
 160 REM S\$=SCANNER LISTEN CODE
 170 REM S=SCANNER #
 180 REM C1=L0 CHANNEL
 190 REM C2=H1 CHANNEL
 200 REM C=TRANSMITTED CHANNEL
 210 REM V=DYN READING
 220 REM R=RPM CHANNEL
 230 PRINT
 240 PRINT
 250 PRINT
 260 PRINT
 270 PRINT
 280 PRINT
 290 DIM XL501,Y[20],Q[10],MC301,Z[50]
 300 MAT X=ZER
 310 MAT Y=ZER
 320 MAT Q=ZER
 330 MAT H=ZER
 340 MAT Z=ZER
 350 DISP "ENTER MONTH, DAY, YEAR OF RUN";
 360 INPUT M[44],X[45],XL46]

```

370 WRITE (15,380)X[44],X[45],X[46]
380 FORMAT "DATE OF RUN: ",F2.0,2X,F3.0,2X,F4.0
390 PRINT
400 PRINT
410 DISP "ENTER RUN #";
420 INPUT X[47]
430 X[49]=1
440 DISP "BAROMETER READING=?";
450 INPUT X[48]
460 PRINT "BAROMETER READING INCHES OF HG="X[48]
470 PRINT
480 PRINT
490 FORMAT B
500 FORMAT 2B
510 FORMAT 4B
520 FORMAT F3.0
530 GOTO 600
540 FOR I=1 TO 42
550 X[I]=0
560 NEXT I
570 FOR I=1 TO 19
580 Y[I]=0
590 NEXT I
600 WRITE (15,610)X[47],X[49]
610 FORMAT /,"RUN #",F3.0,4X,"PT #",F3.0
620 GOSUB 1320
625 PRINT "PRESSURES ? 1=YES 0=NO";
626 INPUT K1
627 IF K1=0 THEN 900
630 PRINT
640 PRINT
650 REM***START OF PROGRAM SEGMENT TO RECORD PRESSURES*****
650 REM***START OF PROGRAM SEGMENT TO RECORD PRESSURES*****
660 WRITE (13,510)256,26,768,512;
670 CMD "?D#","F1R7M3H1H1T3"
680 Y=5
690 R1=1

```

```

700 H2=42
710 S=1
720 CMD "?D"
730 WRITE (13,430)V
740 WRITE (15,750)V
750 FORMAT "SCHNIWALVE #",F3.0,/,," PORT",8X," IN H2O "
760 FOR R=A1 TO R2
770 GOSUB 1040
780 CMD "?D!"
790 WRITE (13,520)V+9
800 CMD "?D#", "13"
810 CMD "?C$"
820 ENTER (13,+)V0
830 X1A1=V0*100000
840 V0=V0*100000
850 WRITE (15,860)P,X1A1
850 FORMAT 1X,F3.0,4X,F8.2
870 CMD "?D!", "C"
880 NEXT A
890 GOTO 900
900 DISP "ENTER TIP VOLTAGE ";
910 INPUT V9
920 P9=(V9-4.5839)/(-0.8248)-4.886
930 WRITE (15,940)P9
940 FORMAT 1X,"TIP POSITION ",F7.3,1X," INCHES"
950 PRINT "-----"
960 DISP "ENTER 1 TO REPEAT";
980 INPUT R
990 X1491=XL491+1
1000 IF R=1 THEN 540
1010 STOP
1020 END
1030 EEM SUBROUTINE "POSIT"
1040 GOSUB 1220
1050 D=R-P
1060 CMD "?D!"

```

```

1070 IF D<0 THEN 1100
1080 IF D>0 THEN 1150
1090 RETURN
1100 REM HOME S/V
1110 WRITE (13,520)V+4
1120 WRITE (13,*)"C"
1130 WAIT 4000
1140 GOTO 1040
1150 REM ADVANCE S/V
1160 FOR I=1 TO B STEP S
1170 WRITE (13,520)V-1
1180 WRITE (13,*)"C"
1190 WAIT 200
1200 NEXT I
1210 GOTO 1040
1220 REM READ S/V ADDRESS
1230 CMD "?G$"
1240 P0=RBYTE13
1250 L=BAND(P0,15)
1260 T=ROT(P0,4)
1270 M=BAND(T,7)
1280 P=10*M+L
1290 WRITE (13,500)256,95;
1300 RETURN
1310 REM****SUBROUTINE TO RECORD TEMPS*****
1320 DIM S$(3)
1330 FORMAT F3.0
1340 FORMAT 3B
1350 FORMAT 4B
1360 REM
1370 OUTPUT (13,1350)256,20,768,512;
1380 CMD "?D$","F1R7M3H1H1T3"
1390 S=2
1400 C1=60
1410 C2=78
1420 S$=?D(

```

```

1430 WRITE (15,1440)S
1440 FORMAT 5X,"SCANNER #",F2.0,/,/,2X,"CHAN",6X,"TEMP DEG. R"
1450 FOR C=C1 TO C2
1460 CMD S$ 
1470 OUTPUT (13,1330)C
1480 CMD "?D#"
1490 OUTPUT (13,1340)256,8,512;
1500 CMD "?C$"
1510 ENTER (13,*)V
1520 B=C-59
1530 Y[B]=V
1540 NEXT C
1550 Y1=Y[1]
1560 FOR I=1 TO 19
1570 Y[1]=Y1+Y[1]
1580 Y[1]=Y[1]/2
1590 Y[1]=FNT(Y[1]*1000)+460-0.42
1600 IF I<14 THEN 1610
1610 Y[1]=Y[1]+1.26
1620 IF I<8 THEN 1630
1630 Y[1]=Y[1]+0.42
1640 WRITE (15,1650)I,Y[1]
1650 FORMAT 2X,F3.0,3X,F14.6
1660 NEXT I
1670 WRITE (15,1680)
1680 FORMAT 1,1
1690 CMD S$, "C"
1700 RETURN
1710 STOP
1720 DEF FNT(Y)
1730 S1=32.0787+46.34*Y-1.0515*Y†2
1740 S2=25.661297*Y-0.61954869*Y†2+0.022181644*Y†3-0.000355009*Y†4
1750 S3=32.0787+9*S2/5
1760 RETURN S3
1770 STOP

```

LIST OF REFERENCES

1. Neumann E. P., Lustwerk, F., "Supersonic Diffusers For Wind Tunnels," Journal of Applied Mechanics, Vol. 16, No. 2, pp. 195-202, June 1949.
2. Lukasiewicz, J. "Diffusers for Supersonic Wind Tunnels," Journal of the Aeronautical Sciences, September 1953, pp. 617-626.
3. Hastings, S.M. and Roberts, R.C., Analysis of the Performance of a Two Dimensional, Variable Area Supersonic Wind Tunnel Diffuser with and without Scavenger Scoop and Model, NAVAIR Report 4384, White Oak Maryland, May 1957.
4. Panesci, J.H., German, R.C., Improved Methods for Determining Second Throat Diffuser Performance of Zero Secondary Flow Ejector Systems, AEDC-TR-65-124, July 1965.
5. Merkli, P.E., "Pressure Recovery in Rectangular Constant Area Supersonic Diffusers," AIAA Journal Vol. 14, No. 2, September 1974, pp. 168-172.
6. Waltrup, P.J., Billig, F.S., "Structure of Shock Waves in Cylindrical Ducts," AIAA Journal Vol. II, No. 1-October 1973, pp. 1404-1408.
7. Ginoux, J.J., Supersonic Ejectors, AGARDograph No. 163, November 1972.
8. Shapiro, A.H., The Dynamics and Thermodynamics of Compressible Fluid Flow, Ronald Press, New York 1953.
9. GeopfARTH, R.N., Development of a Device for the Incorporation of Multiple Scanivalves into a Computer-Controlled Data System, M.S., Thesis Naval Postgraduate School, Monterey, CA, March 1979.
10. American Society of Mechanical Engineers Supplement on Instruments and Apparatus, Flow Measurement, 1959.
11. Bevilaqua, P.M., Combs, C.P., Theory and Practice of Ejector Scaling, Paper at Ejector Workshop for Aerospace Applications Dayton, Ohio, August 1981, (ADP000530)
12. Martin, B.W., Baker, P.J., "Experiments on a Supersonic Parallel Diffuser," Journal Mechanical Engineering Sciences, March 1953, pp. 169-174.

13. McLafferty, G., "Theoretical Pressure Recovery Through a Normal Shock in a Duct with Initial Boundary Layer," Journal of the Aeronautical Sciences, March 1953, pp. 169-174.
14. Amatucci, V.A., Dutton, J.C., Addy, A.L., "Pressure Recovery in a Constant Area Two Stream Supersonic Diffuser," AIAA Journal Vol. 20, No. 9, September 1982, pp. 1308-1309.
15. Johnson, J. A., Wu, B.J.C., Pressure Recovery and Related Properties in Supersonic Diffusers, AFOSR F44620-73-C-0032 April 1974.
16. Welch, D.R., Hot Flow Testing of Multiple Nozzle Exhaust Eductor Systems, M.E. Thesis, Naval Postgraduate School, Monterey, September 1978.

INITIAL DISTRIBUTION LIST

	<u>No. Copies</u>
1. Defense Technical Information Center Cameron Station Alexandria, VA 22314	2
2. Library, Code 0142 Naval Postgraduate School Monterey, CA 93943	2
3. Department Chairman, Code 69 Department of Mechanical Engineering Naval Postgraduate School Monterey, CA 93943	1
4. Professor Paul F. Pucci (Code 69Pc) Department of Mechanical Engineering Naval Postgraduate School Monterey, CA 93943	2
5. Assoc. Professor R.P. Schreeve (Code67Sf) Department of Aeronautics Naval Postgraduate School Monterey, CA 93943	1
6. Mr. J. E. Hammer, Code 67 Department of Aeronautics Naval Postgraduate School Monterey, CA 93943	1
7. Commanding Officer Attention: Mr. Vito Truglio Naval Air Propulsion Center Trenton, New Jersey 08628	3
8. CDR. James W. Molloy, USN 1253 Elm Road Baltimore, MD 21227	2
9. LCDR Thomas H. Walsh, USCG 1908 Carriage Drive Walnut Creek, CA 94598	1

END

FILMED

2-84

DTIC